

2 2004 9758295

This is to certify that the thesis entitled

A MODIFIED "SHIFT-AND-RATIO" METHOD FOR EXTRACTION OF THE EFFECTIVE CHANNEL LENGTH OF DEVICES CONTAINING HALO-IMPLANTS

presented by

Jorge Walter Argandoña

has been accepted towards fulfillment of the requirements for the

M.S. degree in Electrical and Computer Engineering

Major Professor's Signature

2

Date

MSU is an Affirmative Action/Equal Opportunity Institution

LIBRARY Michigan State University

PLACE IN RETURN BOX to remove this checkout from your record.

TO AVOID FINES return on or before date due.

MAY BE RECALLED with earlier due date if requested.

DATE DUE	DATE DUE	DATE DUE

6/01 c:/CIRC/DateDue.p65-p.15

A MODIFIED "SHIFT-AND-RATIO" METHOD FOR EXTRACTION OF THE EFFECTIVE CHANNEL LENGTH OF DEVICES CONTAINING HALO-IMPLANTS

Ву

Jorge Walter Argandoña

A THESIS

Submitted to
Michigan State University
in partial fulfillment of the requirements
for the degree of

MASTER OF SCIENCE

Department of Electrical and Computer Engineering

2004

T

ABSTRACT

A MODIFIED "SHIFT-AND-RATIO" METHOD FOR EXTRACTION OF THE EFFECTIVE CHANNEL LENGTH OF DEVICES CONTAINING HALO-IMPLANTS

By

Jorge Walter Argandoña

The standard shift and ratio method for extracting the effective channel length of a device does not work properly with devices containing halo-implants. This is due to the fact that this standard method makes the assumption that the effective mobility is not dependent on the channel length of a device, which is not the case for devices containing halo-implants. The modified shift and ratio method proposed takes the effective mobility dependence on the channel length of a device into account, and shows potential for solving the issues that exist with the standard shift and ratio method for devices containing halo-implants.

ACKNOWLEDGEMENTS

I would like to take this opportunity to thank everyone that aided in the success of this study. First and foremost Dr. Donnie Reinhard is thanked for aiding me with all the work regarding this research. His immeasurable kindness and patience throughout the entire duration of the project helped make my graduate experience a truly enjoyable one. IBM and Mary Weybright are thanked for providing the wafers with test devices, without which none of this would have been possible, as well as providing us with information regarding the devices and spending the time to review our measurement characteristics.

Thanks are also due to Dr. Timothy Hogan and Dr. Timothy Grotjohn for giving their time to be members of my committee and giving their personal thoughts on the research. Special thanks are extended to my family and friends for all their help and support.

TABLE OF CONTENTS

LIST O	F TABLES	vi
LIST O	F FIGURES	vii
KEY TO	SYMBOLS	ix
СНАРТ	ER 1	1
INTROI	DUCTION	1
1.1	Problem Statement	1
1.2	Thesis Layout	2
СНАРТ	ER 2	4
BACKO	ROUND	4
2.1	Introduction	4
2.2	Extracting the Effective Channel Length	4
2.3	The Standard Shift and Ratio Method	6
2.4	Modified Shift and Ratio Method	11
2.5	SPICE Models	13
СНАРТ	ER 3	14
EXPER	IMENTAL METHODS	14
3.1	Introduction	14
3.2	Devices	14
3.3	Measurement System	19
3.3	.1 Overview	
3.3		
3.3	<u> </u>	
3.3	lacktriangledown	
3.4		
СНАРТ	ER 4	28
SHIFT A	AND RATIO RESULTS	28
	Introduction	
4.2	Non-Halo Devices	
4.3	Halo Devices	
СНАРТ	ER 5	39
SPICE I	MODELING	39
5.1	Introduction	
5.2	Level 2 Models of Non-Halo Devices	
5.3	BSIM3 Modeling	

CHAPTER 6		54
CONC	LUSION	54
6.1	Introduction	
6.2	Summary of Results	
6.3	Future Research	54
APPEN	NDIX A	58
GWBA	ASIC PROGRAM	58
APPEN	NDIX B	65
PROGI	RAM DETAILS	65
APPEN	NDIX C	74
	SUREMENT DATA	
APPEN	NDIX D	90
	MANIPULATION IN EXCEL	
BIBLIC	OGRAPHY	93

LIST OF TABLES

Table 1. Excerpt of I-V data used when applying the shift and ratio method	29
Table 2. Shift and Ratio Data for Non-Halo Devices	74
Table 3. Shift and Ratio Data for Halo Devices with L=0.42μm and L=8.4μm	79
Table 4. Shift and Ratio Data for Halo Devices with L=0.21μm and L=8.4μm	84

LIST OF FIGURES

Figure 1. Various channel length parameters [3]	5
Figure 2. Effective channel length vs. mask length for nMOSFET's [3]	9
Figure 3. nMOS device with halo implants [6]	10
Figure 4. Picture of wafer provided by IBM	15
Figure 5. 2-Terminal setup used to obtain I-V measurements	16
Figure 6. Plot of Id vs. Vd = Vg using data from setup in Figure 5	17
Figure 7. 3-Terminal setup used to obtain I-V data	17
Figure 8. Plot of Id vs. Vd using data from setup in Figure 7	18
Figure 9. Block diagram of equipment setup	20
Figure 10. A picture of the probing station used for I-V measurements	21
Figure 11. A close-up picture of the probed wafer	22
Figure 12. The HP-4145B Semiconductor Parameter Analyzer	23
Figure 13. HP-4145B Source/Monitor Unit Simplified Circuit Diagram [7][7]	24
Figure 14. Semi-log plot of S-function vs. Vg with Vd = 0.05V	29
Figure 15. Ratio plot for various δ 'shift' values	31
Figure 16. Semi-log plot of S-function vs. Vg with Vd=0.05V	33
Figure 17. Ratio plot for various δ 'shift' values	34
Figure 18. Semi-log plot of S-function vs. Vg with Vd = 0.05V	35
Figure 19. Ratio plot for various δ 'shift' values	36
Figure 20. Id vs. Vd = Vg for non-halo device, L = 8.4µm	41
Figure 21. Simulated and measured data using Figure 5 setup	43

Figure 22. Simulated and measured data using Figure 5 setup	44
Figure 23. Simulated and measured data using Figure 7 setup	45
Figure 24. Id vs. Vd = Vg for non-halo device, L = 0.21μm	47
Figure 25. Simulated and measured data using Figure 5 setup	48
Figure 26. I_d vs. $V_d = V_g$ for halo device, $L = 8.4 \mu m$	49
Figure 27. I_d vs. $V_d = V_g$ for halo device, $L = 0.42 \mu m$	50
Figure 28. I_d vs. $V_d = V_g$ for halo device, $L = 0.21 \mu m$	51
Figure 29. Threshold voltage vs. channel length for various devices [10]	52

KEY TO SYMBOLS

Leff Effective channel length

L_{mask} Mask length

Lgate Gate length

L_{met} Metallurgical length

ΔL Delta L

I_{ds} Drain-to-source current

V_{ds} Drain-to-source voltage

μ Effective mobility

C_{ox} Oxide Capacitance

W Width

ε_{ox} Oxide dielectric

εs Semiconductor dielectric

t_{ox} Oxide thickness

Vg, Vgs Gate voltage, Gate-to-Source voltage

Vt Threshold voltage

R_{sd} Source drain resistance

R_{tot} Total resistance

R_{ch} Channel Resistance

 $S(V_g)$ S function

 $r(\delta, V_g)$ Ratio

C Mobility change

MOSFET Metal Oxide Semiconductor Field Effect Transistor

nMOS N-channel Metal Oxide Semiconductor

D Drain

G Gate

S Source

SB Substrate

SMU Source/Monitor Unit

σ Channel length modulation

V_{FB} Flat Band voltage

k Boltzmann's constant

N_A Acceptor concentration

T Temperature

φ_F Fermi potential

n_i Intrinsic carrier concentration

V_{bs} Bulk-to-source voltage

q Charge of an electron

HPIB Hewlett Packard Interface Board

CHAPTER 1

INTRODUCTION

1.1 Problem Statement

Various methods exist to determine the effective channel length of a MOSFET. The effective channel length of a device is of importance to industry for monitoring and modeling purposes. However, with technology changing, current methods can no longer properly extract the effective channel length for certain MOSFET types. Thus new methods are needed in order to determine the effective channel length of these newer devices. The new proposed method described in this paper will be of a modified version of the standard "shift and ratio" method, which is a method that is commonly used due to its accuracy and consistency for extracting the effective channel length. However, this is not the case for devices that contain halo implants. The effective mobility in devices that contain halo implants is different between short and long channel length devices. a difference that normally does not exist when dealing with typical devices. This difference in effective mobility seems to be the main predicament for the shift and ratio method. The proposed shift and ratio method takes this difference into account.

1.2 Thesis Layout

A brief background is given on the importance of extracting the effective channel length. The shift and ratio method is described as well as the proposed modified shift and ratio method. The shift and ratio method is thoroughly described with a series of equations that are used in the extraction of the effective channel length. Similarly, the proposed modified shift and ratio method is described with the same set of equations, but taking into account the effects of halo implants, particularly in that the effective mobility is dependent on the channel length of a device. The importance of the extracted effective channel length for modeling purposes is also noted.

The types of devices as well as the various setups used to obtain I-V measurements are also described. All the main components and their respective roles to obtain measurements are also described in detail.

The results for both the non-halo as well as the halo devices are discussed. The shift and ratio method is first applied to the non-halo devices. The manipulated data is plotted to clearly show how the values needed to apply the shift and ratio method are obtained. For the halo implants we once again apply the shift and ratio method and observe the unphysical results as described by van Meer [1]. The proposed modified shift and ratio method is then applied to these halo devices. The results that are obtained are analyzed and discussed.

The modeling work done on the devices is described in detail. The methods used for extraction of parameters for the SPICE models are described.

The inability to properly model the short channel length devices using level 2

1		

parameters is discussed, as well as the need of higher-level models.

The GWBASIC program used to efficiently obtain I-V measurements is included in Appendix A. Appendix B describes the program coding in detail, such that (if necessary) changes can be made to accommodate other measurements. All the data used for applying the shift and ratio method as well as the modified shift and ratio method is attached in Appendix C. Finally an explanation of how all the calculated values are obtained that are used for applying both methods in the extraction of the effective channel lengths are in Appendix D. Also included are the specific equations used in the Excel files to calculate the values needed.

CHAPTER 2

BACKGROUND

2.1 Introduction

This chapter provides an overview of material important to this thesis.

Section 2.2 notes the importance of knowing L_{eff}, specifically for short channel devices where a small inexactness can make a significant difference in performance. Section 2.3 explains the standard shift and ratio method, which is widely used and considered one of the most accurate and consistent techniques for extracting the effective channel length of a device. Section 2.4 explains a problem that exists with the shift and ratio method when dealing with devices containing halo implants and also gives details of the proposed modified shift and ratio method to take care of devices with halo implants. Modeling with SPICE is discussed in Section 2.5.

2.2 Extracting the Effective Channel Length

By design, physical features of a device are prescribed. However, the actual value of these features change as the devices are processed. Particularly, the effective channel length of a MOSFET is a critical parameter. Engineers use it to monitor lithography and etching during process development and

manufacturing, and designers who model the I-V characteristics of a device need to know the effective channel length of the device they are modeling. [2] Various terms exist to describe the length of a device, as can be seen in Figure 1 [3].

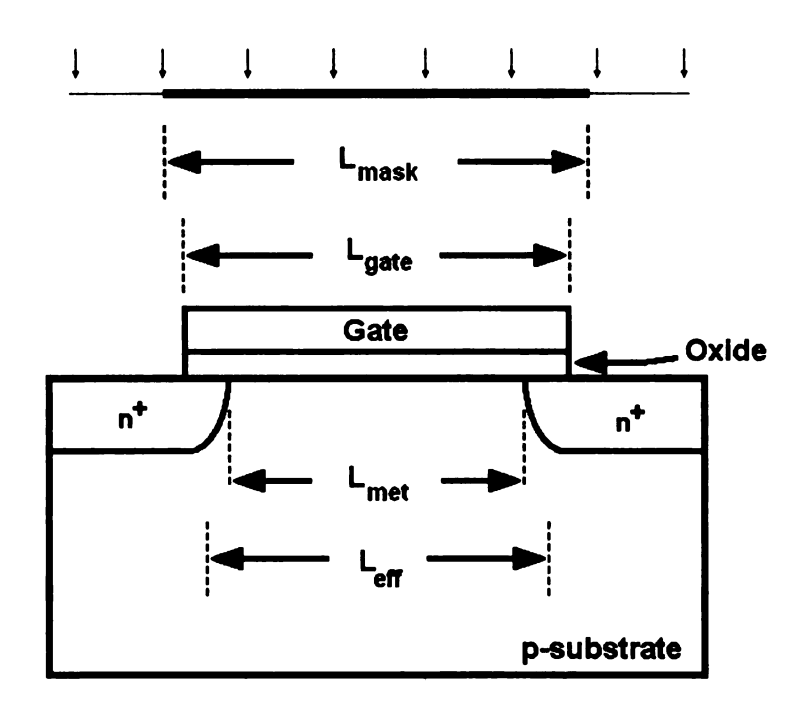


Figure 1. Various channel length parameters [3]

L_{mask} is defined as the design gate length on the etch mask. Through lithography and etching processes, L_{mask} is reproduced on to the wafer, and is defined as L_{gate}, which may be longer or shorter than L_{mask}. The distance between the metallurgical junctions of the source and drain is known as L_{met}. The effective channel length, L_{eff}, isn't strictly a physical parameter and actually is defined through electrical characteristics of the device. L_{eff} is defined as:

$$L_{eff} = L_{mask} - \Delta L \tag{1}$$

where L_{mask} is an initially designed known value, with some changes known as ΔL . This ΔL which is of the order of tens of nanometers, does not really have that much of an effect with large channel length devices. However, with sub-micron channel length devices this small ΔL can significantly affect the manner in which the device works. Different methods exist in order to "accurately" calculate the effective channel length of a device. The shift and ratio method has become a preferred means that is commonly used. It produces accurate estimates of the effective channel length for traditional devices, but has issues with certain newer devices. Specifically the shift and ratio method has problems with devices containing halo implants. A new proposed method based on the shift and ratio method will also be described for devices containing halo implants.

2.3 The Standard Shift and Ratio Method

The standard shift and ratio method is considered one of the most accurate techniques to calculate the effective channel length. Similar to many methods, the shift and ratio method is primarily based on the device current in the linear region [4].

$$I_{ds} = \mu C_{ox} \left(\frac{W}{L_{eff}} \right) \left(\frac{V_g - V_t - V_{ds}}{2} \right) V_{ds}$$
 (2)

where

Ids is the source drain current.

V_{ds} is the source drain voltage.

W is the width of the device.

Leff is the effective channel length of the device.

 μ is the effective mobility.

Vt is the threshold voltage of the device.

V_g is the applied gate voltage.

Cox is the gate oxide capacitance per unit area.

As shown by Taur [3], this equation can be modified to include the parasitic source-drain resistance (R_{sd}).

$$\frac{V_{ds}}{I_{ds}} = R_{tot} = R_{sd} + R_{ch} = R_{sd} + \frac{L_{eff}}{\mu C_{ox} W\left(\frac{V_g - V_t - V_{ds}}{2}\right)}$$
(3)

which can be generalized to the following form which the shift and ratio method is based on.

$$R_{tot}(V_g) = R_{sd} + L_{eff} f(V_g - V_t)$$
(4)

where f is a function of the gate overdrive, V_g - V_t , for all devices. The shift and ratio method continues by taking the derivative of the above equation (4) with respect to V_g . This is defined as the S-function

$$S(V_g) = \frac{dR_{tot}}{dV_g} = L_{eff} \frac{df(V_g - V_t)}{dV_g}$$
 (5)

where R_{sd} and L_{eff} are assumed to be constant with respect to $V_g.$

Using the shift and ratio method requires the use of two devices: one with a long channel and another with a short channel. It is assumed that both devices have the same mobility value such that $\delta f/\delta V_g$ is the same for both devices for a given V_g - V_t . However, the threshold voltage of a short channel device is normally not equal to the threshold of a long channel device. Therefore, in order to solve for the effective channel length of both devices, the S-function of the short channel device is shifted by some δ along the V_g axis. The ratio between the two is then taken

$$r(\delta, V_g) = \frac{S^0(V_g)}{S^i(V_g - \delta)} \tag{6}$$

where the superscript 'i' and '0' denotes the short and long channel device respectively. The quantity δ is equal to the threshold voltage difference between the devices $(V_t^0-V_t^i)$. The ratio equation (6) then reduces to

$$r = \frac{L_{eff}^{0}}{L_{eff}^{i}} = \frac{L_{mask}^{0} - \Delta L}{L_{mask}^{i} - \Delta L}$$
(7)

Since the mask length of both devices is known, ΔL can be solved for. Before ΔL can be determined, however, δ must be found experimentally. This is done by plotting $r(\delta,Vg)$ as a function of V_g for various δ values. The δ that produces a constant r is determined to be V_t^0 - V_t^i .

Thus, ΔL is determined by "shifting" V_g by a δ and documenting the "ratio"

of two device S-functions. This method seems to work fine with most types of devices and the results using this method on typical devices is shown by Taur in Figure 2.

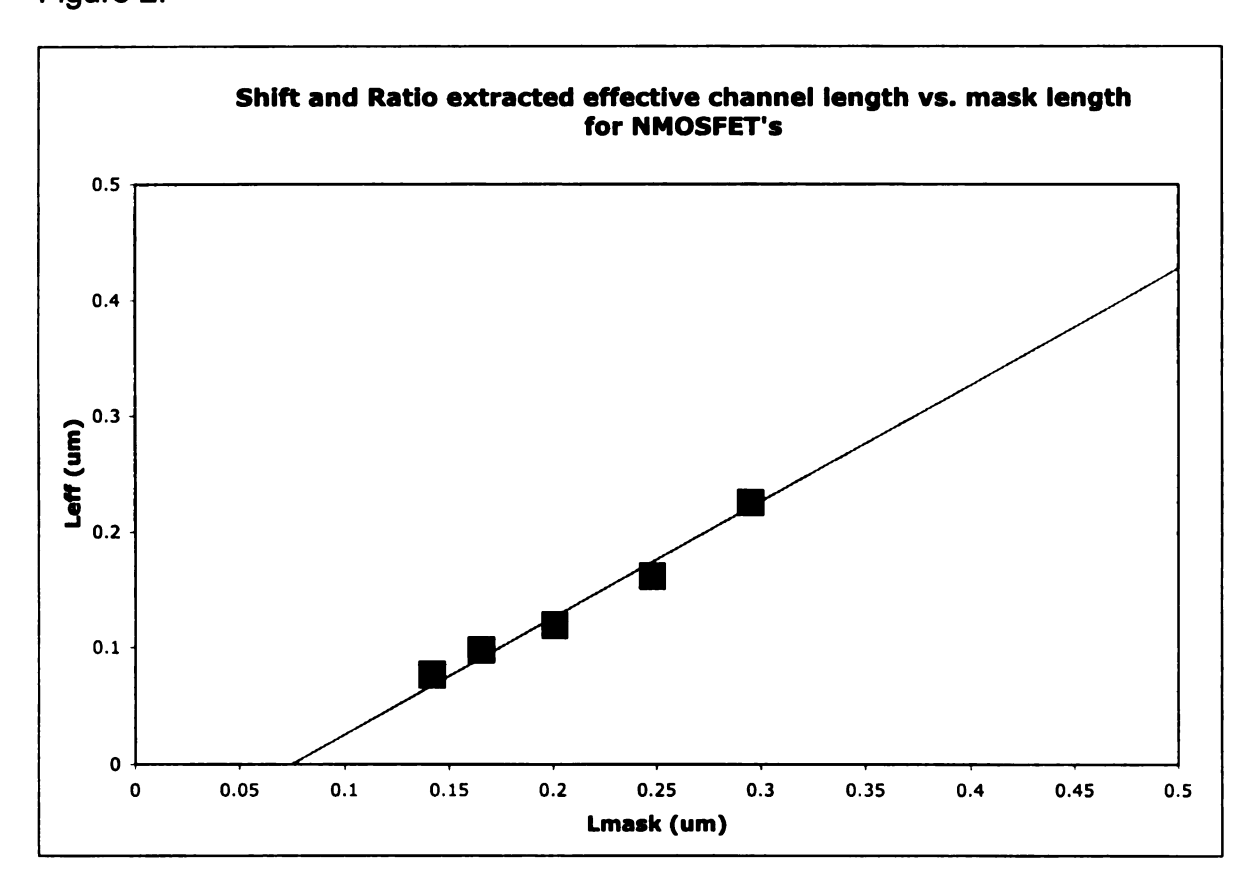


Figure 2. Effective channel length vs. mask length for nMOSFET's [3]

As devices become smaller, halo implants have been included in the fabrication process in order to improve performance. This causes the effective mobility to vary with L, which in turn does not allow one to use the shift and ratio method. One of its primary assumptions is that the effective mobility is the same for both short and long channel devices.

To improve the performance of deep submicron devices, ion implantation is commonly used. Ion implantation is the process of introducing dopants into

the surfactor MeV errat which the implantation containing effective n

It was increases

increases f

^{mask} lengt

method).

the surface layer of a solid substrate by bombarding the solid with ions in the keV to MeV energy range [5]. The penetration of the dopant is dependent on the rate at which the ion loses its energy. The properties of a device change when ion implantations are introduced. In our particular case, we are dealing with devices containing halo implants (Figure 3) and we note the changes it creates in the effective mobility.

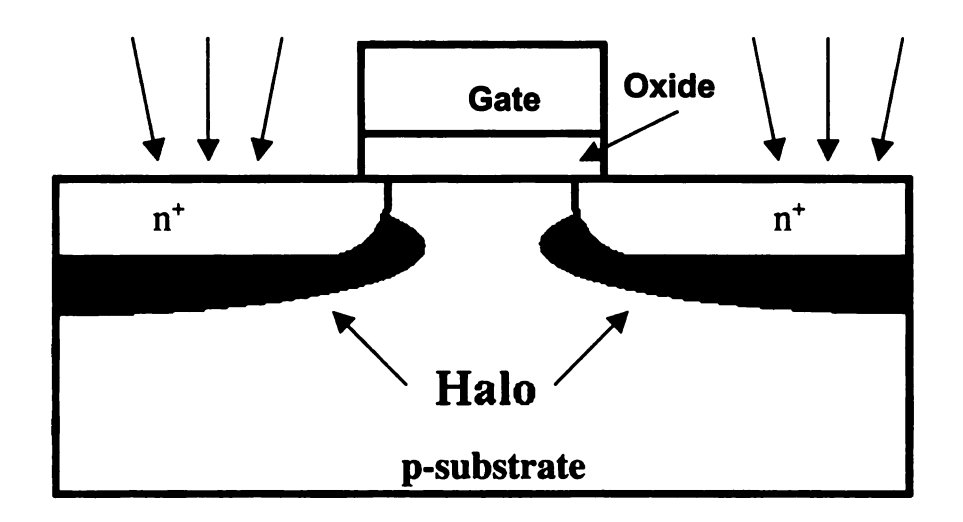


Figure 3. nMOS device with halo implants [6]

It was shown by van Meer [1] that the extracted effective channel length increases for devices with halo implants. When the halo implant doping is high enough, the extracted effective channel length actually becomes greater than the mask length (i.e. negative ΔL values are obtained using the shift and ratio method).

2.4 Modified Shift and Ratio Method

The shift and ratio method works well when extracting L_{eff} for most devices, but has problems when dealing with devices containing halo implants. In a previous study for example, the method produced negative ΔL values and it was concluded that the method produced unphysical results. It is a hypothesis of this thesis that the problem may be due to an assumption made by this method, that the effective mobility of the device is the same for both long and short channel devices, which is not the case for devices with halo implants. Short channel devices with halo implants have a lower effective mobility due to a higher vertical electric field and increased impurity scattering. The new proposed method assumes that the effective mobility of the short channel device is a percentage (less than 100%) of the effective mobility of the larger device.

$$\mu_{short}(V_g - V_t) = C\mu_{long}(V_g - V_t)$$
 (8)

where 'C' is less than 1. Similar to the shift and ratio method, this modified method also assumes that R_{sd} is constant with respect to V_g . The proposed method follows a similar series of steps as the shift and ratio method. The S-function for the long channel device is:

$$S^{0}(V_{g}) = \frac{dR_{tot}^{0}}{dV_{g}} = L_{eff}^{0} \frac{df(V_{g} - V_{t}^{0})}{dV_{g}}$$
(9)

while for the short channel device:

$$S^{i}(V_g) = \frac{dR_{tot}^{i}}{dV_g} = \frac{L_{eff}^{i}}{C} \frac{df(V_g - V_t^{i})}{dV_g}$$
(10)

Note that the 'C' term is the previous constant mentioned that relates the effective mobilities of the long and short channel devices.

As previously done, the ratio between the two devices is taken, where δ again is equal to the threshold voltage difference between the devices (V_t^0 - V_t^i). The ratio equation now reduces to

$$r = C \frac{L_{eff}^{0}}{L_{eff}^{i}} = C \frac{L_{mask}^{0} - \Delta L}{L_{mask}^{i} - \Delta L}$$
(11)

An average constant value of r can be extracted by plotting r vs. V_g . The mask length values are known, but two unknowns exist, C and ΔL .

Let us consider that C = 0.7 with

$$L_{mask}^{0} = 5\mu m$$

$$L_{mask}^{i} = 200nm$$

$$\Delta I_{i}^{0} = \Delta I_{i}^{i} = 50nm$$

Then the value of r using equation 11 would be 23.1. If we were to assume C = 1 which is what is done by the shift and ratio method, with the same two devices previously described, and a measured r value of 23.1, we would calculate $\Delta L = -17$ m using equation 7.

The exact percent change in effective mobility between the long and short channel device is unknown. Thus the proposed method requires measurements for three devices: one long channel device and two short channel devices with different L values. One then makes the assumption that both short channel devices approximately have the same effective mobility. Then for the second

short channel device the ratio equation is.

$$r = C \frac{L_{eff}^{0}}{L_{eff}^{j}} = C \frac{L_{mask}^{0} - \Delta L}{L_{mask}^{j} - \Delta L}$$

$$\tag{12}$$

where 'j' denotes the other short channel device. Now with two equations and two unknowns, one can solve for both C and ΔL . This proposed method would serve to 'more accurately' estimate the effective channel length of devices containing halo implants.

2.5 SPICE Models

The channel length is a primary parameter in SPICE models; small variations in the channel length device can significantly affect its performance, especially when dealing with short channel devices. When creating large circuit models, small inaccuracies that exist in a single device can multiply to create erroneous results. These days with complex devices containing halo implants, high level (BSIM3) SPICE models are necessary in order to accurately simulate them. Obtaining an accurate estimate of the effective channel length can be very useful to engineers creating circuit models. Specific SPICE related issues are discussed further in Chapter 5.

CHAPTER 3

EXPERIMENTAL METHODS

3.1 Introduction

Chapter 3 describes everything related to obtaining and processing the data needed for this project. Specifically section 3.2 explains the setup of the equipment and goes further into detail by explaining the role of all the equipment pertinent to data extraction. Section 3.3 reviews the various methods used when manipulating data to perform the shift and ratio method as well as the new modified method.

3.2 Devices

International Business Machines (IBM) provided eight-inch diameter wafers containing test devices. From these wafers, two particular types of n-channel silicon MOSFET's were used for this project, devices containing halo-implants and other devices that do not contain halo-implants. First measurements were made on the devices that do not contain the halo-implants, to demonstrate the basic method described by Taur [3] using the shift and ratio method with our experimental setup. As mentioned before the shift and ratio method requires measurements to be made for two devices, a long channel

device and a short channel device. The long channel device had gate dimensions of W = $8.4\mu m$ and L = $8.4\mu m$. The short channel device had gate dimensions W = $8.4\mu m$ and L = $0.21\mu m$. Note the width of both devices is the same.

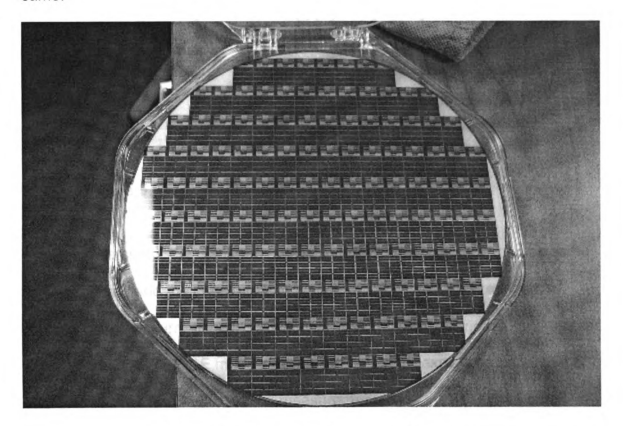


Figure 4. Picture of wafer provided by IBM

For each device, two types of I-V measurements were made. First I-V data was obtained using the setup pictured below in Figure 5.

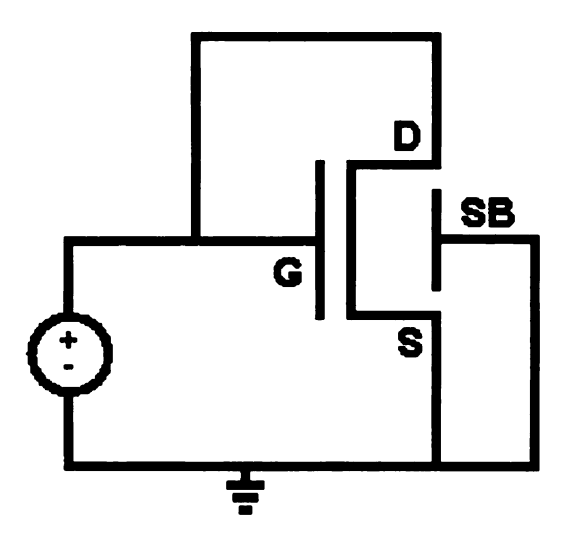


Figure 5. 2-Terminal setup used to obtain I-V measurements

In this setup, the drain and gate of the device are connected to the same voltage source and the substrate and source of the device are grounded.

Plotting the drain current vs. the voltage allows one to extract some important parameters for the SPICE models, which will be further explained in Chapter 5.

Representative data for this device measurement using the setup in Figure 5 is shown in Figure 6.

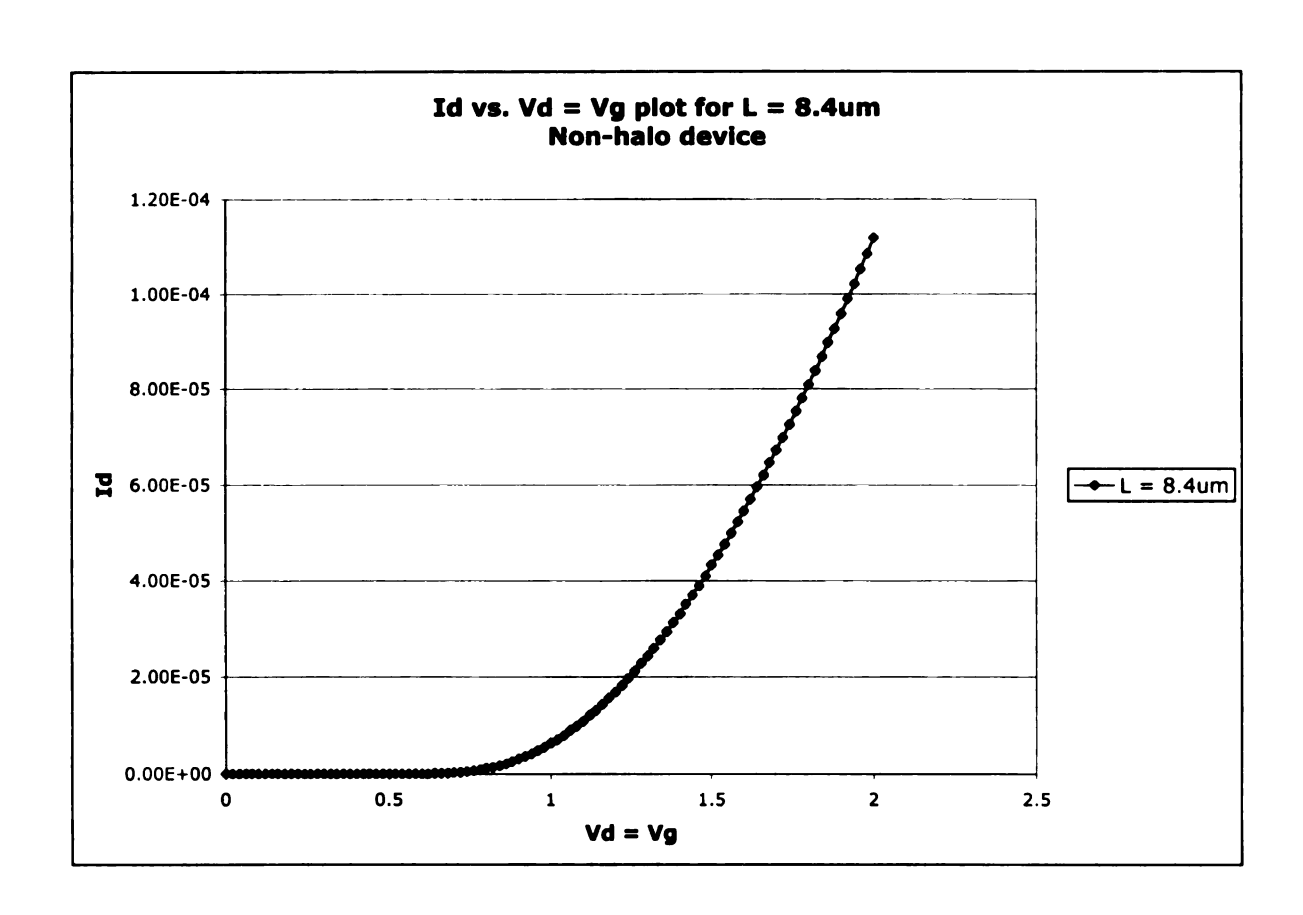


Figure 6. Plot of Id vs. Vd = Vg using data from setup in Figure 5

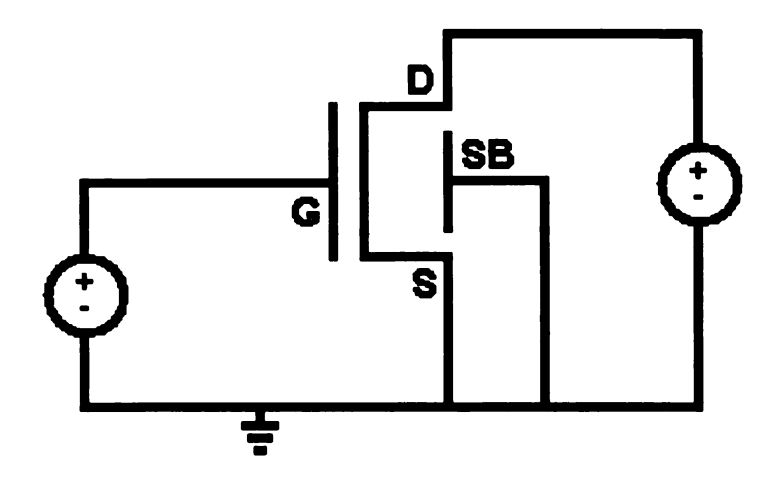


Figure 7. 3-Terminal setup used to obtain I-V data

Secondly, measurements were made using the following setup. Here the

source and the substrate are grounded. The gate of the device is connected to a step function voltage source. The drain of the device is connected to a sweeping function voltage source. Typically the drain current is plotted vs. the drain voltage for various gate voltages, providing a family of curves. This setup provides data that is used for the shift and ratio method, where the drain voltage is kept small (such that the device stays within the linear region) for various gate voltages. This data is also to be used for comparison with the created SPICE models, to observe how well they compare with the actual data from the devices. Representative data for this device measurement using the setup in Figure 7 is shown in Figure 8.

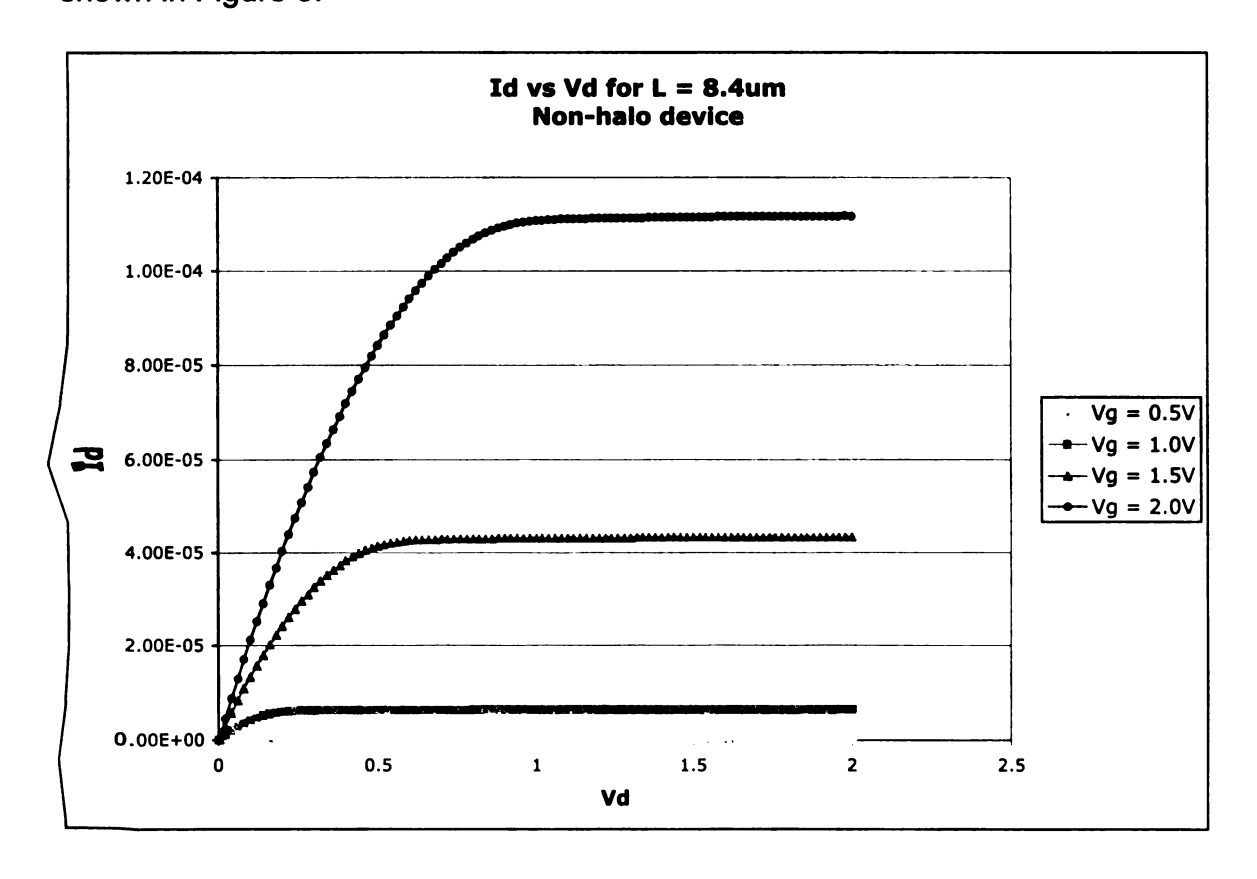


Figure 8. Plot of Id vs. Vd using data from setup in Figure 7

Both of the previous two measurements setups are also used for the devices containing halo-implants, but I-V measurements were measured for three devices. Two of them have the same gate dimensions as the devices not containing halo-implants. The third device has dimensions of W = 8.4 μ m and L = 0.42 μ m, which is the other short channel device that is assumed to have approximately the same effective mobility as the device with L = 0.21 μ m. The purpose of using three devices is to implement the modified shift and ratio method describe in Section 2.4

3.3 Measurement System

3.3.1 Overview

The main components of our setup to obtain I-V measurements, is shown below in Figure 9, in the form of a simplified block diagram. A brief summary of the main components and their respective roles is also discussed. The probes along with the shielded probing station provide protection for the data from outside noise. The HP-4145B is the equipment used to make the I-V measurements. The HPIB card and computer program are used to control the HP-4145B remotely, as well as simplify the setup procedure, and allow for efficient collection of the data.

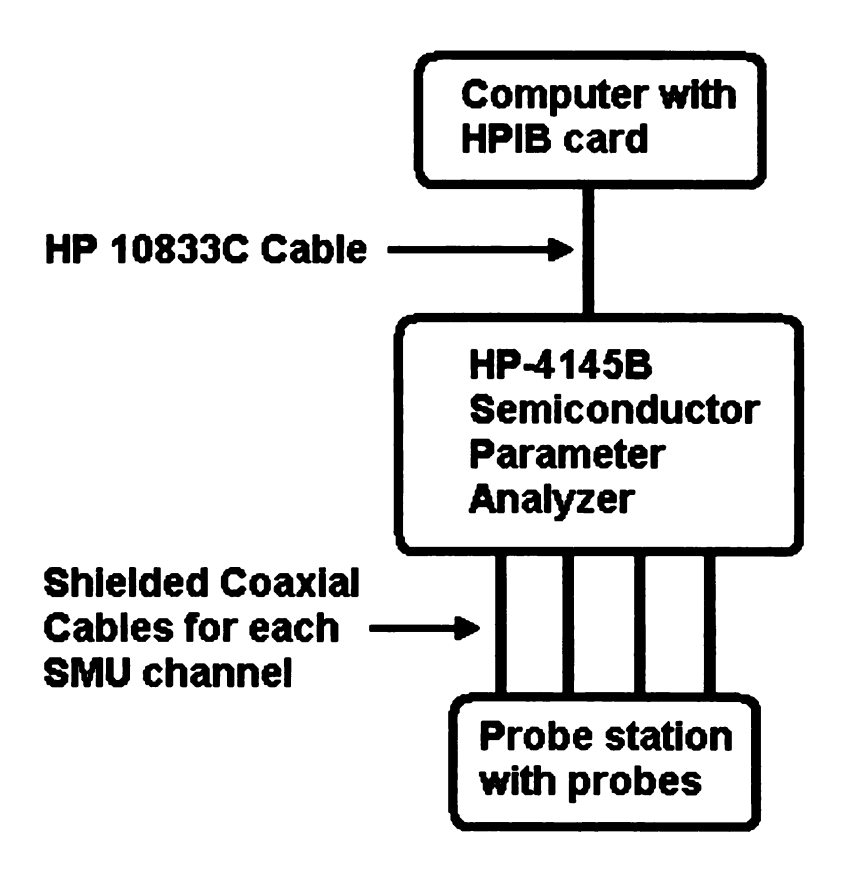


Figure 9. Block diagram of equipment setup

3.3.2 Probes and Probing Station

The wafer used to obtain I-V measurements was placed within a shielded probing station. The Signatone S-1160 High Frequency Probing System is a general-purpose analytical probe station designed for probing various geometries from 10 mils to 1 micron. It is equipped with a Signatone QuieTemp DC Hot Chuck System model S-1060. The system is capable of conducting measurements in a temperature range from room temperature to 300°C. However, for this study room temperature was used.

A set of four multipurpose, high speed, passive, model 10 GGB picoprobes are used with this probing station. The range of operation for those

specific picoprobes is dc to 3.5Ghz. Although only dc was used here, the probe construction is of advantage for low noise measurement. The probes used have shielded coaxial connections and gold plated tips. The whole system is shielded with a Signatone Light-Tight box model PSDB-1160 to protect the measurements from any noise signals (photoconductive) that may disturb the accuracy of the output measurements. Additionally, electromagnetic shielding was used. Figure 10 shows the probing station and Figure 11 shows a close-up of the probed wafer.

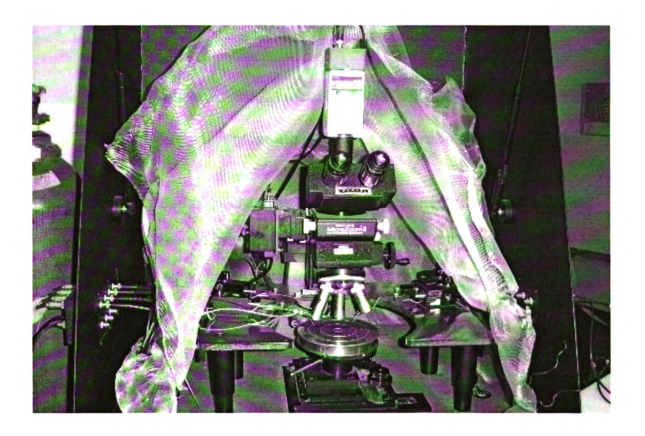


Figure 10. A picture of the probing station used for I-V measurements

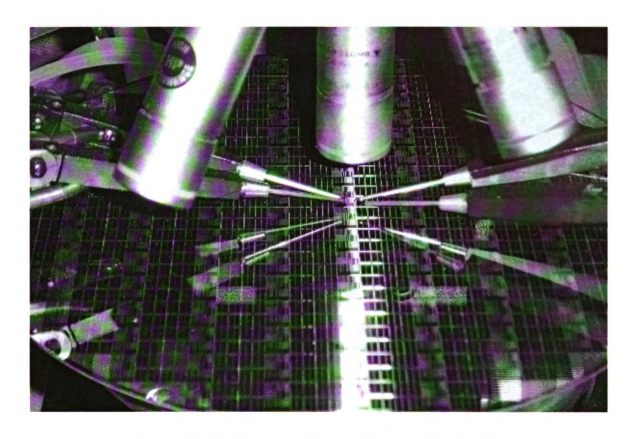


Figure 11. A close-up picture of the probed wafer

Furthermore shielded coaxial cables were used to connect each SMU channel from the probe station to the HP-4145B. The shielding from the probe to the HP-4145B helps in keeping the I-V data from being corrupted by other nearby equipment operating.

3.3.3 HP-4145B Semiconductor Parameter Analyzer

The HP-4145B Semiconductor Parameter Analyzer and later variations on this model, represent a popular piece of equipment used to obtain I-V data. It is equipped with four programmable Source/Monitor units (SMU's). Each SMU can be set up to function as a voltage source/monitor, current source/monitor, or



Figure 12. The HP-4145B Semiconductor Parameter Analyzer

common source (ground). A simplified circuit diagram of an SMU is illustrated in Figure 13.

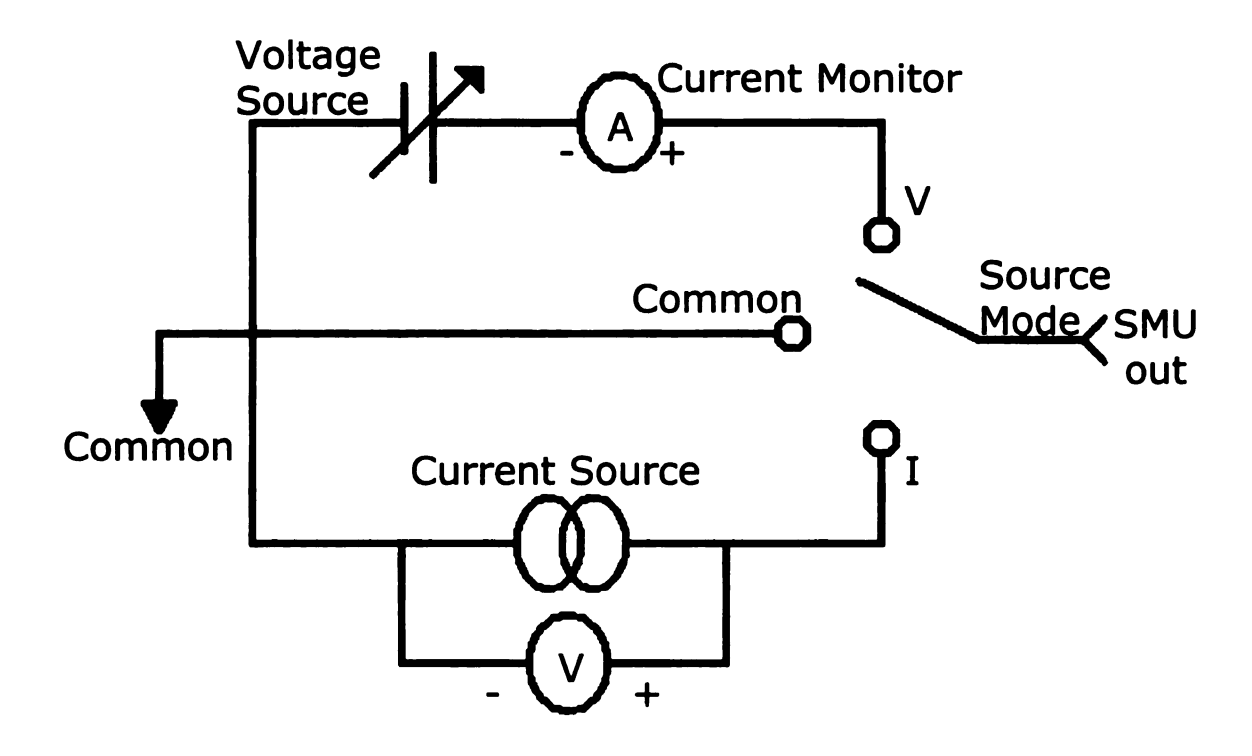


Figure 13. HP-4145B Source/Monitor Unit Simplified Circuit Diagram [7]

The particular model of the HP-4145B we were dealing with used its proprietary operating system that was not compatible with Windows/DOS.

Therefore data could not be simply transferred using a diskette. Also setting up the HP-4145B to take measurements is not very simple and takes a bit of time, since large amounts of data was needed. Thus to solve these two issues, a computer program using GWBASIC was created to setup and transfer measured data from the HP-4145B.

Another important thing to note about the HP-4145B is that it should be kept on for a good amount of time (+1 hour) before taking any measurements. It was noticed that when the HP-4145B was turned on and then repeated I-V measurements were made on a diode, the data was not consistent. When the

HP-4145B was left on overnight and then measurements were made that data was consistent in its repeatability.

3.3.4 HPIB Card and Program

The Hewlett Packard Interface Bus (HPIB) card is essentially used for communication with various instruments and particularly in this case to communicate with the HP-4145B. The HPIB card is what allows us to 'talk' and 'listen' to the HP-4145B using a computer. What is meant by 'talking' is the computer sends information to the HP-4145B, for example how to set up the equipment, how to display the measured data and when to begin to take measurements. 'Listening' primarily refers to the transferring of data from the HP-4145B to the computer. Details for how to exactly 'talk' and 'listen' to the HP-4145B are found in Appendix B.

The GWBASIC program running under DOS that was written to remotely control the HP-4145B was an essential part of the project to obtain large amounts of I-V data. The program itself is attached as Appendix A, as well as a detailed summary of the program used attached in Appendix B. The program was not completely perfected. It had certain issues that were not resolved due to time restrictions, but still was good enough for extracting the needed data.

One of the issues that could not be resolved was the 'random crashing' of the program. The program would stop at random times and about 1 out of every 10 measurements crashed. Sometimes it would crash when setting up the HP-4145B and other times when transferring the data from the HP-4145B to the

computer. Due to the crashing randomness and time constraints the problem was not looked into with great detail nor resolved. A computer with a better processor and more memory was used but showed no improvement. Even with this problem, using the program was much more efficient that not using it.

Another issue that existed was specifically for setting up the stepping function. It was found that the amount of steps per measurement could only be 30 or less. When a number of steps value larger than 30 was entered the HP-4145B would set the number of steps to 5. While this little annoyance was not resolved it was fine due to the fact the larger the number of data points the program needed to transfer, the more likely chance it would crash.

3.4 Data Manipulation

The drain current data required for the shift and ratio method as well as the modified shift and ratio method contains noise even with all the shielding used. Thus a 'running average' was used to 'average out' random noise in the data. This was done for each gate voltage by adding to its S-function value the S-function value of two voltage steps above and two voltage steps below that particular voltage and then dividing by five to obtain the averaged S-function value.

For the shift and ratio method the derivative is needed of the total resistance with respect to the drain voltage to obtain the S-function value for a particular gate voltage. The derivative for a particular voltage was obtained numerically by determining the slope of a line connecting a one data point above

and one below this particular point. Excel was used for all data manipulation, i.e. obtaining the running averages, the slopes, and the r values as a function of δ (see Section 2.3).

CHAPTER 4

SHIFT AND RATIO RESULTS

4.1 Introduction

Chapter 4 reviews the shift and ratio results obtained in this project.

Section 4.2 reviews the results for devices that do not contain halo implants.

Using the shift and ratio method as described in Taur's publication [3] we attempt to find the effective channel length of these particular devices given to us by IBM.

Section 4.3 describes the results obtained using both the shift and ratio method and the modified shift and ratio method on devices containing halo implants.

4.2 Non-Halo Devices

Once all the necessary I-V data needed is obtained as described in Section 3.2 the data was placed into an Excel file. The r values and the S-functions for both long and short channel devices are calculated for each gate

Table 1. Excerpt of I-V data used when applying the shift and ratio method

		L = .21	L = 8.4	L = .21	L = 8.4	L = .21	L = 8.4
Vd	Vg	ld	ld	Rd	Rd	Sfunc	Sfunc
0.05	0.80	2.86E-05	6.90E-07	1.75E+03	7.25E+04	1.67E+04	7.28E+05
0.05	0.81	3.14E-05	7.60E-07	1.59E+03	6.58E+04	1.43E+04	6.17E+05
0.05	0.82	3.42E-05	8.31E-07	1.46E+03	6.02E+04	1.25E+04	5.30E+05
0.05	0.83	3.72E-05	9.05E-07	1.34E+03	5.52E+04	1.08E+04	4.64E+05
0.05	0.84	4.02E-05	9.83E-07	1.24E+03	5.09E+04	9.54E+03	4.16E+05
0.05	0.85	4.34E-05	1.07E-06	1.15E+03	4.69E+04	8.51E+03	3.69E+05
0.05	0.86	4.65E-05	1.15E-06	1.07E+03	4.35E+04	7.42E+03	3.18E+05

voltage as described in Section 2.3 and as illustrated in Table 1. Once all the S-functions are calculated, they are plotted as can be seen in Figure 14 below. For specific information on the methods used to calculate the S-function as well as the ratio r for different δ shifts refer to Appendix D.

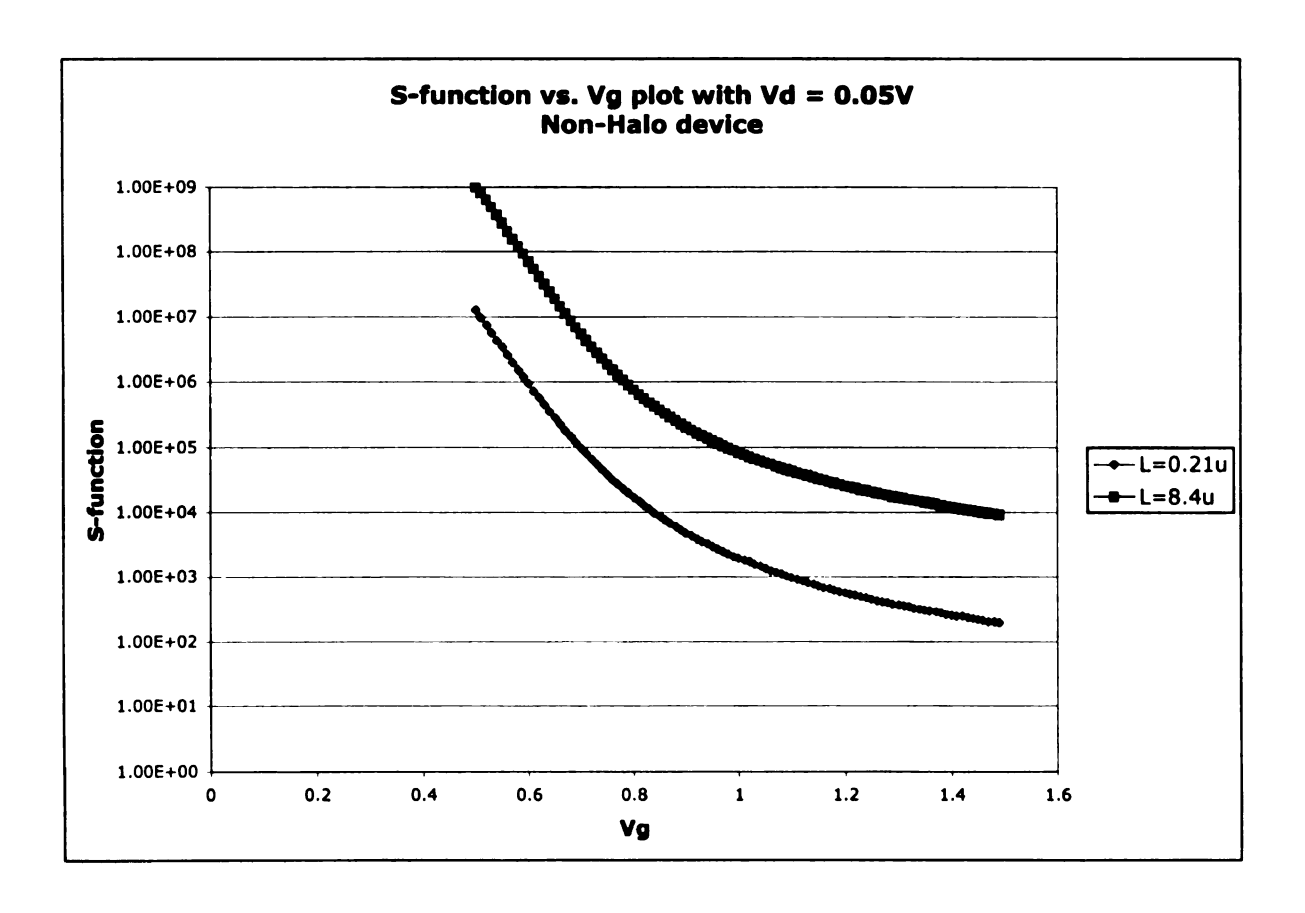


Figure 14. Semi-log plot of S-function vs. Vg with Vd = 0.05V

The short channel device S-function data S^i is then shifted by δ values. Next the ratio between the S-function of the long channel device S^0 over the S-function of the short channel device for different δ shifts in the short channel device is calculated and plotted. For example, to shift V_t for the smaller device, V_t^i , by -0.01 volts relative to the large device, such that

$$\delta = V_t^0 - V_t^i = 0.01 \text{ volts} \tag{13}$$

we plot using Excel $S^0(N)$ and $S^i(N-1)$ vs. $V_g(N)$. For each shift of ' Δ ' rows, the ratio of S-functions,

$$r = \frac{S^0(N)}{S^i(N+\Delta)} \tag{14}$$

is calculated and plotted. Detailed discussion of the spreadsheet manipulation is in Appendix D. The results can be observed in Figure 15.

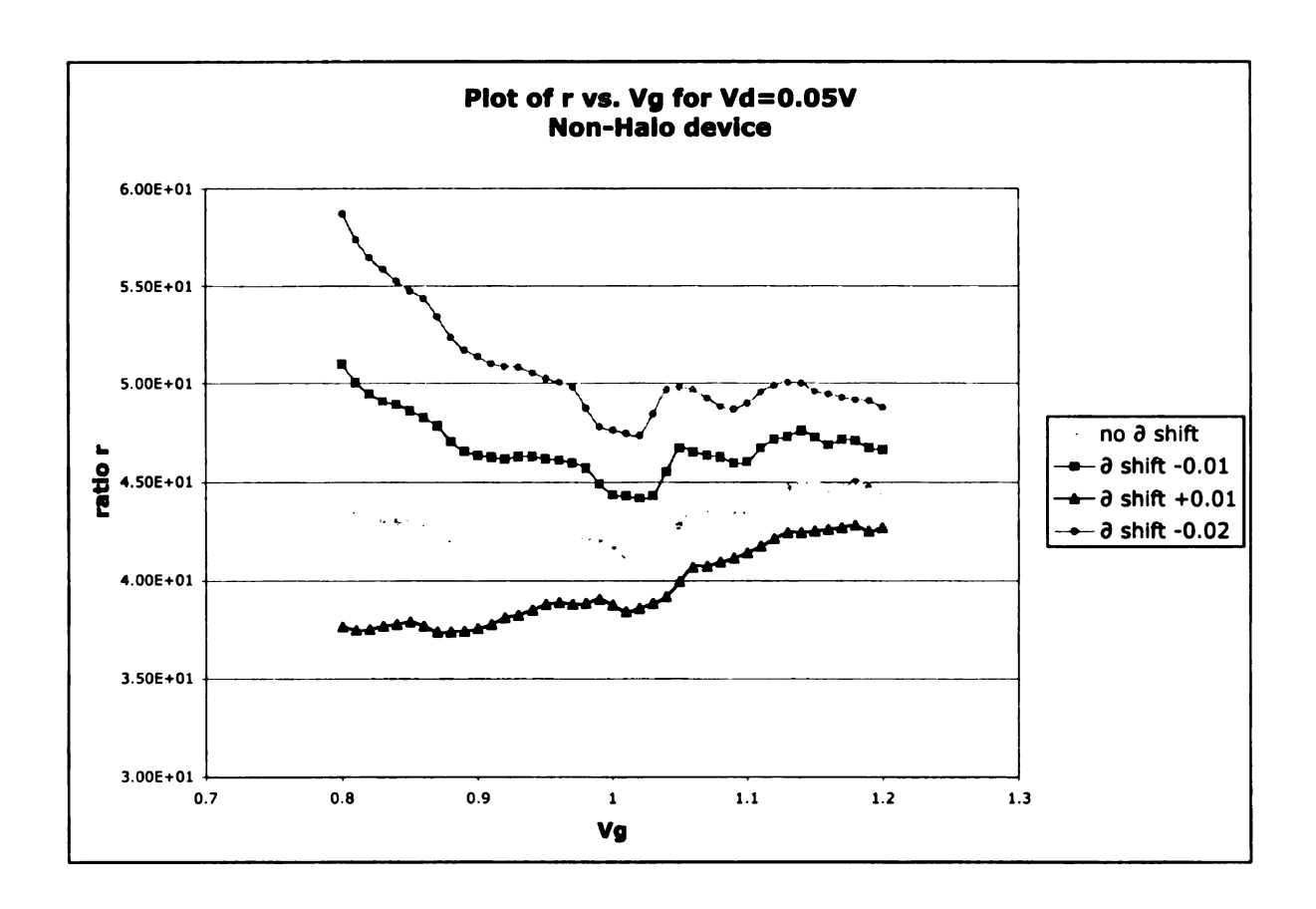


Figure 15. Ratio plot for various & 'shift' values

The ratio plotted in Figure 15 shows a positive slope for a δ shift of +0.01V, a primarily positive slope for no shift, and a primarily negative slope for a δ shift of -0.01V. The data shows more experimental variation then would be ideally desired. However, it was estimated from this data that a δ shift of -0.005V gives the closest to zero slope, and that the ratio value for this shift is approximately 45. Since a ratio 'r' value of 45 does not equal the geometric mask ratio of 40, the shift and ratio method indicates a non-zero Δ L. The calculations are as follows.

$$L_{mask}^i = 0.21 \mu m$$

$$L_{mask}^{0} = 8.4 \mu m$$

 $r \approx 45$ which is obtained from Figure 15

Using these values along with equation 7 we can calculate a ΔL value using the shift and ratio method a described in Section 2.3.

$$45 \cdot (0.21\mu m - \Delta L) = (8.4\mu m - \Delta L) \Rightarrow 44 \cdot \Delta L = 45 \cdot 0.21\mu m - 8.4\mu m \Rightarrow \Delta L = 0.0255\mu m = 25.5nm$$
(15)

The ΔL value obtained is a reasonable result. In comparison, Taur obtained a value of about 60nm [3]. A difference is not unexpected since the devices used by Taur had a traditional source and drain, while the devices used in this project are devices with lightly doped drains (LDDs). This is known to cause variations when solving for ΔL using the shift and ratio method [3].

4.3 Halo Devices

After the data for devices containing the halo implants was obtained, the data was placed into an Excel file and its manipulated as described in Section 3.4 as well as Appendix D. First the S-functions for the devices with gate length $L = 0.21 \mu m$ and $L = 8.4 \mu m$ are plotted, as can be seen in Figure 16 below.

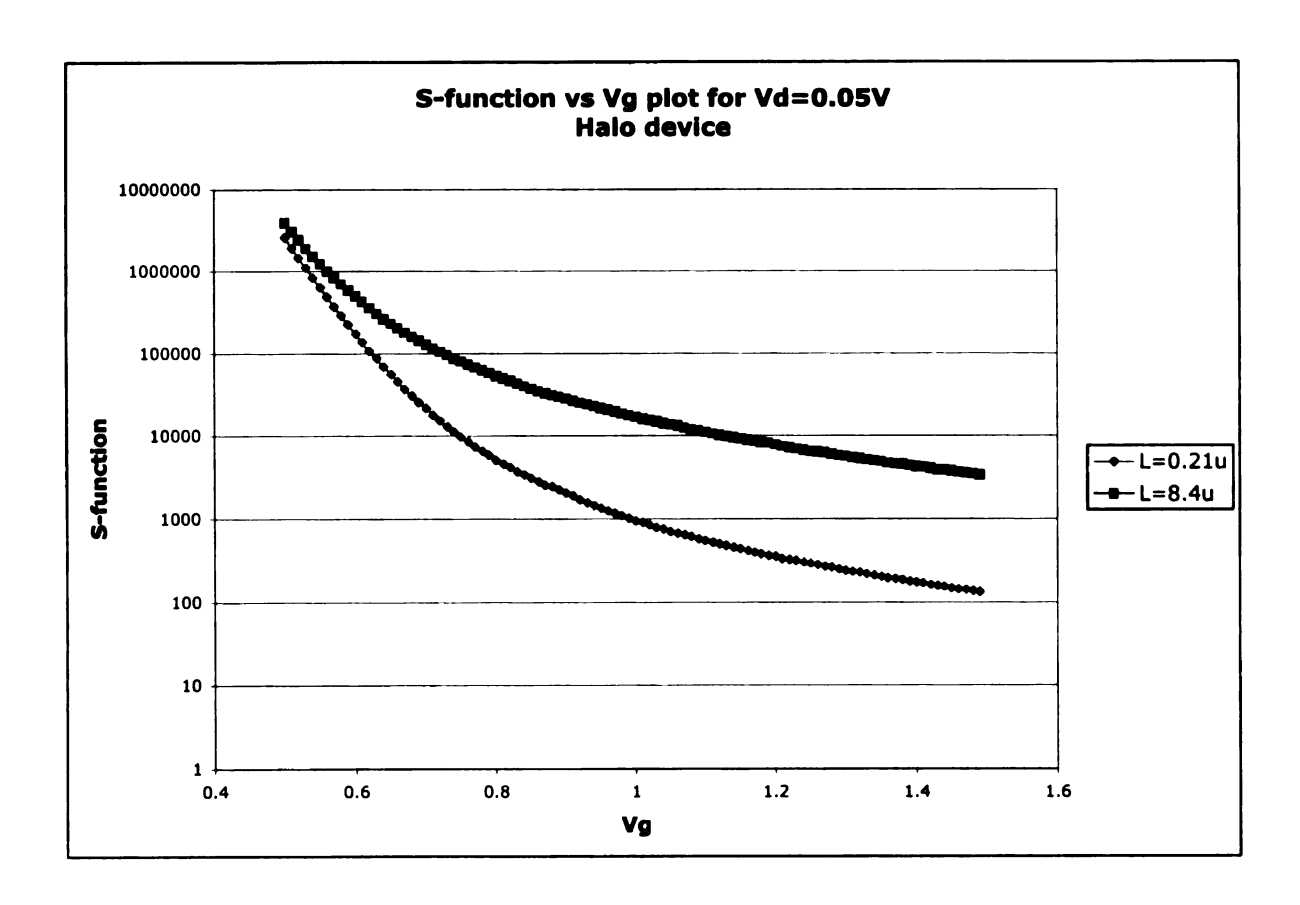


Figure 16. Semi-log plot of S-function vs. Vg with Vd=0.05V

The short channel device S-function data is then shifted to the left in order to find δ as described in Section 2.4. Figure 17 shows the plot of $r(\delta,V_g)$ vs. V_g for different δ values.

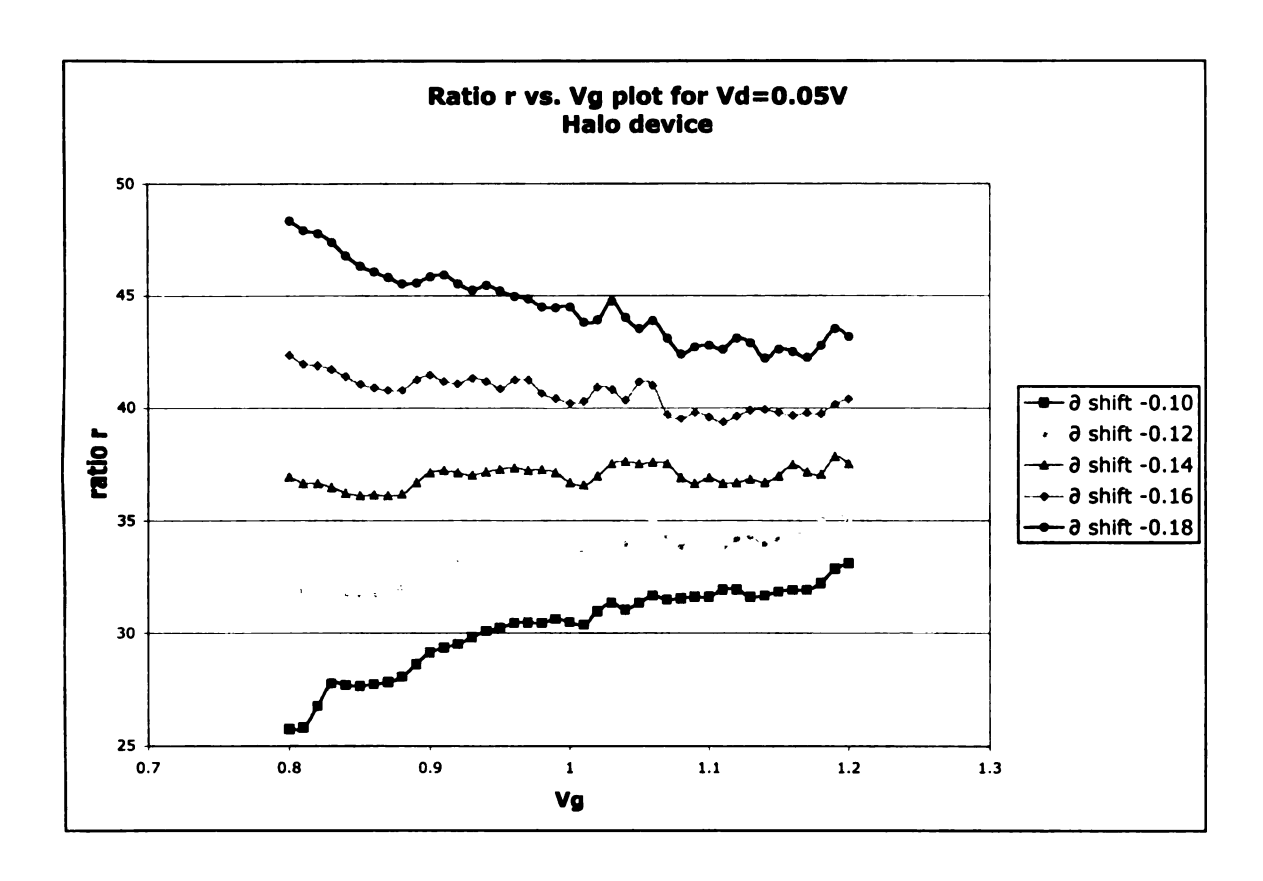


Figure 17. Ratio plot for various δ 'shift' values

The ratio plotted in Figure 17 shows a positive slope for a δ of -0.12 and a primary negative slope for a shift of -0.16. From the plotted data it was estimated that a δ of -0.14 gives the closest to zero slope, and that the ratio value for this shift is approximately 37. Since a ratio 'r' value of 37 does not equal the geometric mask ratio of 40, the shift and ratio method once again indicates a non-zero ΔL . Using the above information, we apply the shift and ratio method on these devices containing halo implants. Using equation 7 as well as the following values listed below a ΔL value is calculated.

$$L_{mask}^{i} = 0.21 \mu m$$

$$L_{mask}^0 = 8.4 \mu m$$

 $r \approx 37$ which is obtained from Figure 17

$$37 \cdot (0.21\mu m - \Delta L) = (8.4\mu m - \Delta L) \Rightarrow$$

$$36 \cdot \Delta L = 37 \cdot 0.21\mu m - 8.4\mu m \Rightarrow \Delta L = -0.0175\mu m = -17.5nm$$
(16)

The negative ΔL value that is obtained appears unphysical, however it actually agrees with van Meer's publication [1] on the issues that exist when applying the shift and ratio method on devices containing halo implants. A negative ΔL from the shift and ratio is a motivation for the modified shift and ratio method.

In order to apply the modified shift and ratio method a second short channel device is required. The S-functions for the devices with gate length L = $0.42\mu m$ and L = $8.4\mu m$ are similarly plotted, as can be seen in Figure 18 below.

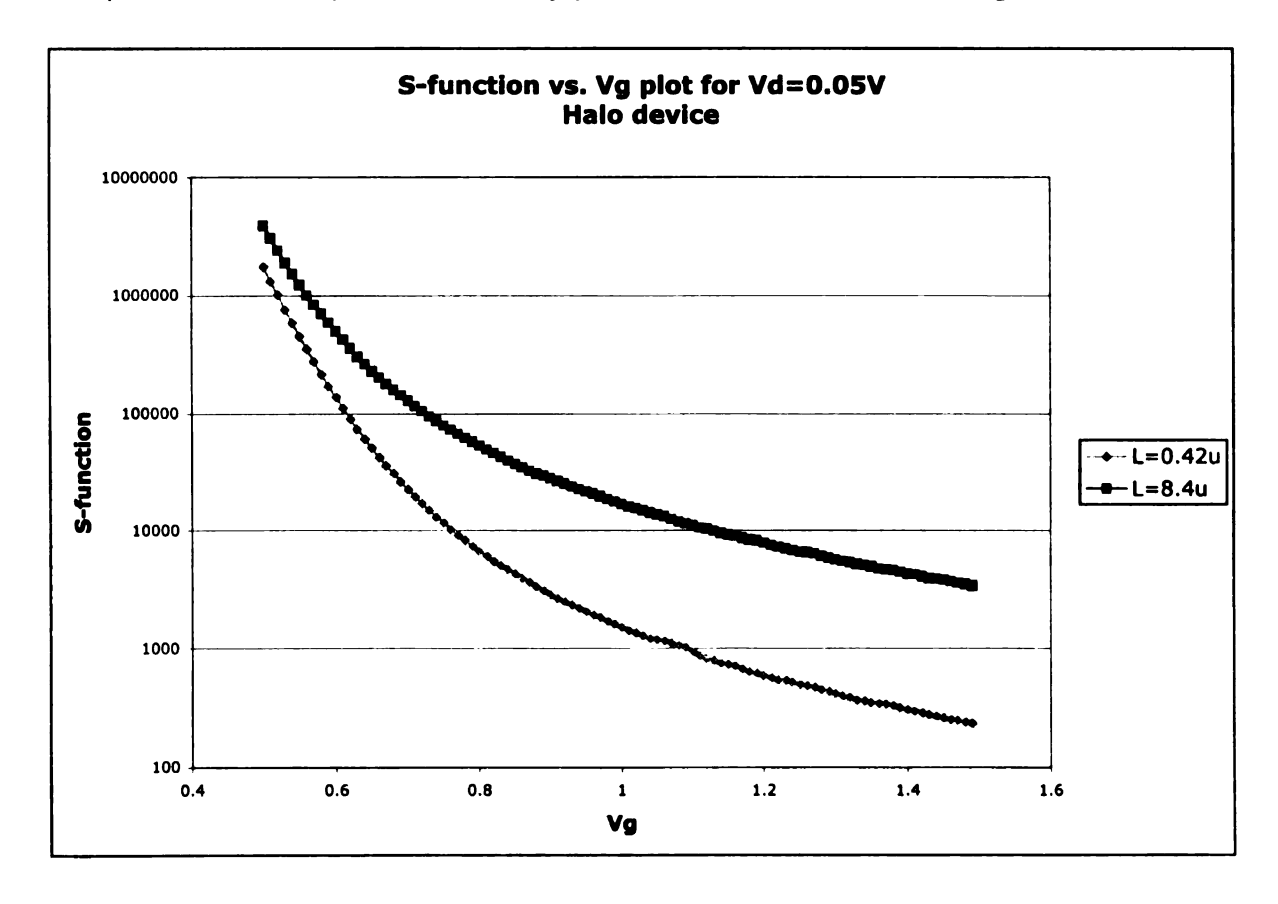


Figure 18. Semi-log plot of S-function vs. Vg with Vd = 0.05V

The short channel device S-function data is then shifted to the left in order to find δ as described in Section 2.4. Figure 19 shows the plot of $r(\delta, V_g)$ vs. V_g for different δ values.

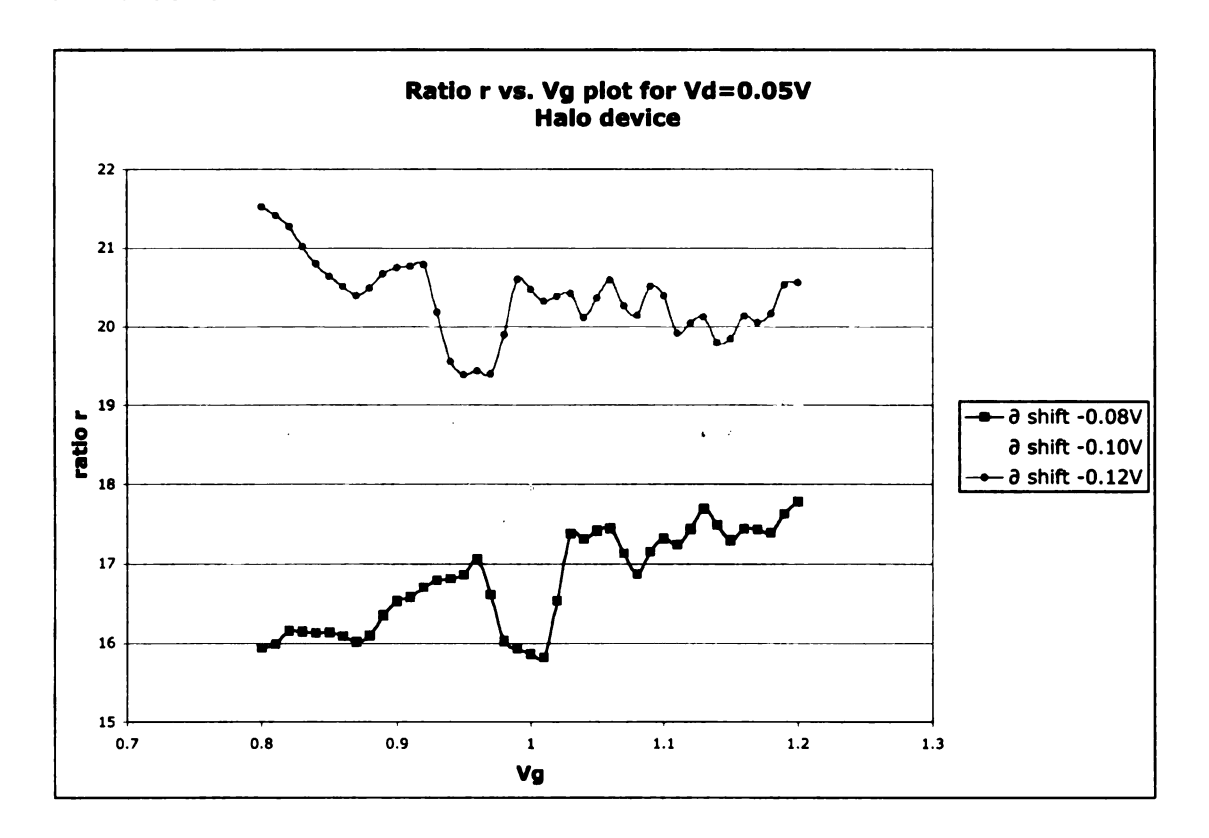


Figure 19. Ratio plot for various δ 'shift' values

The ratio plotted in Figure 19 shows a primarily positive slope for a δ of -0.08 and a primarily negative slope for a shift of -0.12. From the plotted data it was estimated that a δ of -0.10 gives the closest to zero slope, and that the ratio value for this shift is approximately 18.5. Since a ratio r value of 18.5 does not equal the geometric mask ratio of 20, the shift and ratio method again indicates a non-zero ΔL . Using the above information, we apply the shift and ratio method on this other pair of devices containing halo implants. Using equation 7 as well

as the following values listed below a ΔL value is calculated.

$$L_{mask}^{j} = 0.42 \mu m$$

$$L_{mask}^{0} = 8.4 \mu m$$

 $r \approx 18.5$ which is obtained from Figure 19

$$18.5 \cdot (0.42\mu m - \Delta L) = (8.4\mu m - \Delta L) \Rightarrow 17.5 \cdot \Delta L = 18.5 \cdot 0.42\mu m - 8.4\mu m \Rightarrow \Delta L = -0.036\mu m = -36nm$$
(17)

This negative ΔL value that is obtain once again agrees with van Meer's publication [1] on the issues that exist when applying the shift and ratio method on devices containing halo implants.

Observing that the application of the shift and ratio method to the two short channel devices along with the long channel device results in unphysical results, the modified shift and ratio method is now applied.

For 0.21µm and 8.4µm channel length devices:

$$L_{mask}^{i} = 0.21 \mu m$$

$$L_{mask}^0 = 8.4 \mu m$$

 $r \approx 37$ this value is obtained from Figure 17

For 0.42µm and 8.4µm channel length devices:

$$L_{mask}^{j} = 0.42 \mu m$$

$$L_{mask}^{0} = 8.4 \mu m$$

 $r \approx 18.5$ this value is obtained from Figure 19

Using these values as well as equations 11 and 12, we obtain two equations and two unknowns:

$$37 = C \cdot \frac{(8.4\,\mu m - \Delta L)}{(0.21\,\mu m - \Delta L)} \tag{18}$$

$$18.5 = C \cdot \frac{(8.4 \,\mu m - \Delta L)}{(.42 \,\mu m - \Delta L)} \tag{19}$$

Dividing equation 18 by 19 reduces the two equations with two unknowns to a single equation that now can be solved for ΔL .

$$2.0 = \frac{(0.42\mu m - \Delta L)}{(0.21\mu m - \Delta L)} \Rightarrow \Delta L = 0 \tag{20}$$

With a $\Delta L = 0$, C can now be solved for and yields: C = 0.925. The results are consistent with the initial hypothesis of the long and short channel length devices having a different effective mobility. The results indicate that the modified shift and ratio method does offer the potential to resolve the issue that existed of obtaining negative ΔL values when applying the standard shift and ratio method.

A detailed error analysis of the experimental results has not been performed. However, examination of Figures 17 and 19 indicate an approximate uncertainty in ratio r values of $\pm 2\%$. With this uncertainty one could conservatively consider that our r values could range from 36 to 38 for the L = 0.21mm device and from 18 to 19 for the L = 0.42mm device. Using equations 18 and 19 we find the resulting ΔL can range from -25nm to +21nm. Note that the small amount of error in the ratio r value can produce significant variation in ΔL results. A larger amount of measurements can be taken and averaged to reduce the amount of uncertainty that exists.

CHAPTER 5

SPICE MODELING

5.1 Introduction

The SPICE modeling portion of this work is of a preliminary nature. In this investigation, the process of creating a device model began with a low level SPICE model, level 2, due to its relative simplicity when compared to higher-level models. Level 2 models do not include enough parameters to take into account various effects for short channel devices, however they can produce a useful basis for more advanced models. Section 5.2 discusses our attempts to create level 2 models for the non-halo devices, and the issues that prevent us from creating a reasonable model for the short channel devices at this model level. Furthermore, some key parameters for the halo devices are also extracted and discussed. Section 5.3 explains the need of a higher-level model to properly design a model for the non-halo and halo devices.

5.2 Level 2 Models of Non-Halo Devices

In level 2, the DC I-V characteristics are primarily modeled by the equation shown below [8].

$$I_{ds} = \mu \cdot \frac{\varepsilon_{ox}}{t_{ox}} \left(\frac{W}{L_{eff}} \right) \left(\frac{1}{1 - \sigma \cdot V_{ds}} \right) \begin{cases} \left[V_{gs} - V_{FB} - 2 \cdot |\phi_F| - \frac{V_{ds}}{2} \right] \cdot V_{ds} \\ -\frac{2}{3} \cdot \chi \left[V_{ds} - V_{bs} + 2 \cdot |\phi_F| \right] \frac{3}{2} - (V_{bs}) + 2 \cdot |\phi_F| \frac{3}{2} \end{cases}$$
(21)

In this expression,

$$|\phi_F| = \frac{kT}{q} \ln \left(\frac{N_A}{n_i} \right), \tag{22}$$

$$\chi = \frac{\sqrt{2 \cdot \varepsilon_S \cdot q \cdot N_A}}{\varepsilon_{OX}} \cdot t_{OX}, \qquad (23)$$

and σ accounts for channel length modulation. Thus, for a given semiconductor and temperature, one provides geometric information (W, L, t_{ox}) and processing parameters (N_A, V_{FB} or V_t).

In order to extract parameters to create a level 2 SPICE model for the non-halo devices we first obtain I-V measurement data. The data is obtained using the 2-terminal measurement setup described in Section 3.2 and seen in Figure 5. First for the long channel length device we plot the square root of the drain current (I_d) vs. its respective gate/drain voltage (V_d = V_g). The results are plotted in Figure 20. A straight line along the curve is then drawn to approximately find where the line intersects the V_d = V_g axis. For the long channel non-halo device, the line intersects at approximately 0.6775 volts; this value is defined as the threshold voltage for this particular device.

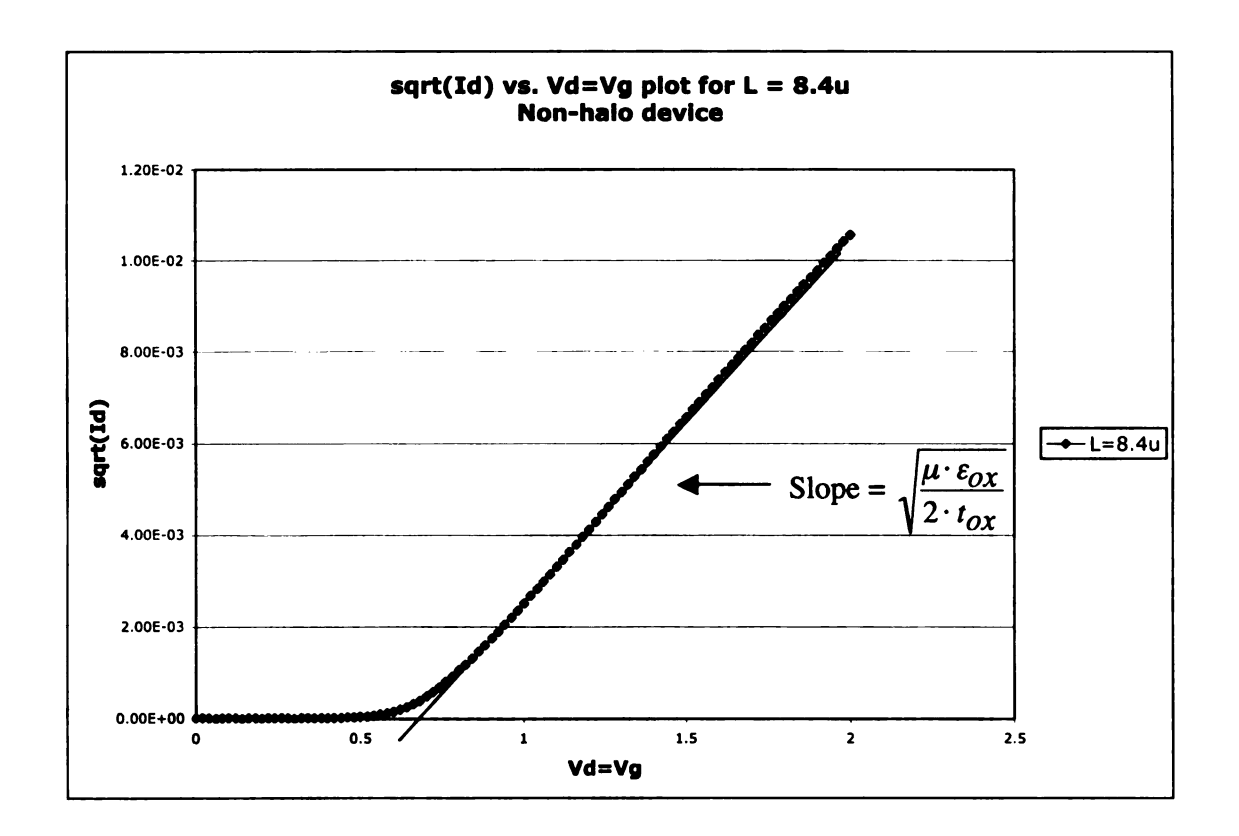


Figure 20. Id vs. Vd = Vg for non-halo device, L = 8.4μm

The slope of this line used to find the threshold voltage is also used to determine μ / t_{ox} , as seen from the SPICE level 1 equation,

$$I_{d} = \frac{1}{2} \frac{W}{L} \frac{\varepsilon_{ox}}{t_{ox}} \mu \left(V_{gs} - V_{t} \right)^{2} \Rightarrow \frac{\Delta \sqrt{I_{d}}}{\Delta V_{gs}} = \sqrt{\frac{\mu \cdot \varepsilon_{ox}}{2 \cdot t_{ox}}}$$
 (24)

We were informed by IBM that the non-halo devices were thick oxide devices with $t_{\rm OX}$ = 5.8nm. This allowed us to calculate the effective mobility, μ , using the above equation to obtain the following result:

$$\sqrt{\frac{\mu \cdot \varepsilon_{ox}}{2 \cdot t_{ox}}} = 8.09 \times 10^{-3} \Rightarrow \mu = 221 cm^2 / V \cdot s \tag{25}$$

In level 2, the NFS parameter is used to model sub-threshold current.

Changes were made to this parameter until the SPICE model and actual data agreed. A value of $3.7 \times 10^{12} \text{ cm}^{-2}$ was chosen for NFS. The channel mobility is smaller than the bulk material because of increased scattering at the Si/SiO₂ interface and is approximately half the bulk mobility [9]. Thus using this mobility value, if taken to be half the bulk mobility, would indicate a substrate doping of approximately $4 \times 10^{17} \text{ cm}^{-2}$.

However, modeling results show that this value was too high, and changes were made to this parameter until the simulation data matched the experimental data. A final NSUB value of 2 x $10^{16} cm^{-3}$ was chosen. In actuality, the device is formed in an n-type well, with a higher concentration near the surface (which determines μ) and a lower concentration at depth (which effects Φ_F). Using all the parameters described above, the final SPICE model used was:

PSPICE NFTK MOSFET L = 8.4

VS1 1 0 2

M1 1 1 0 0 N84

.DC VS1 0.02 2 .02

.MODEL N84 NMOS(LEVEL=2 L=8.4u W=8.4u VTO=0.6775 UO=221

+TOX=5.8n NFS=3.7e12 NSUB=2e16)

.PRINT DC ID(M1)

.PROBE

.END

The results of the model compared to the actual 2 terminal I-V data are shown in

Figure 21 (linear scale) and Figure 22 (semi-logarithmic scale). Excellent agreement is observed for both low and high currents.

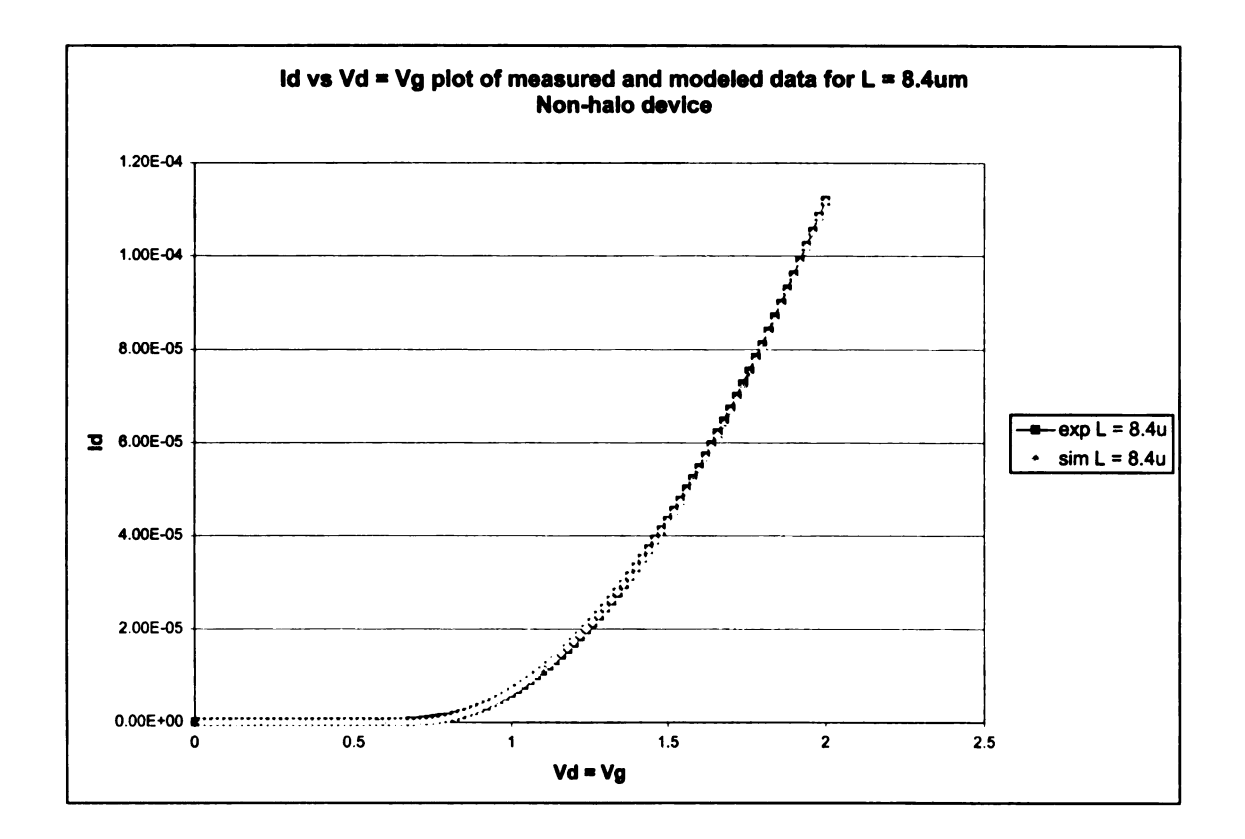


Figure 21. Simulated and measured data using Figure 5 setup (Linear Scale)

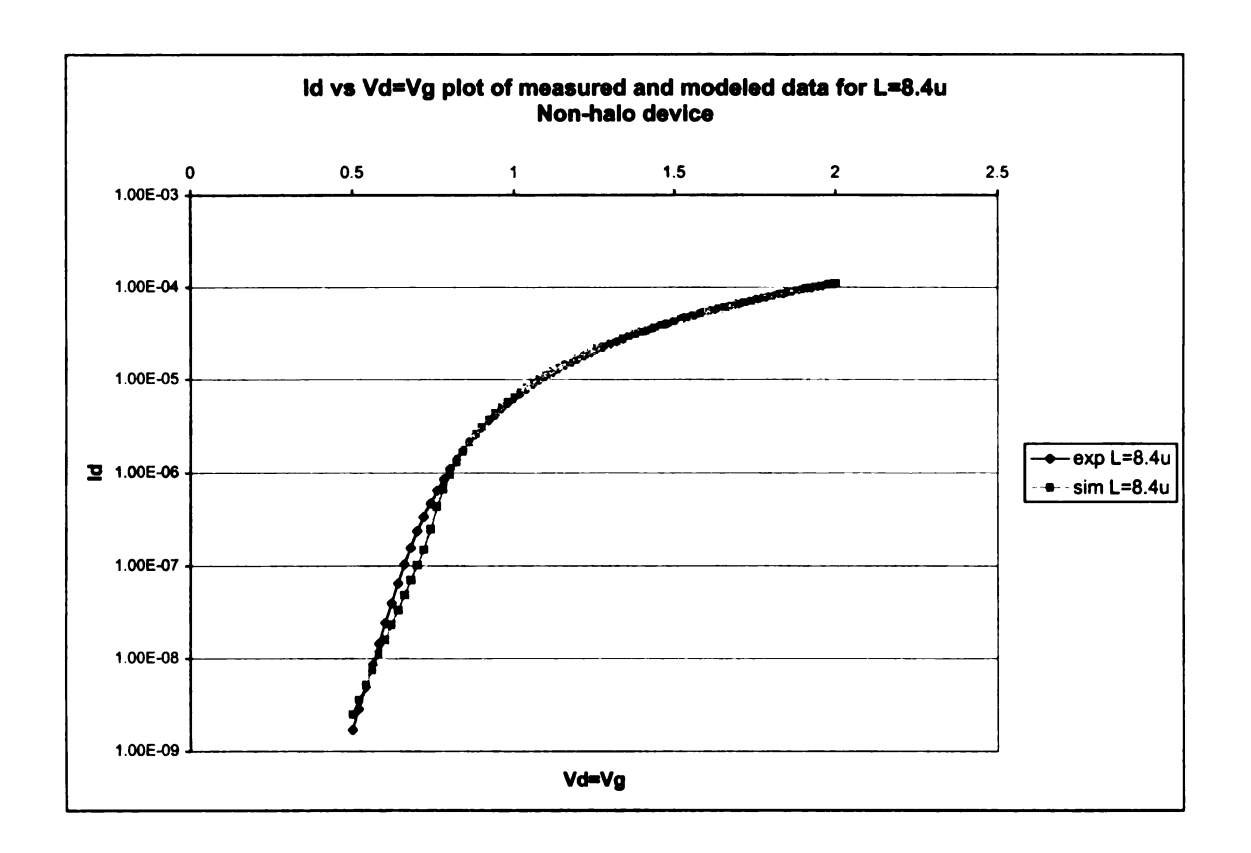


Figure 22. Simulated and measured data using Figure 5 setup (Semi-log Scale)

Family of curve measurements and modeling were also made using the 3-terminal setup described in section 3.2 and seen in Figure 7. A SPICE model was created using the same parameters used for the previous model.

PSPICE NFTK MOSFET L = 8.4

VS1 1 0 2

VS2 2 0 2

M1 1 2 0 0 N84

.DC VS1 0.02 2 .02

.STEP VS2 0.5V 2V .5V

.MODEL N84A NMOS(LEVEL=2 L=8.4u W=8.4u VTO=0.6775 UO=221

+TOX=5.8n NFS=3.7e12 NSUB=2e16)

.PRINT DC ID(M1)

.PROBE

.END

For the family of curves configuration, where $V_g \neq V_d$, the simulation data from the SPICE model does not match the measured data as well as when V_g is constrained to equal V_d in the two terminal case. The modeling vs. experimental result is shown in the Figure 23.

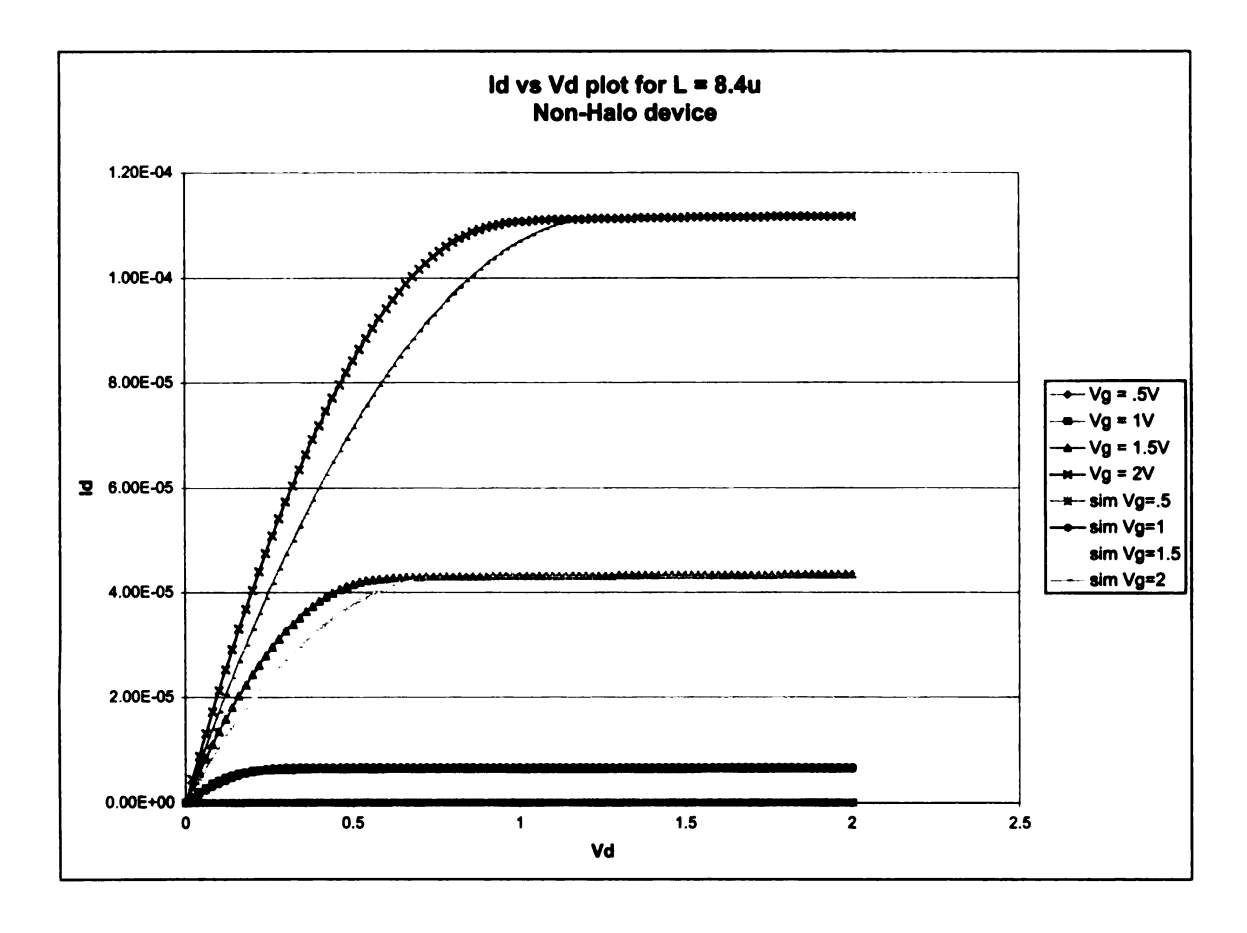


Figure 23. Simulated and measured data using Figure 7 setup

Here, one sees that the simulation and experimental agree well in saturation, where $(V_g - V_d) < V_t$. However, in the linear region where $(V_g - V_d) > V_t$, the simulation produces a smaller current than actually measured.

We then similarly extracted the threshold voltage of the short channel length device to create a SPICE model of this device. Using the same technique described above, a threshold voltage, V_t = 0.593 V is obtained. Note that the difference in extrapolated threshold voltages is about 0.1 volts, and recall that the δ shift found for the non-halo devices was only 0.005 volts in Section 4.2. In principal, one would expect to find the same result from both methods for finding δ , as for example observed by Taur. The difference may again be due to the fact that different

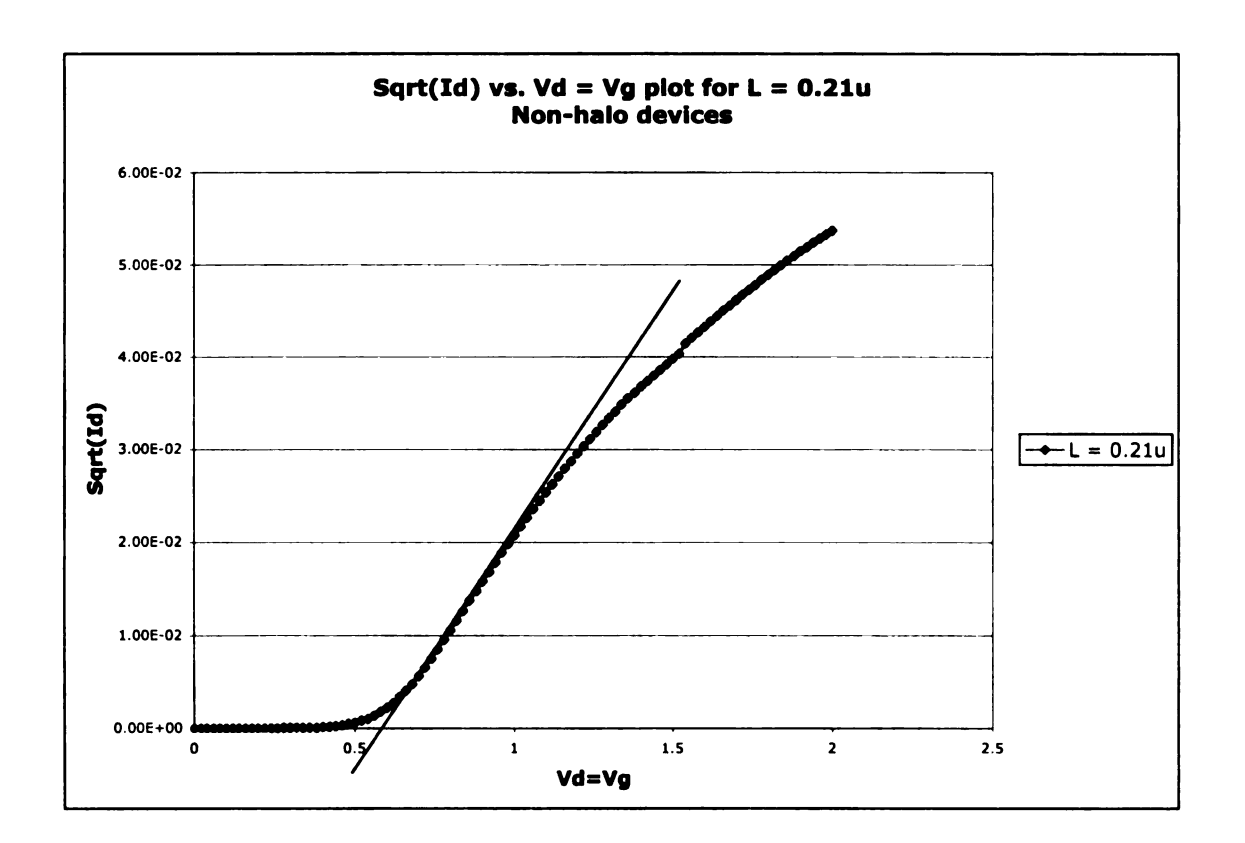


Figure 24. Id vs. Vd = Vg for non-halo device, $L = 0.21 \mu m$

devices were used in comparison to Taur's. The devices we used had lightly doped drains (LDDs), which is known to create issues for the extraction of the effective channel length of devices [3]. One may also observe drain-to-source electric field dependent mobility in Figure 24, at higher drain voltages.

Using these values another SPICE model was created for the short channel device.

PSPICE NFTK MOSFET L = .21

VS1 1 0 2

M1 1 1 0 0 N21

.DC VS1 .02 2 .02

.MODEL N21 NMOS(LEVEL=2 L=.21u W=8.4u VTO=0.593 UO=221

+TOX=5.8n NFS=3.7e12 NSUB=2e16)

.PROBE

.PRINT DC ID(M1)

.END

As might be anticipated, this SPICE model did not correlate well at all with the measured short channel data. The ΔL value was then taken into account, but not much of an improvement at all was noticed. The comparison of the simulation data with the actual data is plotted below in Figure 25 with a linear scale.

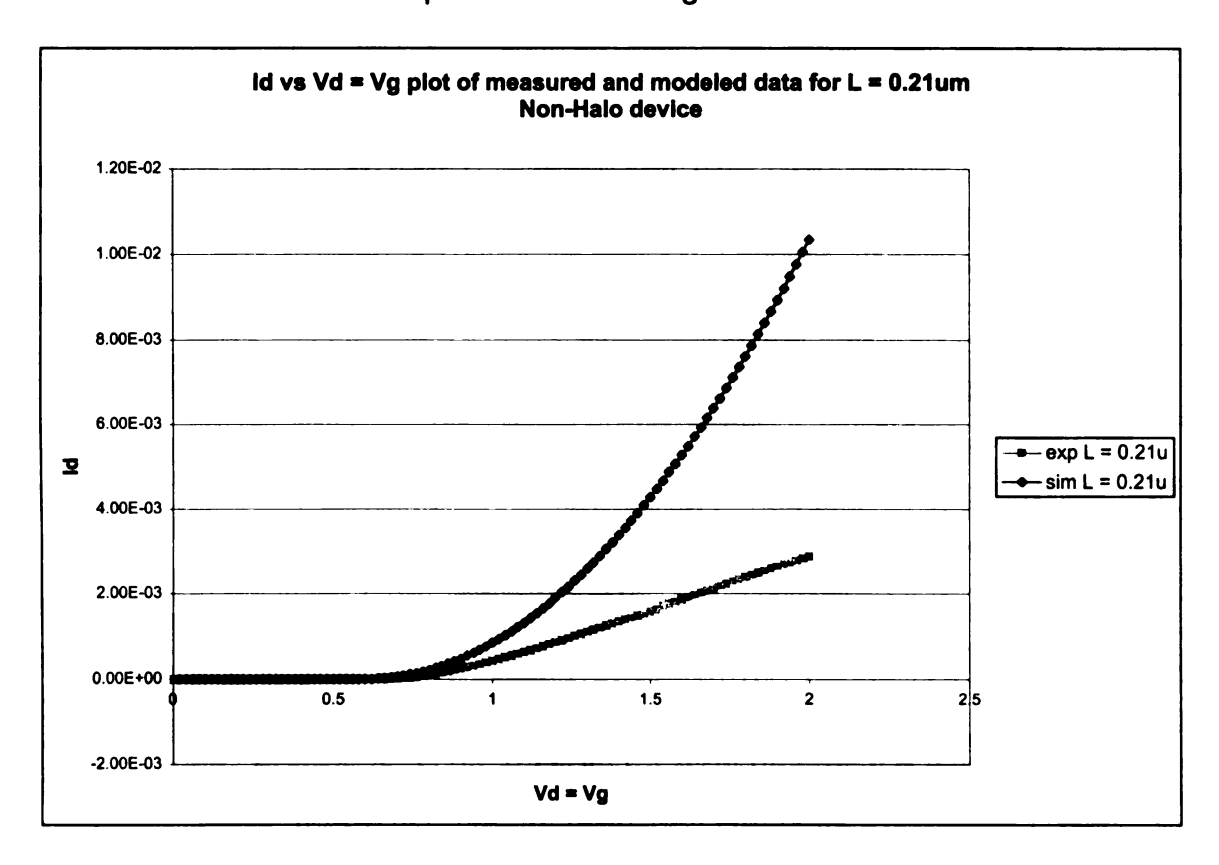


Figure 25. Simulated and measured data using Figure 5 setup

Many short channel length attributes cannot be modeled properly with low-level

SPICE models and the results show that higher-level models would be necessary to accurately model these devices.

Although SPICE modeling was not performed with the halo devices, the measured data to be compared against simulation is presented here. The threshold voltages for all three of the halo devices were extracted as described previously in this section. Figure 26 shows the square root of the drain current vs. gate voltage for the long channel device.

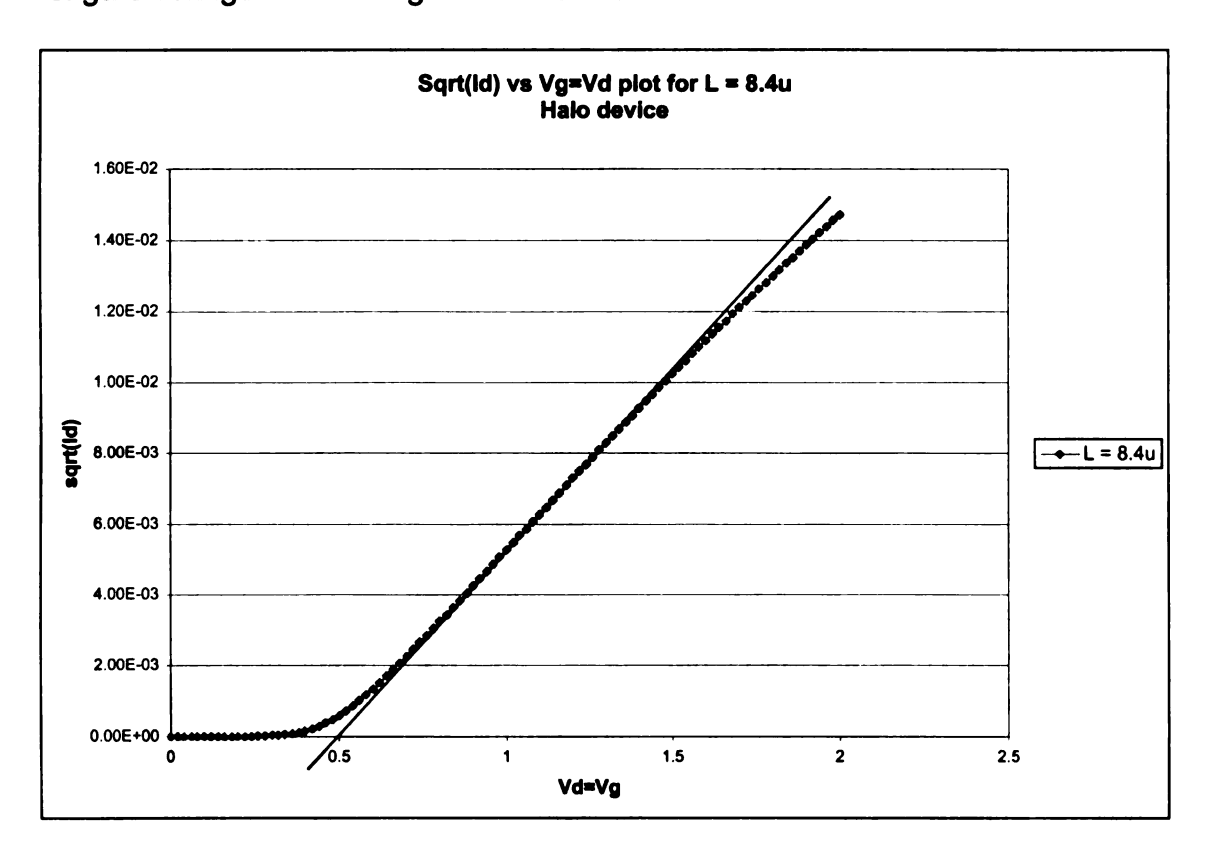


Figure 26. I_d vs. $V_d = V_g$ for halo device, $L = 8.4 \mu m$

A threshold voltage of, V_t = 0.5 V is extracted from the Figure 26. This value along with the threshold voltage of both of the short channel devices allows us to analyze the δ shift value we obtained by performing the modified shift and

ratio method. Figure 27 plots the drain current vs. the gate and drain voltage for the device with $L=0.42\mu m$.

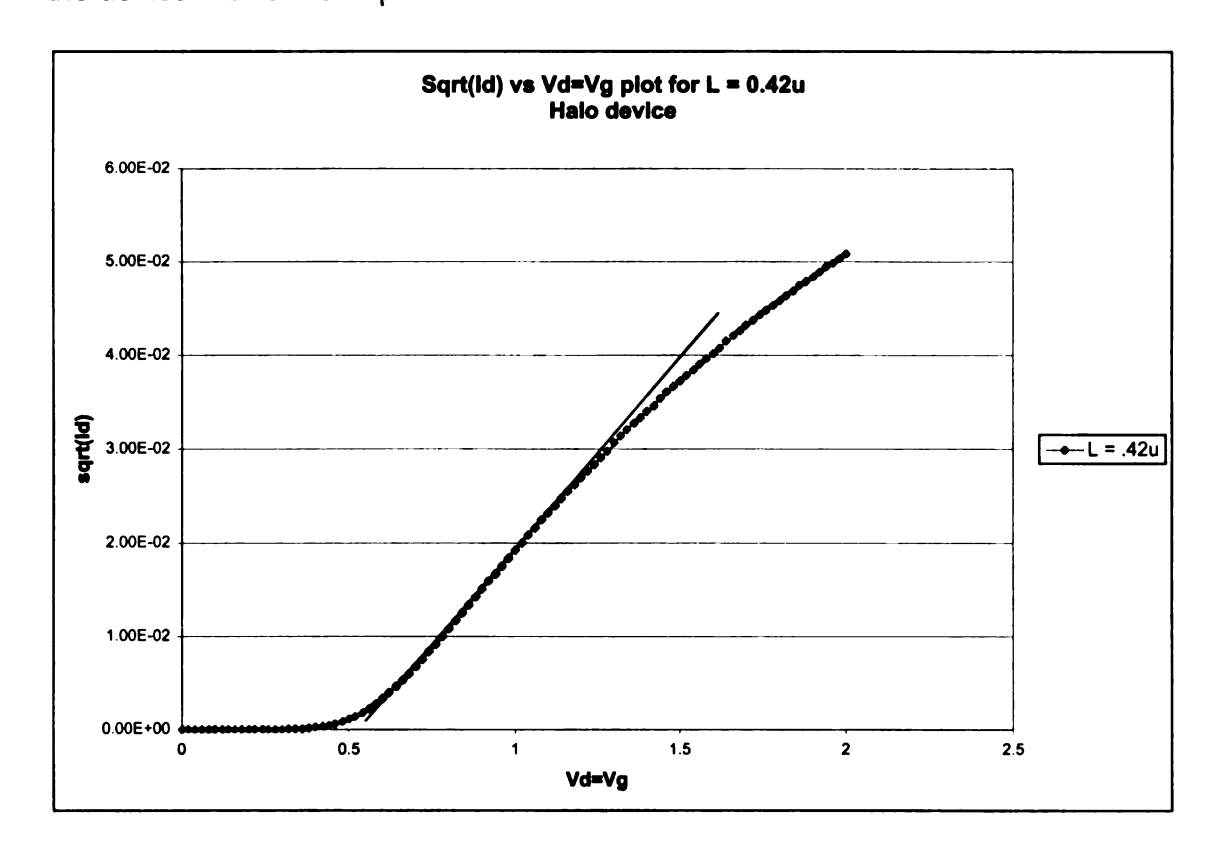


Figure 27. I_d vs. $V_d = V_g$ for halo device, $L = 0.42 \mu m$

A threshold voltage of 0.54 V was extracted from Figure 27, which would indicate $V_t^0 - V_t^i = -0.04$ V. However, the δ needed to find a constant ratio r value was of -0.1 V which, as was the case for the non-halo devices, different than the plot extraction using the shift and ratio method.

Similarly for the short channel device with L = $0.21\mu m$, a threshold voltage value of V_t = 0.58 V was extracted from the Figure 28.

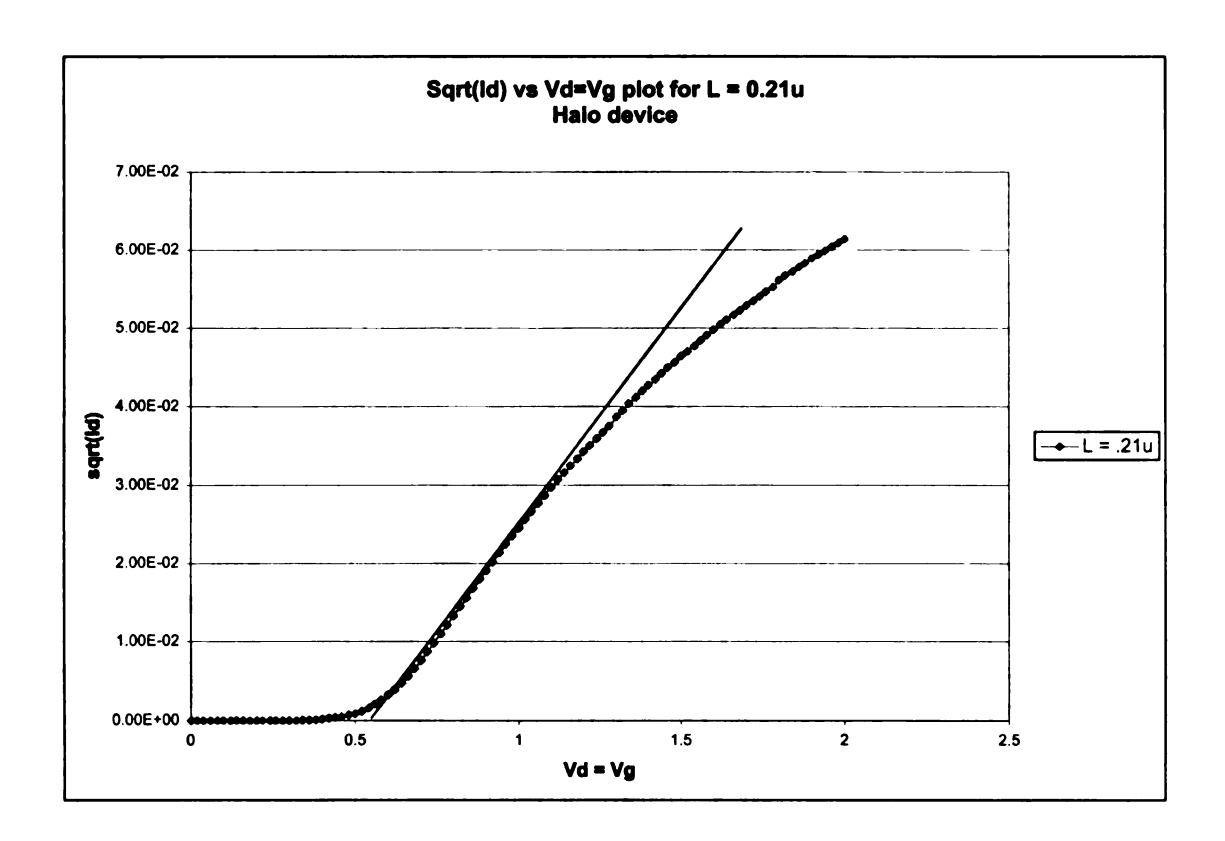


Figure 28. I_d vs. $V_d = V_g$ for halo device, L = 0.21 μ m

The expected $\delta = V_t^0 - V_t^i = -0.08$ value once again does not match the actual δ (-0.14V) shift required to obtain a constant ratio r value. It appears that the δ shift value does not necessarily have to be the difference in extrapolated threshold voltages for devices containing halo implants.

We also note for the devices containing halo implants that the short channel devices have a larger threshold voltage when compared to the threshold voltage of the long channel device. Furthermore, publications found online state the large increase in threshold voltage for short channel devices containing halo implants [10]. Figure 29 shows a comparison of threshold voltage from that source as a function of the channel length, for devices with no halo, halo, and

strong halo implants.

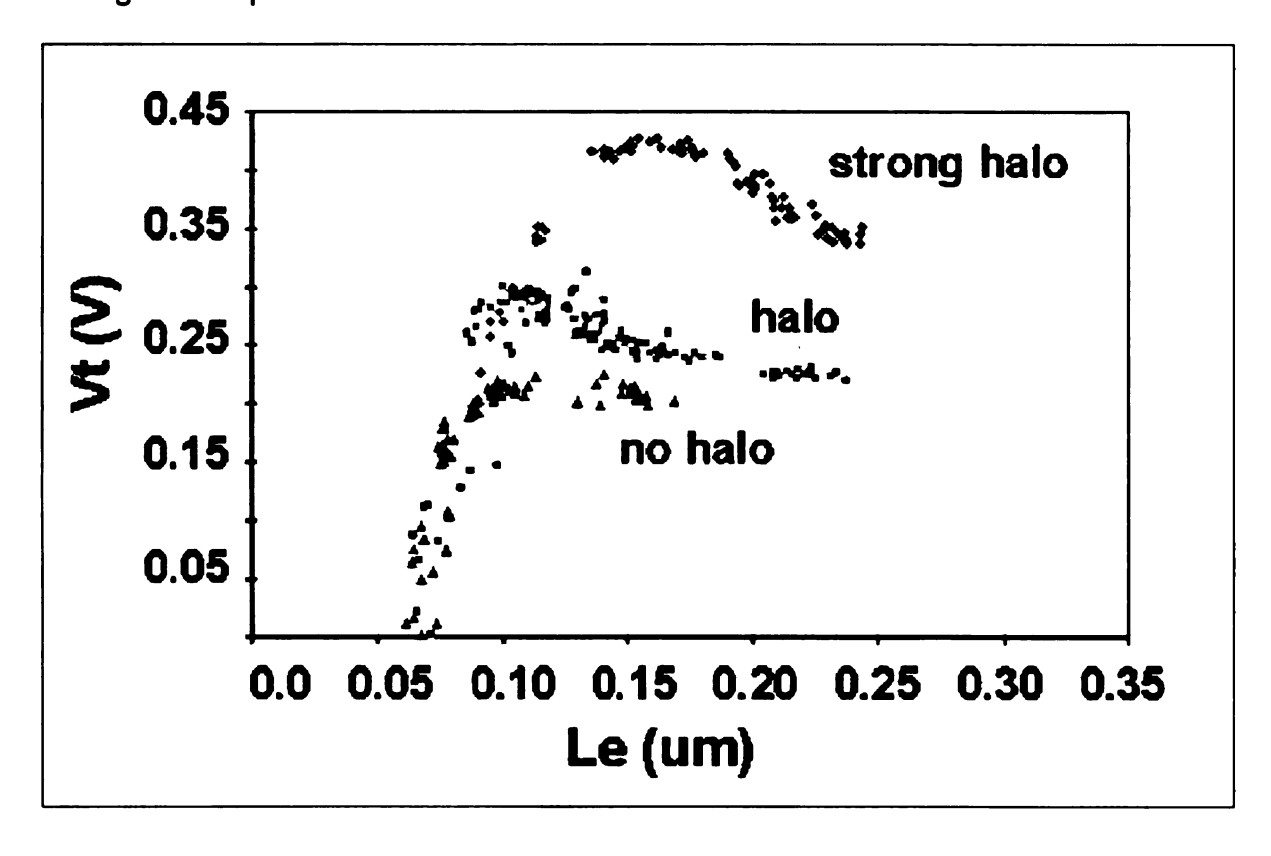


Figure 29. Threshold voltage vs. channel length for various devices [10]

From the previous level 2 SPICE models one can conclude that higher-level models are needed to properly model these devices, which are not typical. According to the SPICE manual, BSIM3 models are known to be able to model major effects in deep-submicrometer MOSFET's, including nonuniform doping.

5.3 BSIM3 Modeling

In order to properly model the short channel devices along with the devices containing halo implants a higher level SPICE model is needed. The BSIM3 model has the ability to incorporate many of the features found in the

devices in this study, such as with lightly doped drains (LDDs) and halo implants. The BSIM3 model also includes many parameters that can model many of the short channel effects that exist. Unfortunately, due to the limited amount of time and the high degree of complexity these models can reach, BSIM3 models for the devices we used were not created in this investigation.

CHAPTER 6

CONCLUSION

6.1 Introduction

Chapter 6 wraps up the thesis. Section 6.2 describes what has been accomplished and what the results mean. Section 6.3 suggests the possibilities in terms of future work with this modified shift and ratio method.

6.2 Summary of Results

The modified shift and ratio method seems to have provided some fair results. Even though a ΔL value of zero was found, a C value less than one was also found. This value of C represents that the effective mobility in the short channel device is indeed smaller than in the long channel device. Also when initially applying the shift and ratio method to the devices containing halo implants, we obtained unphysical negative ΔL values, but when applying the modified shift and ratio, we obtain a more physically realistic result.

6.3 Future Research

The results obtained with work done with the devices provided shows that the modified shift and ratio method may work for devices containing halo implants. To further verify the results obtained, an SEM cross-section of the

devices measured would give insight to how accurate the results obtained were.

From that point on one could improve the modified shift and ratio method depending on how close the extracted effective channel length is to the actual length of the device.

Work can also be continued on the modeling of the devices for both the halo and non-halo devices. From the results obtained from the modeling it is a clear assessment that higher-level models will be needed to not only properly model the devices containing halo implants, but also to model the short channel length devices with lightly doped drains.

APPENDICES

APPENDIX A

GWBASIC PROGRAM

```
5 'Copyright Hewlett-Packard 1984, 1985, 1989
10 '
15 ' Set up program for MS-DOS HP-IB I/O Library
20 ' For use independent of the PC instrument bus system
25 '
30 DEF SEG
35 DATA &H32CD. &H00CB
40 DIM GETDS%(2)
45 READ GETDS%(0): READ GETDS%(1)
50 ADDR% = VARPTR(GETDS%(0))
55 CALL ADDR%
60 CLEAR .&HFC00
65 I=&HFC00
70 '
75 ' PCIB.DIR$ represents the directory where the library files
80 '
       are located
85 ' PCIB is an environment variable which should be set from MS-DOS
90 ' i.e. A:> SET PCIB=A:\LIB
95 '
100 '
       If there is insufficient environment space a direct assignment
105 '
       can be made here, i.e
110 '
         PCIB.DIR$ = "A:\LIB"
115 '
       Using the environment variable is the preferred method
120 '
125 PCIB.DIR$ = ENVIRON$("PCIB")
130 I$ = PCIB.DIR$ + "\IBHPIB.LIB"
135 BLOAD I$,&HFC00
140 CALL I(I%)
145 PCIB.SEG = 1%
150 '
155 ' Define entry points for setup routines
160 '
165 DEF SEG = PCIB.SEG
170 IOABORT
                = 3
175 IOCLEAR
               = 6
180 | OCONTROL = 9
185 IODMA
              = 12
190 IOENTER
               = 15
195 IOENTERA = 18
200 | OENTERAB = 21
205 IOENTERB = 24
210 IOENTERS = 27
215 IOEOI
             = 30
              = 33
220 IOEOL
222 IOFASTOUT = 36
225 \mid OGETTERM = 39
```

```
230 IOLLOCKOUT = 42
235 IOLOCAL = 45
240 IOMATCH = 48
245 IOOUTPUT = 51
250 IOOUTPUTA = 54
255 IOOUTPUTAB = 57
260 \mid OOUTPUTB = 60
265 IOOUTPUTS = 63
270 IOPEN
            = 66
275 IOPPOLL = 69
280 IOPPOLLC
              = 72
285 IOPPOLLU = 75
290 IOREMOTE = 78
295 IORESET = 81
300 \mid OSEND = 84
305 IOSPOLL = 87
310 IOSTATUS = 90
315 IOTIMEOUT = 93
320 IOTRIGGER = 96
325 DEF.ERR = 99
330 '
335 ' Establish error variables and ON ERROR branching
340 '
345 PCIB.ERR$ = STRING$(64,32) : PCIB.ERR = 0
350 PCIB.NAME$ = STRING$(16.32) : PCIB.GLBERR = 0
355 CALL DEF.ERR(PCIB.ERR,PCIB.ERR$,PCIB.NAME$,PCIB.GLBERR)
360 PCIB.BASERR = 255
365 ON ERROR GOTO 395
370 '
375 GOTO 460
380 '
385 ' Error handling routine
390 '
395 IF ERR=PCIB.BASERR THEN GOTO 410
400 PRINT "BASIC error #"; ERR; "occurred in line "; ERL
405 STOP
410 TMPERR = PCIB.ERR
415 IF TMPERR = 0 THEN TMPERR = PCIB.GLBERR
420 PRINT "HPIB error #":TMPERR:" detected at line ":ERL
425 PRINT "Error: ";PCIB.ERR$
430 STOP
435 '
440 ' COMMON declarations are needed if your program is going to chain
      to other programs. When chaining, be sure to call DEF.ERR as
450 '
      well upon entering the chained-to program
455 '
```

```
465 COMMON
DEF.ERR,PCIB.BASERR,PCIB.ERR,PCIB.ERR$,PCIB.NAME$,PCIB.GLBERR
470 COMMON
IOABORT, IOCLEAR, IOCONTROL, IOENTER, IOENTERA, IOENTERS, IOEOI, IOE
OL, IOGETTERM, IOLLOCKOUT, IOLOCAL, IOMATCH, IOOUTPUT, IOOUTPUTA, I
OOUTPUTS
475 COMMON
IOPPOLL, IOPPOLLC, IOPPOLLU, IOREMOTE, IORESET, IOSEND, IOSPOLL, IOS
TATUS, IOTIMEOUT, IOTRIGGER, IODMA, IOPEN, IOENTERB, IOENTERAB, IOO
UTPUTB, IOOUTPUTAB, IOFASTOUT
480 '
485 \text{ FALSE} = 0
490 TRUE = NOT FALSE
495 NOERR = 0
500 EUNKNOWN = 100001!
505 ESEL = 100002!
510 ERANGE = 100003!
515 ETIME = 100004!
520 ECTRL = 100005!
525 EPASS = 100006!
530 ENUM = 100007!
535 EADDR = 100008!
540 COMMON FALSE, TRUE, NOERR, EUNKNOWN, ESEL, ERANGE.
ETIME, ECTRL, EPASS, ENUM, EADDR
545 '
550 'End Program Set-up
555 'User program can begin anywhere past this point
1010 ' Connect to HP4145B, Begin Remote control
1030 OPTION BASE 1
1040 \text{ INFO$} = \text{SPACE$}(13)
1050 DINFO = 20
1060 \text{ CODES} = \text{SPACE}(50)
1070 ISC=7: PARA=17
1080 HP4145B = ISC * 100 + PARA
1090 CALL IORESET (ISC)
1100 IF PCIB.ERR <> NOERR THEN ERROR PCIB.BASERR
1110 \text{ TIMEOUT} = 5
1120 CALL IOTIMEOUT (ISC, TIMEOUT)
1130 IF PCIB.ERR <> NOERR THEN ERROR PCIB.BASERR
1140 CALL IOCLEAR (ISC)
1150 IF PCIB.ERR <> NOERR THEN ERROR PCIB.BASERR
1160 CALL IOREMOTE (ISC)
1170 IF PCIB.ERR <> NOERR THEN ERROR PCIB.BASERR
```

460 COMMON PCIB.DIR\$,PCIB.SEG

```
4010 CLS: LOCATE 5, 15
4020 PRINT "This program will perform a 3 terminal MOS measurement!"
4030 CLS: LOCATE 6, 15
4040 PRINT "Perform the following connections before beginning
measurements:"
4050 PRINT ""
4060 LOCATE 8, 20
4070 PRINT "- Connect the Source to SMU1"
4080 LOCATE 9, 20
4090 PRINT "- Connect the Gate to SMU2"
4100 LOCATE 10, 20
4110 PRINT "- Connect the Drain to SMU3"
4111 LOCATE 11, 20
4112 PRINT "- Connect the Substrate to SMU4"
4120 LOCATE 15, 15
4130 PRINT "Once finished choose one of the options below"
4140 LOCATE 16, 20
4150 PRINT "B - To Begin taking measurements"
4180 LOCATE 17, 20
4190 PRINT " Q - To QUIT program "
4200 INPUT "ENTER LETTER OF YOUR CHOICE: "; B$
4210 IF B$ = "B" OR B$ = "b" THEN CLS : GOTO 4300
4230 IF B$ = "Q" OR B$ = "q" THEN GOTO 9000
4240 GOTO 4200
4310 INPUT "Give filename where data will be stored ":FPUT$
4320 FPUT$=FPUT$+".DAT"
4330 INPUT "Start drain voltage (V): ";SVD
4340 INPUT "End drain voltage (V): "; EVD
4350 INPUT "Drain voltage step (V): "; VDSTEP
4360 INPUT "Start gate voltage (V): ":SVG
4370 INPUT "Step gate voltage (V): ";VGSTEP
4380 INPUT "Number of steps for gate voltage: ";NUMSTEPS
4390 NDAT=(ABS(EVD-SVD)/VDSTEP)+1
4400 GOSUB 8000 'Initialize data file
4410 CLS
4420 PRINT ""
4430 PRINT ""
4450 PRINT " Setting Up HP4145B - Measurements will begin shortly "
4460 PRINT "**"
4470 PRINT ""
4480 '****** Setting up 4145B ******
4490 CODES$="IT1 CA1 DR0 BC" : GOSUB 8500
```

```
4500 CODES$="DE CH1,'VS','IS',3,3" : GOSUB 8500
4510 CODES$="CH2,"VG','IG',1,2" : GOSUB 8500
4520 CODES$="CH3,"VD','ID',1,1": GOSUB 8500
4530 CODES$="CH4,"VSB','ISB',3,3": GOSUB 8500
4540 CODES$="VS1:VS2:VM1:VM2": GOSUB 8500
4550 CODES$="SS
VR1,"+STR$(SVD)+","+STR$(EVD)+","+STR$(VDSTEP)+",.1": GOSUB 8500
4560 CODES$="VP
"+STR$(SVG)+","+STR$(VGSTEP)+","+STR$(NUMSTEPS)+"..1": GOSUB 8500
4570 CODES$="SM DM1 XN 'VD',1,"+STR$(SVD)+","+STR$(EVD): GOSUB
8500
4580 CODES$="YA 'ID'.1.0..1": GOSUB 8500
4590 CODES$="MD ME1": GOSUB 8500
4600 INPUT "Press F once HP4145B has finished taking measurements": F$
4610 IF F$ = "F" OR F$ = "f" THEN CLS : GOTO 4630
4620 GOTO 4600
4630 PRINT ""
4650 PRINT "Transferring and Saving Data to Computer "
4670 PRINT ""
4680 CODES$="DO 'ID"" : GOSUB 8500
4690 FOR M=1 TO NUMSTEPS
4700 FOR N=1 TO NDAT
4710
        GOSUB 8700 'GET DATA
4720
        OPEN FPUTS FOR APPEND AS #1
        VDrain = SVD+(VDSTEP*N)-VDSTEP
4730
       VGate = SVG+VGSTEP*M-VGSTEP
4740
4750
        PRINT VDrain VGate INFO$
4760
        PRINT #1, VDrain, VGate, mid$(INFO$,2,12)
4770
        CLOSE(1)
      NEXT N
4780
4790 NEXT M
4800 GOTO 8800
8010 OPEN FPUT$ FOR APPEND AS #1
8020 PRINT #1."%*********
8030 '** PRINT #1."% SAMPLE: ": SAMPLE$
8040 PRINT #1,"IV measurement using HP4145B and probe station"
8130 CLOSE(1)
8140 RETURN
8310 OPEN FPUT$ FOR APPEND AS #1
8320 CLOSE(1)
8330 RETURN
```

```
8510 LENGTH=LEN(CODES$)
8520 CALL IOOUTPUTS(HP4145B,CODES$,LENGTH)
8530 IF PCIB.ERR <> NOERR THEN ERROR PCIB.BASERR
8540 RETURN
8710 CALL IOENTERS(HP4145B,INFO$,DINFO,ACINFO)
8720 IF PCIB.ERR <> NOERR THEN ERROR PCIB.BASERR
8730 RETURN
8810 GOSUB 8300
8820 PRINT ""
8830 PRINT "*****************
8840 PRINT " Data Transfer Complete "
8850 PRINT "*****************
8860 PRINT ""
8870 INPUT "Press W once you have finished viewing data from HP4145B";
H$
8880 GOTO 1000
9000 END
```

APPENDIX B

PROGRAM DETAILS

In order to efficiently extract large amounts data from the provided wafers a program had to be written that would interact with the HP-4145B Semiconductor Parameter Analyzer. This particular HP-4145B was also an older model, which saved all the data in its own format, which is not compatible with a PC. The program used was created using GWBASIC code [11].

After installing the HPIB card software, a file (SETUP.BAS) is available that contains the initializing/set-up code. This code is to be used at the beginning of every program written, and runs from lines 5->555. These lines of codes should not be changed, at line 1000 the user's program begins. Note that the 'is used to make comments in the program. At line 1030 the code sets the array base to 1, so that numbering of the array elements begins at 1 instead of 0. Variables are also defined, particularly the variables CODES\$ and INFO\$. These are actually string variables of lengths 50 and 13 respectively, that are used to send information to setup the HP-4145B and used to transfer the data from the HP-4145B to the computer respectively. At line 1050, DINFO is defined as a value that is used in other commands in the program and it specifies the maximum number of elements to be read. Then in the program one has to define the Interface select code (ISC) and Parameter Address (PARA). These values are manually set on the card by switches or jumpers and on the HP-4145B by back panel switches respectively. Whatever values are selected must be defined in the program. Using the ISC and PARA, a new variable, 'HP4145B' is defined. This value is used in various commands that talk and listen to the HP-4145B. Line 1090 sets the interface to its default configuration. The next line is

an error checking line that appears after every library command, which goes to an error handling routine in the setup code. The next pair of lines (1110->1120) defines a system timeout of 5 seconds in the event of a communication problem. Line 1140 puts the HP-4145B into a device dependent state and line 1160 sets the device in Remote. Both of these states are necessary for computer control of the instrument.

The program then prints out on the screen a set of instructions for the setup (lines 4000 -> 4240) of the probes (SMU's). The screen is first cleared using the CLS command, then the cursor is located to a particular point on the screen using the LOCATE command. The PRINT command prints out text on the screen. Then the program is stopped giving the user time to setup the probes and also the option to continue or quit. A pair of if/then statements observe and perform the choice of the user. For this particular program, SMU1 is the source, SMU2 is the gate, SMU3 is the drain, and SMU4 is the substrate.

Next a user interface is created such that the user can enter the voltage values (lines 4300->4400) for the desired current measurements. First the user is asked to give a filename (less than or equal to 8 characters) to store the obtained data. Then the range of voltage values for the drain and gate is requested. All these values are stored in variables that are then used to setup the HP-4145B. Before the setup begins though, the program goes to a subroutine that initializes and creates the data file. This occurs at lines 8000-> 8140. Once finished with the subroutine, the program returns to setting up the HP-4145B.

First a subroutine is needed that will communicate to the HP-4145B what type of source each probe will represent, over what range each source will vary, as well as data display options. This subroutine is lines 8500-8540 in the program. The subroutine sends the 'CODES\$' string to the HP-4145B and sets up the HP-4145B just as one would normally do manually. The 'CODES\$' string is first defined using program codes found in the HP-4145B manual [7]. Then the information is sent to the HP-4145B, using the IOOUTPUTS command. This occurs multiple times until the setup of the HP-4145B is complete.

First the method to take measurements is defined, also known as the Integration Time, where 3 choices are available. IT1: short, IT2: medium, IT3: long. This determines how long it takes the HP-4145B to take measurements, and the longer the time the more accurate the measurement. Auto calibration is turned on with code 'CA1' and data ready service request is turned off with code 'DR0'. The HPIB data output buffer must also be cleared before performing data output from the HP-4145B. This is accomplished by sending a 'BC' code. In the program these can be seen in line 4490.

4490 CODES\$="IT1 CA1 DR0 BC" : GOSUB 8500

The channel definition page defines the connections that are being used (in this case) to probe the wafer. The probe station has 4 connections (SMU's) and each one of these must be defined, and for this program the source is defined as follows:

4500 CODES\$="DE CH1,"VS',"IS',3,3" : GOSUB 8500

DE: Defines that you want to setup the channel definition page

1 to 1 to 1 to 1

CH1: This is the connection we are setting up, in this case SMU1.

VS: Names the source voltage as VS.

IS: Names the source current as IS.

3 (first): This defines that SMU1 is COM, i.e. the common, or ground connection.

3 (second): This defines that SMU1 is a constant function.

The gate is then defined as follows:

4510 CODES\$="CH2,'VG','IG',1,2" : GOSUB 8500

CH2: This is the connection we are setting up, SMU2.

VG: Names the gate voltage as VG.

IG: Names the gate current as IG.

1: This defines that SMU2 is a voltage source.

2: This defines that SMU2 is a step function variable (On the HP-4145B display screen, VAR2 is used for step functions).

The drain is then defined as follows:

4520 CODES\$="CH3,'VD','ID',1,1": GOSUB 8500

CH3: This is the connection we are setting up, SMU3.

VD: Names the drain voltage as VD.

ID: Names the drain current as ID.

1 (first): This defines that SMU3 is a voltage source.

1 (second): This defines that SMU3 is a sweep variable function (On the HP-

4145B display screen, VAR1 is used for sweep functions).

The substrate is then defined as follows:

4530 CODES\$="CH4,"VSB','ISB',3,3": GOSUB 8500

CH4: This is the connection we are setting up, SMU4.

VSB: Names the substrate voltage as VSB.

ISB: Names the substrate current as ISB.

3 (first): This defines that SMU4 is COM.

3 (second): This defines that SMU4 is a constant function.

Line 4540 turns off the other 4 SMU channels, which are not used:

(VS1, VS2, VM1, VM2)

4540 CODES\$="VS1;VS2;VM1;VM2": GOSUB 8500

Then the source setup page for this particular case allows the user to define the gate and drain voltages to be used to take current measurements.

The program first sets the drain voltage up as follows:

4550 CODES\$="SS

VR1,"+STR\$(SVD)+","+STR\$(EVD)+","+STR\$(VDSTEP)+",.1" GOSUB 8500

SS: Defines you want to setup the source setup page

VR1: This defines VAR1 to be a voltage source with a linear sweep. (VR2 would be a log 10 sweep)

+STR\$(SVD)+: Defines the start value, which was previously defined by the user and stored as variable SVD.

+STR\$(EVD)+: Defines the stop value, which was previously defined by the user and stored as variable EVD.

+STR\$(VDSTEP)+: Defines the step value, which was previously defined by the user and stored as variable VDSTEP.

.1: defines the current compliance value in amperes.

The gate voltage is setup as follows:

4560 CODES\$="VP

"+STR\$(SVG)+","+STR\$(VGSTEP)+","+STR\$(NUMSTEPS)+",.1": GOSUB 8500

VP: This defines VAR2 to be a voltage source. VAR2 is a step function.

+STR\$(SVG)+: Defines the start value, which was previously defined by the user and stored as variable SVG.

+STR\$(VGSTEP)+: Defines the step value, which was previously defined by the user and stored as variable VGSTEP.

+STR\$(NUMSTEPS)+: Defines the number of steps to be taken, which was previously defined by the user and stored as variable NUMSTEPS.

.1: defines the current compliance value in amperes.

Then the measurement and display mode setup page is defined using some of the previously values defined by the user.

4570 CODES\$="SM DM1 XN 'VD',1,"+STR\$(SVD)+","+STR\$(EVD): GOSUB 8500

SM: Defines you want to setup the measurement and display mode setup page DM1: Defines that we want to display the data in graphics form. (DM2 would display in list form)

XN: Defines that you want to setup the x-axis

VD: Defines that we want the x-axis to be the drain voltage

1: Define the x-axis to have a linear scale (2 would indicates log scale)

+STR\$(SVD)+: minimum value for the x-axis

+STR\$(EVD): maximum value for the x-axis

The y-axis is then setup is the next line of the program:

4580 CODES\$="YA 'ID',1,0,.1": GOSUB 8500

YA: Defines that you want to setup the y-axis

ID: Defines that we want the y-axis to be the drain current

1: Define the y-axis to have a linear scale

0: minimum value for the y-axis

.1: maximum value for the y-axis

Then to begin to take measurements, measurement codes are used:

4590 CODES\$="MD ME1": GOSUB 8500

MD: Defines that you will be defining measurement codes

ME1: Defines that a single measurement is to be taken. Other options allow multiple runs to be taken and averaged.

Once the previous line runs, the measurements begin to be taken. When the HP-4145B is taking measurements, a red LED on the front panel lights up, and once finished, this LED shuts off. The user should not make keyboard entries until this LED turns off. Once the light shuts off, the user should then continue running the program by entering 'F' as requested by the program, this

allows the data needs to be transferred to the computer, which is done by putting the data into the 'Data Output Channel' using the following program codes:

4680 CODES\$="DO 'ID"" : GOSUB 8500

DO: Defines what to put into the Data Output Channel

ID: Tells the HP-4145B to put the drain current data into the Data Output Channel

Then a nested 'for' loop is created to transfer the drain current data with respect to a specific drain and gate voltage. A subroutine within the nested 'for' loop transfers the data into the Data Output Channel to the computer in the INFO\$ string.

8710 CALL IOENTERS(HP4145B,INFO\$,DINFO,ACINFO)

8720 IF PCIB.ERR <> NOERR THEN ERROR PCIB.BASERR

8730 RETURN

This string is then copied onto the data file along with its respective drain and gate voltage. This is repeated until the nested 'for' loop ends, when all the values measured are transferred.

For further reference on can check both the HP-4145B instruction manual as well as the HP-IB Command Library.

APPENDIX C

MEASUREMENT DATA

Table 2. Shift and Ratio Data for Non-Halo Devices

Ratio d Shift02		3.85E+00	4.60E+00	5.18E+00	2.86E+00	1.45E+00	1.22E+00	9.88E-01	6.72E-01	4.26E-01	2.60E-01	8.56E-02	6.59E-02	1.14E-02	9.83E-03	3.71E-02	7.22E-02	8.24E-02	1.75E-01	1.32E+00	4.05E+01	1.11E+02	3.07E+02	4.63E+02	5.20E+02	4.14E+02	4.56E+02	2.73E+02	3.56E+02
Ratio d Shift01		2.02E+00	3.49E+00	4.41E+00	5.33E+00	1.71E+00	1.67E+00	1.53E+00	9.67E-01	6.37E-01	5.40E-01	2.44E-01	6.70E-02	5.75E-02	1.09E-02	5.65E-02	6.83E-02	8.26E-02	8.74E-02	1.11E+00	3.60E+00	4.54E+01	1.64E+02	3.13E+02	3.97E+02	3.43E+02	3.94E+02	2.37E+02	2.95E+02
Ratio No d shift		1.04E+00	1.83E+00	3.34E+00	4.53E+00	3.18E+00	1.96E+00	2.09E+00	1.50E+00	9.17E-01	8.06E-01	5.05E-01	1.91E-01	5.84E-02	5.51E-02	6.29E-02	1.04E-01	7.81E-02	8.75E-02	5.54E-01	3.04E+00	4.03E+00	6.72E+01	1.67E+02	2.68E+02	2.62E+02	3.27E+02	2.05E+02	2.56E+02
Ratio d Shift +.01		9.44E-01	1.75E+00	3.44E+00	2.71E+00	3.65E+00	2.46E+00	2.04E+00	1.42E+00	1.16E+00	7.54E-01	3.95E-01	1.66E-01	5.60E-02	3.17E-01	1.16E-01	1.19E-01	8.28E-02	5.55E-01	1.51E+00	3.41E+00	5.98E+00	6.86E+01	1.44E+02	1.77E+02	2.50E+02	1.70E+02	2.22E+02	2.27E+02
Ratio d Shift +.02		9.04E-01	1.80E+00	2.05E+00	3.11E+00	4.57E+00	2.40E+00	1.94E+00	1.80E+00	1.09E+00	5.90E-01	3.45E-01	1.59E-01	3.22E-01	5.83E-01	1.32E-01	1.26E-01	5.25E-01	1.52E+00	1.70E+00	5.05E+00	6.10E+00	5.88E+01	9.48E+01	1.69E+02	1.30E+02	1.84E+02	1.97E+02	1.48E+02
L = 8.4 Sfunc c	8.89E+09 7.76E+09	3.42E+09	2.10E+10	9.26E+09	4.15E+09	5.82E+09	4.67E+09	2.91E+09	1.32E+10	1.19E+10	4.99E+09	2.70E+09	1.24E+10	1.03E+10	2.71E+09	7.36E+08	1.53E+09	1.44E+11	1.44E+11	4.46E+10	2.08E+10	1.90E+12	4.04E+12	8.91E+11	3.37E+12	2.31E+11	4.08E+11	1.00E+12	6.12E+11
L = .21 Sfunc	2.49E+10 1.23E+10	4.94E+09	4.90E+09	1.24E+09	1.56E+09	4.13E+08	1.79E+09	3.42E+09	8.50E+09	4.32E+09	7.09E+09	1.56E+10	2.05E+10	3.62E+10	9.42E+10	3.27E+11	2.37E+10	2.05E+12	3.23E+11	1.56E+12	9.32E+10	3.17E+10	1.34E+10	8.22E+09	5.34E+09	3.55E+09	2.73E+09	2.66E+09	2.90E+09
L = 8.4 Rd 2.02E+09	1.87E+09 1.84E+09	2.02E+09	1.77E+09	1.61E+09	1.58E+09	1.52E+09	1.47E+09	1.62E+09	1.53E+09	1.35E+09	1.29E+09	1.25E+09	1.23E+09	1.50E+09	1.44E+09	1.45E+09	1.46E+09	1.41E+09	4.33E+09	4.29E+09	3.44E+09	3.88E+09	-3.45E+10	-7.69E+10	-1.67E+10	-9.62E+09	-1.20E+10	-1.45E+09	8.00E+09
L = .21 Rd -1.58E+09	-1.30E+09 -1.09E+09	-1.05E+09	-9.88E+08	-9.57E+08	-9.63E+08	-9.88E+08	-9.55E+08	-9.52E+08	-1.02E+09	-1.12E+09	-1.11E+09	-1.26E+09	-1.42E+09	-1.68E+09	-2.15E+09	-3.56E+09	-8.70E+09	-4.03E+09	3.23E+10	2.43E+09	1.03E+09	5.63E+08	3.93E+08	2.94E+08	2.29E+08	1.88E+08	1.58E+08	1.33E+08	1.04E+08
L = 8.4 Id 2.48E-11	2.68E-11 2.72E-11	2.47E-11	2.83E-11	3.12E-11	3.16E-11	3.29E-11	3.40E-11	3.10E-11	3.28E-11	3.70E-11	3.88E-11	4.00E-11	4.05E-11	3.33E-11	3.47E-11	3.46E-11	3.43E-11	3.54E-11	1.16E-11	1.17E-11	1.46E-11	1.29E-11	-1.45E-12	-6.50E-13	-3.00E-12	-5.20E-12	-4.15E-12	-3.45E-11	6.25E-12
L = .21 Id -3.16F-11	-3.84E-11 -4.60E-11	-4.74E-11	-5.06E-11	-5.23E-11	-5.19E-11	-5.06E-11	-5.23E-11	-5.25E-11	-4.89E-11	-4.45E-11	4.51E-11	-3.96E-11	-3.52E-11	-2.99E-11	-2.33E-11	-1.41E-11	-5.75E-12	-1.24E-11	1.55E-12	2.06E-11	4.87E-11	8.88E-11	1.27E-10	1.70E-10	2.19E-10	2.66E-10	3.17E-10	3.76E-10	4.79E-10
Vd Vg	0.05 0.01			0.05 0.05	0.05 0.06	0.05 0.07	0.05 0.08	0.05 0.09	0.05 0.10	0.05 0.11	0.05 0.12	0.05 0.13	0.05 0.14	0.05 0.15	0.05 0.16	0.05 0.17	0.05 0.18	0.05 0.19	0.05 0.20	0.05 0.21	0.05 0.22	0.05 0.23		0.05 0.25	0.05 0.26	0.05 0.27	0.05 0.28	0.05 0.29	0.05 0.30

Ratio .01 d Shift02	-02 4.20E+02				-02 1.24E+03	-03 1.98E+03	-03 4.11E+03								0044460														. N O 4 4 4 W O		. N O 4 4 4 W O	. w w w w o o o o o o o o o o o o o o o	. w w w w o o o o o o o o o o o o o o o	· · · · · · · · · · · · · · · · · · ·	. W W W W W W W W W W W W W W W W W W W	· · · · · · · · · · · · · · · · · · ·
R d Shift01)2 9.82E+02	3 1.53E+03	3 3.09E+03	3 4.10E+03		3 5.19E+03																								8 8 8 8 8 8 8 8 8 8 8 8 8 8 8 8 8 8 8	8 8 8 8 8 8 8 8 8 8 8 8 8 8 8 8 8 8 8	8 8 8 8 8 8 8 8 8 8 8 8 8 8 8 8 8 8 8
Ratio I No d shift				2 2.00E+02	2 7.65E+02	3 1.21E+03	3 2.38E+03	3 3.08E+03	3 3.87E+03		3 2.85E+03																									
Ratio d Shift +.01	1.71E+02	1.45E+02	1.45E+02	5.78E+02	9.41E+02	1.88E+03	2.38E+03	2.91E+03	2.13E+03	2 155102	Z. 13E10	2.14E+02	2.14E+02 1.61E+02	2.14E+02 2.14E+02 1.61E+02 1.13E+02	2.14E+02 2.14E+02 1.61E+02 1.13E+02 8.39E+01	2.14E+02 2.14E+02 1.13E+02 8.39E+01 6.70E+01	2.14E+02 2.14E+02 1.61E+02 1.13E+02 8.39E+01 6.70E+01	2.14E+02 2.14E+02 1.61E+02 1.13E+02 8.39E+01 6.70E+01 5.62E+01	2.14E+02 2.14E+02 1.16TE+02 8.39E+0 6.70E+0 5.62E+0 5.63E+0	2.14E+02 2.14E+02 1.61E+02 1.13E+02 8.39E+01 6.70E+01 5.62E+01 5.63E+01	2.14E+02 2.14E+02 1.13E+02 8.39E+01 6.70E+01 5.62E+01 5.63E+01 6.18E+01	2.14 2.14 2.14 3.14 3.39 6.70 6.70 6.70 6.70 6.70 6.70 6.70 6.70	2.14E+02 2.14E+02 1.61E+02 8.39E+01 6.70E+01 5.62E+01 5.63E+01 6.18E+01 6.54E+01	2.14 2.14 1.61 1.13 1.13 1.13 1.13 1.13 1.13 1.13	2.14E+0.7 2.14E+0.7 2.14E+0.7 3.00E+	2.14E+0.7 2.14E+0.7 2.14E+0.7 3.39E+0.7 3.62E+0.7 3.62E+0.7 3.63E+0.7 6.54E+0.7 6.7 6.7 6.7 6.7 6.7 6.7 6.7 6.7 6.7 6	2.14E+02 1.61E+02 1.13E+04 6.70E+0 6.70E+0 5.62E+0 5.63E+0 6.54E+0 6.63E+0 6.63E+0 6.63E+0 6.63E+0 6.63E+0 6.63E+0 6.63E+0	2.14E+0.7 1.61E+0.7 1.13E+0.7 6.70E+0.7 5.62E+0.7 5.63E+0.7 6.54E+0.7 6.63E+0.7 6.7 6.7 6.7 6.7 6.7 6.7 6.7 6.7 6.7 6	2.14E+02 1.61E+02 1.13E+04 6.70E+04 5.62E+04 5.62E+04 5.63E+04 6.18E+04 6.18E+04 6.18E+04 6.18E+04 6.18E+04 6.05E+04 6.05E+04 6.06E+04 6.06E+04 6.06E+04	2.14E+02 1.61E+02 1.13E+02 1.13E+02 6.70E+01 6.70E+01 5.62E+01 6.54E+01 6.54E+01 6.63E+01 6.17E+01 6.05E+01 6.05E+01 6.06E+01 6.06E+01	2.14 1.14 1.15	2.14E+02 1.15TE+02 8.39E+0-02 6.70E+0-03 6.70E+0-0	6.05 Help (1.5) (1	6.05 E + O + O + O + O + O + O + O + O + O +	6.05 E + O + O + O + O + O + O + O + O + O +	2.14 1.61 1.61 8.39 6.70 6.70 6.70 6.70 6.70 6.70 6.70 6.70
Ratio d Shift +.02	1.20E+02	1.09E+02	4.18E+02	7.11E+02	1.46E+03	1.88E+03	2.24E+03	1.60E+03	1.60E+03	1 R1E+02	10.1.0.	1.22E+02	1.22E+02 8.65E+01	1.22E+02 8.65E+01 6.41E+01	1.22E+02 8.65E+01 6.41E+01 5.08E+01	1.22E+02 8.65E+01 6.41E+01 5.08E+01	1.22E+02 8.65E+01 6.41E+01 5.08E+01 4.47E+01	8.65E+02 8.65E+01 6.41E+01 5.08E+01 4.30E+01 4.30E+01	8.65E+01 8.65E+01 6.41E+01 5.08E+01 4.30E+01 4.30E+01	8.65E+01 8.65E+01 6.41E+01 5.08E+01 4.47E+01 4.30E+01 4.44E+01	8.65E+01 8.65E+01 6.41E+01 5.08E+01 4.30E+01 4.30E+01 4.71E+01 5.00E+01	8.65E+01 8.65E+01 6.41E+01 5.08E+01 4.30E+01 4.30E+01 4.71E+01 5.00E+01	8.65E+01 8.65E+01 6.41E+01 4.47E+01 4.30E+01 4.71E+01 4.71E+01 5.00E+01 5.08E+01	8.65E+01 8.65E+01 6.41E+01 5.08E+01 4.30E+01 4.30E+01 4.71E+01 5.00E+01 5.08E+01 4.96E+01	8.65E+01 8.65E+01 6.41E+01 5.08E+01 4.30E+01 4.30E+01 4.71E+01 5.00E+01 5.08E+01 4.96E+01 4.96E+01	1.22E+02 8.65E+01 6.41E+01 5.08E+01 4.30E+01 4.30E+01 4.71E+01 5.00E+01 5.08E+01 4.86E+01 4.70E+01	8.65E+02 8.65E+01 6.41E+01 5.08E+01 4.47E+01 4.30E+01 4.71E+01 5.00E+01 4.96E+01 4.70E+01 4.70E+01 4.66E+01	8.65E+02 8.65E+01 6.41E+01 5.08E+01 4.30E+01 4.30E+01 4.71E+01 5.08E+01 4.70E+01 4.96E+01 4.96E+01 4.96E+01 4.96E+01 4.96E+01 4.96E+01 4.96E+01 4.96E+01	8.65E+02 8.65E+01 6.41E+01 5.08E+01 4.47E+01 4.30E+01 4.71E+01 5.08E+01 4.71E+01 5.08E+01 4.71E+01 4.71E+01 4.71E+01 4.70E+01 4.66E+01 4.66E+01 4.67E+01	8.65E+02 8.65E+01 6.41E+01 5.08E+01 4.47E+01 4.30E+01 4.71E+01 5.00E+01 4.96E+01 4.96E+01 4.70E+01 4.66E+01 4.67E+01 4.57E+01	8.65E+02 8.65E+01 6.41E+01 5.08E+01 4.47E+01 4.30E+01 4.71E+01 5.00E+01 4.96E+01 4.96E+01 4.66E+01 4.66E+01 4.67E+01 4.57E+01 4.57E+01	8.65E+02 8.65E+01 6.41E+01 6.41E+01 4.47E+01 4.30E+01 4.71E+01 5.00E+01 4.96E+01 4.66E+01 4.67E+01 4.67E+01 4.67E+01 4.67E+01 4.57E+01 4.57E+01 4.57E+01	8.65E+02 8.65E+01 6.41E+01 6.41E+01 4.47E+01 4.30E+01 4.30E+01 4.96E+01 4.66E+01 4.67E+01 4.67E+01 4.67E+01 4.67E+01 4.67E+01 4.67E+01 4.67E+01 4.67E+01 4.67E+01 4.67E+01 4.67E+01 4.67E+01 4.67E+01 4.67E+01 4.67E+01	8.65E+02 8.65E+01 6.41E+01 6.41E+01 4.47E+01 4.30E+01 4.36E+01 4.96E+01 4.67E+01 4.67E+01 4.67E+01 4.57E+01 4.57E+01 4.57E+01 4.57E+01 4.57E+01 4.57E+01	8.65E+02 8.65E+01 6.41E+01 6.41E+01 4.47E+01 4.30E+01 4.30E+01 4.96E+01 4.67E+01 4.67E+01 4.67E+01 4.57E+01 4.57E+01 4.57E+01 4.57E+01 4.57E+01 4.57E+01 4.57E+01 4.57E+01	8.65E+02 8.65E+01 6.41E+01 6.41E+01 4.47E+01 4.30E+01 4.44E+01 4.30E+01 4.67E+01
L = 8.4 Sfunc	6.69E+11	4.68E+11	5.14E+10	2.65E+10	7.50E+10	3.44E+11	2.29E+12	6.94E+11	1.94E+12	7.05E+10		4.40E+10	4.40E+10 2.27E+10	4.40E+10 2.27E+10 1.21E+10	4.40E+10 2.27E+10 1.21E+10 6.56E+09	4.40E+10 2.27E+10 1.21E+10 6.56E+09 3.91E+09	4.40E+10 2.27E+10 1.21E+10 6.56E+09 3.91E+09 2.71E+09	4.40E+10 2.27E+10 1.21E+10 6.56E+09 3.91E+09 2.71E+09	4.40E+10 2.27E+10 1.21E+10 6.56E+09 3.91E+09 2.71E+09 1.92E+09	4.40E+10 2.27E+10 1.21E+10 6.56E+09 3.91E+09 2.71E+09 1.92E+09 1.39E+09	4.40E+10 2.27E+10 1.21E+10 6.56E+09 3.91E+09 2.71E+09 1.32E+09 1.39E+09 9.51E+08	4.40E+10 2.27E+10 1.21E+10 6.56E+09 3.91E+09 2.71E+09 1.39E+09 1.39E+09 9.51E+08 8.10E+08	4.40E+10 2.27E+10 1.21E+10 6.56E+09 3.91E+09 2.71E+09 1.92E+09 1.39E+09 9.51E+08 8.10E+08	4.40E+10 2.27E+10 1.21E+10 6.56E+09 3.91E+09 2.71E+09 1.92E+09 1.39E+09 1.08E+09 9.51E+08 8.10E+08 6.24E+08	4.40E+10 2.27E+10 1.21E+10 6.56E+09 3.91E+09 2.71E+09 1.92E+09 1.39E+09 9.51E+08 8.10E+08 6.24E+08 3.30E+08	4.40E+10 2.27E+10 1.21E+10 6.56E+09 3.91E+09 1.92E+09 1.39E+09 1.08E+09 9.51E+08 8.10E+08 6.24E+08 3.30E+08	4.40E+10 2.27E+10 1.21E+10 6.56E+09 3.91E+09 1.39E+09 1.39E+09 9.51E+08 8.10E+08 6.24E+08 4.53E+08	4.40E+10 2.27E+10 1.21E+10 6.56E+09 3.91E+09 1.39E+09 1.39E+09 9.51E+08 8.10E+08 6.24E+08 4.53E+08 3.30E+08	4.40E+10 2.27E+10 1.21E+10 6.56E+09 3.91E+09 1.92E+09 1.39E+09 9.51E+08 8.10E+08 6.24E+08 4.53E+08 3.30E+08 1.91E+08	4.40E+10 2.27E+10 6.56E+09 3.91E+09 1.92E+09 1.39E+09 9.51E+08 8.10E+08 6.24E+08 4.53E+08 3.30E+08 1.91E+08 1.91E+08	4.40E+10 2.27E+10 6.56E+09 3.91E+09 1.92E+09 1.39E+09 9.51E+08 8.10E+08 6.24E+08 4.53E+08 3.30E+08 1.91E+08 1.91E+08	4.40E+10 2.27E+10 6.56E+09 3.91E+09 1.39E+09 1.39E+09 9.51E+08 8.10E+08 6.24E+08 4.53E+08 3.30E+08 4.53E+08 1.91E+08 8.70E+08 1.91E+08	4.40E+10 2.27E+10 6.56E+09 3.91E+09 1.39E+09 1.39E+09 9.51E+08 8.10E+08 6.24E+08 4.53E+08 3.30E+08 1.91E+08 1.91E+08 8.70E+08 1.91E+08 3.30E+08 3.30E+08 4.53E+08 3.30E+08 3.30E+08 4.55E+08 1.47E+08 1.91E+08	4.40E+10 2.27E+10 6.56E+09 3.91E+09 1.92E+09 1.39E+09 9.51E+08 8.10E+08 6.24E+08 4.53E+08 3.30E+08 4.53E+08 1.91E+08 1.91E+08 3.30E+08 4.53E+08 1.91E+08 3.30E+08 3.30E+08 4.53E+08 3.30E+08 3.30E+08 4.53E+08 1.47E+08 1.47E+08	4.40E+10 2.27E+10 6.56E+09 3.91E+09 2.71E+09 1.92E+09 1.39E+09 9.51E+08 8.10E+08 6.24E+08 4.53E+08 3.30E+08 1.91E+08 1.91E+08 3.30E+08 3.30E+08 4.53E+08 3.30E+08 3.30E+08 3.30E+08 3.30E+08 3.30E+08 4.55E+08 3.30E+08 3.30E+08 3.30E+08	4.40E+10 2.27E+10 6.56E+09 3.91E+09 2.71E+09 1.92E+09 1.39E+09 9.51E+08 8.10E+08 6.24E+08 4.53E+08 3.30E+08 1.91E+08 1.91E+08 1.91E+08 3.30E+08 3.30E+08 3.30E+08 2.45E+08 1.47E+08 1.11E+08 3.76E+07 2.93E+07
L = .21 Sfunc	2.41E+09	1.61E+09	1.13E+09	8.30E+08	6.91E+08	5.64E+08	4.36E+08	3.19E+08	2.35E+08	1.75E+08	90.1740.4	- JUNE 100	1.05E+08	1.05E+08 7.91E+07	1.05E+08 7.91E+07 5.95E+07	1.05E+08 1.05E+08 7.91E+07 5.95E+07 4.58E+07	1.05E+08 7.91E+07 5.95E+07 4.58E+07 3.51E+07	1.05E+08 7.91E+07 5.95E+07 4.58E+07 3.51E+07	1.05E+08 1.05E+08 7.91E+07 5.95E+07 4.58E+07 3.51E+07 2.67E+07	1.05E+08 1.05E+08 7.91E+07 5.95E+07 4.58E+07 2.67E+07 2.02E+07	1.05E+08 1.05E+08 7.91E+07 5.95E+07 4.58E+07 3.51E+07 2.67E+07 1.54E+07	1.05E+08 1.05E+08 7.91E+07 5.95E+07 4.58E+07 3.51E+07 2.67E+07 2.02E+07 1.54E+07 1.18E+07	1.05E+08 1.05E+08 7.91E+07 5.95E+07 4.58E+07 2.67E+07 2.02E+07 1.54E+07 1.18E+07 9.03E+06	1.05E+08 1.05E+08 7.91E+07 5.95E+07 4.58E+07 2.67E+07 2.02E+07 1.54E+07 1.54E+07 0.03E+06 6.86E+06	1.05E+08 1.05E+08 7.91E+07 5.95E+07 3.51E+07 2.67E+07 2.02E+07 1.54E+07 1.54E+07 9.03E+06 6.86E+06 5.29E+06	1.05E+08 1.05E+08 7.91E+07 4.58E+07 3.51E+07 2.07E+07 1.54E+07 1.54E+07 0.03E+06 6.86E+06 5.29E+06 3.13E+06	1.05E+08 7.91E+07 5.95E+07 3.51E+07 2.02E+07 1.54E+07 1.54E+07 0.03E+06 6.86E+06 5.29E+06 3.13E+06	1.05E+08 7.91E+07 5.95E+07 3.51E+07 2.02E+07 1.54E+07 1.54E+07 0.03E+06 6.86E+06 5.29E+06 3.13E+06 2.40E+06	1.05E+08 7.91E+07 5.95E+07 3.51E+07 2.02E+07 1.18E+07 9.03E+06 6.86E+06 5.29E+06 4.09E+06 1.45E+06	1.05E+08 1.05E+08 7.91E+07 2.05E+07 2.05E+07 1.54E+07 1.18E+07 9.03E+06 6.86E+06 6.86E+06 5.29E+06 3.13E+06 1.45E+06 1.45E+06	1.05E+08 1.05E+08 2.95E+07 3.51E+07 2.02E+07 1.54E+07 1.18E+07 9.03E+06 6.86E+06 5.29E+06 2.40E+06 1.45E+06 1.45E+06 8.65E+06 8.65E+06	1.05E+08 7.91E+07 5.95E+07 3.51E+07 2.02E+07 1.54E+07 1.18E+07 9.03E+06 6.86E+06 6.86E+06 5.29E+06 1.95E+06 1.85E+06 1.44E+06 1.13E+06 6.86E+06 8.65E+05 6.86E+06	1.05E+08 7.91E+07 7.91E+07 2.02E+07 2.02E+07 1.54E+07 1.18E+07 9.03E+06 6.86E+06 6.86E+06 7.99E+06 1.44E+06 1.13E+06 6.86E+06 6.86E+06 6.86E+06 7.99E+	1.05E+08 7.91E+07 7.91E+07 2.05E+07 2.05E+07 1.54E+07 1.18E+07 9.03E+06 6.86E+06 6.86E+06 7.99E+06 1.44E+06 1.13E+06 1.13E+06 6.86E+06 6.86E+06 6.86E+06 7.99E+	1.05E+08 7.91E+07 7.91E+07 2.05E+07 2.05E+07 2.02E+07 1.18E+07 1.18E+07 9.03E+06 6.86E+06 6.86E+06 7.99E+06 1.14E+06 1.13E+06 1.13E+06 1.13E+06 3.13E+06 3.13E+06 4.09E+06 3.13E+06 3.13E+06 3.13E+06 3.13E+06 3.13E+06 4.09E+06 3.13E+	1.05E+08 1.05E+08 2.95E+07 2.05E+07 2.02E+07 1.54E+07 1.18E+07 9.03E+06 6.86E+06 6.86E+06 1.45E+06 1.13E+06 1.13E+06 6.81E+05 5.39E+05 5.39E+05 3.34E+05 3.34E+05
r = 8.4 Rd 4	-1.37E+10	-5.38E+09	-4.35E+09	-4.35E+09	-4.88E+09	-5.85E+09	-1.18E+10	4.00E+10	2.12E+09	1.30E+09	7 14F+08																		• • • • • • • • • • • • • • • • • • • •	• • • • • • • • • • • • • • • • • • • •	• • • • • • • • • • • • • • • • • • • •	• • • • • • • • • • • • • • • • • • • •		• • • • • • • • • • • • • • • • • • • •		
R .	7.51E+07	5.62E+07	4.28E+07	3.37E+07	2.62E+07	1.99E+07	1.49E+07	1.12E+07	8.49E+06	6.49E+06	A QRE+OR	100:1																								
L = 8.4 Id = 4.4	-3.65E-12		-1.15E-11	-1.15E-11	-1.03E-11	-8.55E-12	4.25E-12	1.25E-12	2.36E-11	3.85E-11	7 OOF-11		1.20E-10	1.20E-10 1.92E-10	1.20E-10 1.92E-10 2.85E-10	1.20E-10 1.92E-10 2.85E-10 3.86E-10	1.20E-10 1.92E-10 2.85E-10 3.86E-10 5.14E-10	1.20E-10 1.92E-10 2.85E-10 3.86E-10 5.14E-10	1.20E-10 1.92E-10 2.85E-10 3.86E-10 6.64E-10 8.49E-10	1.20E-10 1.92E-10 2.85E-10 3.86E-10 5.14E-10 6.64E-10 1.05E-09	1.92E-10 2.85E-10 3.86E-10 5.14E-10 6.64E-10 1.05E-09	1.92E-10 2.85E-10 3.86E-10 5.14E-10 6.64E-10 1.05E-09 1.34E-09	1.20E-10 1.20E-10 2.85E-10 3.86E-10 5.14E-10 6.64E-10 1.05E-09 1.76E-09	1.20E-10 1.92E-10 2.85E-10 3.86E-10 6.64E-10 1.05E-09 1.34E-09 2.36E-09	1.20E-10 1.92E-10 2.85E-10 3.86E-10 6.64E-10 1.05E-09 1.34E-09 2.36E-09 3.14E-09	1.20E-10 1.92E-10 2.85E-10 3.86E-10 6.64E-10 1.05E-09 1.34E-09 2.36E-09 3.14E-09 3.14E-09 5.35E-09	1.20E-10 1.92E-10 2.85E-10 3.86E-10 6.64E-10 1.05E-09 1.34E-09 1.76E-09 3.14E-09 3.14E-09 5.35E-09 6.92E-09	1.20E-10 1.92E-10 2.85E-10 3.86E-10 6.64E-10 6.64E-10 1.05E-09 1.34E-09 3.14E-09 3.14E-09 6.92E-09 9.06E-09	1.20E-10 1.92E-10 2.85E-10 3.86E-10 6.64E-10 6.64E-10 1.05E-09 1.76E-09 3.14E-09 3.14E-09 5.35E-09 6.92E-09 9.06E-09	1.92E-10 2.85E-10 3.86E-10 6.64E-10 6.64E-10 1.05E-09 1.76E-09 3.14E-09 3.14E-09 5.35E-09 6.92E-09 1.17E-08	1.92E-10 2.85E-10 3.86E-10 6.64E-10 6.64E-10 1.05E-09 1.34E-09 2.36E-09 3.14E-09 5.35E-09 6.92E-09 1.77E-08 1.52E-08	1.92E-10 2.85E-10 3.86E-10 6.64E-10 6.64E-10 1.05E-09 1.34E-09 2.36E-09 3.14E-09 3.14E-09 5.35E-09 6.92E-09 1.77E-08 1.52E-08	1.92E-10 2.85E-10 3.86E-10 6.64E-10 6.64E-10 1.05E-09 1.34E-09 2.36E-09 3.14E-09 5.35E-09 6.92E-09 1.52E-08 1.52E-08 3.23E-08	1.92E-10 2.85E-10 3.86E-10 6.64E-10 6.64E-10 1.05E-09 1.34E-09 3.14E-09 5.35E-09 6.92E-09 1.52E-08 3.23E-08 3.23E-08	1.92E-10 2.85E-10 3.86E-10 6.64E-10 6.64E-10 1.05E-09 1.34E-09 2.36E-09 6.92E-09 9.06E-09 9.06E-09 1.52E-08 3.23E-08 3.23E-08 5.35E-08	1.92E-10 2.85E-10 3.86E-10 6.64E-10 6.64E-10 1.05E-09 1.34E-09 2.36E-09 2.36E-09 6.92E-09 9.06E-09 9.06E-09 2.54E-08 3.23E-08 6.52E-08
L = .21 Id	6.66E-10	8.89E-10	1.17E-09	1.48E-09	1.91E-09	2.51E-09	3.36E-09	4.47E-09	5.89E-09	7.71E-09	4 00 00	20100.	1.32E-08	1.32E-08 1.74E-08	1.32E-08 1.74E-08 2.27E-08	1.32E-08 1.32E-08 1.74E-08 2.27E-08 2.96E-08	1.32E-08 1.74E-08 2.27E-08 2.96E-08 3.88E-08	1.32E-08 1.74E-08 2.27E-08 2.96E-08 3.88E-08	1.32E-08 1.32E-08 1.74E-08 2.27E-08 2.96E-08 3.88E-08 5.07E-08	1.32E-08 1.32E-08 1.74E-08 2.96E-08 3.88E-08 5.07E-08 6.62E-08	1.32E-08 1.32E-08 1.74E-08 2.96E-08 3.88E-08 5.07E-08 6.62E-08 8.60E-08	1.32E-08 1.32E-08 2.27E-08 2.96E-08 3.88E-08 5.07E-08 6.62E-08 1.12E-07	1.32E-08 1.32E-08 2.27E-08 2.96E-08 3.88E-08 5.07E-08 6.62E-08 8.60E-08 1.12E-07	1.32E-08 1.74E-08 2.27E-08 2.96E-08 3.88E-08 5.07E-08 6.62E-08 1.12E-07 1.45E-07	1.32E-08 1.74E-08 2.27E-08 2.96E-08 3.88E-08 6.62E-08 8.60E-08 1.12E-07 1.87E-07 3.10E-07	1.32E-08 1.74E-08 2.27E-08 2.96E-08 3.88E-08 6.62E-08 8.60E-08 1.12E-07 1.87E-07 3.10E-07	1.32E-08 1.32E-08 2.27E-08 2.96E-08 3.88E-08 6.62E-08 8.60E-08 1.12E-07 1.45E-07 3.10E-07 5.07E-07	1.32E-08 1.32E-08 2.27E-08 2.96E-08 3.88E-08 6.62E-08 1.12E-07 1.45E-07 3.10E-07 5.07E-07	1.32E-08 1.74E-08 2.27E-08 2.96E-08 3.88E-08 6.62E-08 1.12E-07 1.87E-07 3.10E-07 3.98E-07 3.98E-07 8.13E-07	1.32E-08 1.74E-08 2.27E-08 2.96E-08 3.88E-08 6.62E-08 1.12E-07 1.87E-07 3.10E-07 3.10E-07 3.98E-07 3.98E-07 1.02E-07	1.32E-08 1.74E-08 2.27E-08 2.96E-08 3.88E-08 6.62E-08 6.62E-08 1.12E-07 1.87E-07 3.10E-07 3.98E-07 3.98E-07 1.02E-06 1.29E-06	1.32E-08 1.74E-08 2.27E-08 2.96E-08 3.88E-08 6.62E-08 6.62E-08 1.12E-07 1.87E-07 3.98E-07 3.98E-07 1.02E-06 1.29E-06	1.32E-08 1.32E-08 2.27E-08 2.96E-08 3.88E-08 6.62E-08 6.62E-08 1.12E-07 1.87E-07 3.98E-07 3.98E-07 1.02E-06 1.29E-06 1.59E-06	1.32E-08 1.32E-08 2.27E-08 2.96E-08 3.88E-08 6.62E-08 6.62E-08 1.12E-07 1.87E-07 3.98E-07 3.98E-07 1.02E-06 1.29E-06 1.59E-06	1.32E-08 1.32E-08 2.27E-08 2.96E-08 3.88E-08 6.62E-08 6.62E-08 1.12E-07 1.87E-07 3.98E-07 3.98E-07 1.02E-06 1.29E-06 1.59E-06 2.41E-06	1.32E-08 1.32E-08 2.27E-08 2.96E-08 3.88E-08 6.62E-08 6.62E-08 1.12E-07 1.87E-07 3.98E-07 3.98E-07 1.02E-06 1.29E-06 1.59E-06 2.94E-06 3.56E-06
8																																				
₽	0.05	0.05	0.05	0.05	0.05	0.05	0.05	0.05	0.05	0.05		0.05	0.05	0.05 0.05 0.05	0.05 0.05 0.05 0.05	0.05 0.05 0.05 0.05	0.05 0.05 0.05 0.05 0.05	0.05 0.05 0.05 0.05 0.05	0.00 0.00 0.00 0.00 0.00 0.00 0.00	0.05 0.05 0.05 0.05 0.05 0.05 0.05	0.05 0.05 0.05 0.05 0.05 0.05 0.05	0.05 0.05 0.05 0.05 0.05 0.05 0.05 0.05	0.05 0.05 0.05 0.05 0.05 0.05 0.05 0.05	0.000000000000000000000000000000000000	0.000000000000000000000000000000000000	0.05 0.05 0.05 0.05 0.05 0.05 0.05 0.05	0.05 0.05 0.05 0.05 0.05 0.05 0.05 0.05	00000000000000000000000000000000000000	0.05 0.05 0.05 0.05 0.05 0.05 0.05 0.05	0.05 0.05 0.05 0.05 0.05 0.05 0.05 0.05	00000000000000000000000000000000000000	000000000000000000000000000000000000000	00000000000000000000000000000000000000	0.05 0.05 0.05 0.05 0.05 0.05 0.05 0.05	0.05 0.05 0.05 0.05 0.05 0.05 0.05 0.05	0 0 0 0 0 0 0 0 0 0 0 0 0 0 0 0 0 0 0

Ratio	Shift02	4.84E+01	4.97E+01	4.98E+01	4.97E+01	4.93E+01	4.88E+01	4.87E+01	4.90E+01	4.95E+01	4.99E+01	5.01E+01	5.00E+01	4.96E+01	4.95E+01	4.93E+01	4.91E+01	4.91E+01	4.88E+01	4.90E+01	4.91E+01	4.92E+01	4.93E+01	4.93E+01	4.91E+01	4.91E+01	4.87E+01	4.88E+01	4.94E+01	4.97E+01	4.95E+01	4.95E+01	4.97E+01	4.94E+01	4 94F+01	֡֝֝֝֝֝֡֓֝֝֝֓֓֓֝֝֝֡֓֓֓֝֝֡֓֓֓֓֓֓֜֝֡֓֜֝֓֓֜֝֡֓֜֜֜֝֡֓֓֓֡֓֡֓֡֡֝֡֡֡
2	H Sh	_	4.9	4. 9.	4.9	.9.	4. 8.	4.8	છ.4	4.9	4.9	5.0	5.0	2. 20.4	4.9	4.9	4.9	4.9	4.8	- 4.9	4.9	4.9	4.9	_	4.9	4.9	4.8	_	_		4.9	_	_	4. Q.	4	
Ratio	d Shift01	4.43E+01	4.55E+01	4.67E+01	4.65E+01	4.63E+01	4.62E+01	4.59E+01	4.60E+01	4.67E+01	4.71E+01	4.73E+01	4.76E+01	4.72E+01	4.69E+01	4.71E+01	4.71E+01	4.67E+01	4.66E+01	4.70E+01	4.68E+01	4.67E+01	4.72E+01	4.75E+01	4.71E+01	4.71E+01	4.73E+01	4.70E+01	4.71E+01	4.78E+01	4.79E+01	4.81E+01	4.79E+01	4.75E+01	4 78F+01	
Ratio	No d shift	4.13E+01	4.16E+01	4.28E+01	4.36E+01	4.34E+01	4.35E+01	4.35E+01	4.34E+01	4.38E+01	4.44E+01	4.47E+01	4.49E+01	4.49E+01	4.47E+01	4.47E+01	4.50E+01	4.47E+01	4.44E+01	4.49E+01	4.49E+01	4.45E+01	4.48E+01	4.55E+01	4.54E+01	4.53E+01	4.55E+01	4.56E+01	4.53E+01	4.55E+01	4.61E+01	4.67E+01	4.66E+01	4.58E+01	4.59F+01	
Ratio	d Shift +.01	3.88E+01	3.92E+01	4.00E+01	4.07E+01	4.07E+01	4.09E+01	4.11E+01	4.14E+01	4.17E+01	4.21E+01	4.24E+01	4.24E+01	4.25E+01	4.26E+01	4.27E+01	4.28E+01	4.25E+01	4.27E+01	4.29E+01	4.27E+01	4.28E+01	4.32E+01	4.35E+01	4.36E+01	4.37E+01	4.38E+01	4.40E+01	4.38E+01	4.39E+01	4.48E+01	4.52E+01	4.46E+01	4.43E+01	4 45F+01	
Ratio	d Shift +.02	3.65E+01	3.66E+01	3.73E+01	3.82E+01	3.83E+01	3.87E+01	3.92E+01	3.94E+01	3.95E+01	4.00E+01	4.01E+01	4.01E+01	4.05E+01	4.07E+01	4.05E+01	4.07E+01	4.09E+01	4.08E+01	4.08E+01	4.10E+01	4.12E+01	4.13E+01	4.18E+01	4.20E+01	4.21E+01	4.22E+01	4.25E+01	4.22E+01	4.27E+01	4.34E+01	4.32E+01	4.31E+01	4.29E+01	4 25F+01	
L = 8.4	Sfunc	6.57E+04	6.20E+04	5.79E+04	5.43E+04	5.17E+04	4.64E+04	4.38E+04	4.23E+04	4.02E+04	3.93E+04	3.64E+04	3.40E+04	3.23E+04	3.11E+04	2.98E+04	2.75E+04	2.67E+04	2.57E+04	2.41E+04	2.31E+04	2.27E+04	2.14E+04	1.99E+04	1.97E+04	1.92E+04	1.81E+04	1.75E+04	1.66E+04	1.64E+04	1.61E+04	1.52E+04	1.46E+04	1.45E+04	1 40F+04	
L = .21	Sfunc	1.66E+03	1.43E+03	1.36E+03	1.23E+03	1.14E+03	1.09E+03	1.04E+03	9.83E+02	9.06E+02	8.65E+02	8.14E+02	7.59E+02	7.34E+02	6.82E+02	6.49E+02	6.36E+02	5.97E+02	5.61E+02	5.46E+02	5.23E+02	4.97E+02	4.77E+02	4.53E+02	4.31E+02	4.03E+02	4.03E+02	3.96E+02	3.70E+02	3.53E+02	3.47E+02	3.32E+02	3.10E+02	3.03E+02	3 02F+02	
L = 8.4	Rd	1.87E+04	1.80E+04	1.74E+04	1.69E+04	1.63E+04	1.58E+04	1.54E+04	1.50E+04	1.45E+04	1.42E+04	1.38E+04	1.34E+04	1.31E+04	1.28E+04	1.25E+04	1.22E+04	1.19E+04	1.16E+04	1.14E+04	1.12E+04	1.09E+04	1.07E+04	1.05E+04	1.03E+04	1.01E+04	9.93E+03	9.75E+03	9.58E+03	9.42E+03	9.25E+03	9.10E+03	8.95E+03	8.81E+03	8 66F+03	
L = .21	Rd	4.80E+02	4.65E+02	4.51E+02	4.38E+02	4.27E+02	4.15E+02	4.05E+02	3.95E+02	3.85E+02	3.77E+02	3.68E+02	3.60E+02	3.53E+02	3.46E+02	3.39E+02	3.33E+02	3.26E+02	3.21E+02	3.15E+02	3.10E+02	3.05E+02	3.00E+02	2.95E+02	2.91E+02	2.87E+02	2.83E+02	2.78E+02	2.75E+02	2.71E+02	2.68E+02	2.64E+02	2.61E+02	2.58E+02	2.55F+02	,
L = 8.4	₽	2.68E-06	2.77E-06	2.87E-06	2.97E-06	3.06E-06	3.16E-06	3.25E-06	3.34E-06	3.44E-06	3.53E-06	3.63E-06	3.72E-06	3.82E-06	3.91E-06	4.01E-06	4.10E-06	4.20E-06	4.29E-06	4.39E-06	4.48E-06	4.57E-06	4.67E-06	4.76E-06	4.85E-06	4.94E-06	5.04E-06	5.13E-06	5.22E-06	5.31E-06	5.40E-06	5.49E-06	5.59E-06	5.68E-06	5 78F-06	
L = .21	D	1.04E-04	1.07E-04	1.11E-04	1.14E-04	1.17E-04	1.20E-04	1.24E-04	1.27E-04	1.30E-04	1.33E-04	1.36E-04	1.39E-04	1.42E-04	1.45E-04	1.47E-04	1.50E-04	1.53E-04	1.56E-04	1.59E-04	1.61E-04	1.64E-04	1.67E-04	1.69E-04	1.72E-04	1.75E-04	1.77E-04	1.80E-04	1.82E-04	1.84E-04	1.87E-04	1.89E-04	1.92E-04	1.94E-04	1.96E-04	
	6	1.03	5	1.05	1.06	1.07	1.08	1.09	1.1	1.11	1.12	1.13	1.14	1.15	1.16	1.17	1.18	1.19	1.2	1.21	1.22	1.23	1.24	1.25	1.26	1.27	1.28	1.29	د .	1.31	1.32	1.33	1.3	1.35	1.36	
	P	0.05	0.05	0.05	0.05	0.05	0.05	0.05	0.05	0.05	0.05	0.05	0.05	0.05	0.05	0.05	0.05	0.05	0.05	0.05	0.05	0.05	0.05	0.05	0.05	0.05	0.05	0.05	0.05	0.05	0.05	0.05	0.05	0.05	0.05	

	L = .21	L = 8.4	L = .21	L = 8.4	L = .21	L = 8.4	Ratio	Ratio	Ratio	Ratio	Ratio
	9	ᅙ	Rd	Rd	Sfunc	Sfunc	d Shift +.02	d Shift +.01	No d shift	d Shift01	d Shift02
7	2.03E-04	6.04E-06	2.46E+02	8.27E+03	2.52E+02	1.24E+04	4.29E+01	4.4E+01	4.56E+01	4.78E+01	4.91E+01
7	2.05E-04		2.44E+02	8.15E+03	2.56E+02	1.17E+04	4.37E+01	4.49E+01	4.66E+01	4.78E+01	4.84E+01
ď	07E-04		2.41E+02	8.04E+03	2.56E+02	1.16E+04	4.36E+01	4.49E+01	4.61E+01	4.67E+01	4.83E+01
7	09E-04			7.92E+03	2.42E+02	1.12E+04	4.27E+01	4.41E+01	4.54E+01	4.69E+01	4.92E+01
Ŋ	12E-04		2.36E+02	7.82E+03	2.43E+02	1.08E+04	4.29E+01	4.42E+01	4.56E+01	4.78E+01	4.94E+01
~	.14E-04		2.34E+02	7.71E+03	2.38E+02	1.07E+04	4.37E+01	4.50E+01	4.63E+01	4.78E+01	4.96E+01
~	.16E-04			7.60E+03	2.15E+02	1.01E+04	4.40E+01	4.51E+01	4.64E+01	4.81E+01	5.04E+01
N	18E-04	6.66E-06		7.50E+03	2.00E+02	9.90E+03	4.43E+01	4.56E+01	4.67E+01	4.90E+01	4.94E+01
N	.20E-04		2.28E+02	7.40E+03	2.07E+02	9.63E+03	4.49E+01	4.64E+01	4.78E+01	4.82E+01	4.87E+01
N	.22E-04		2.25E+02	7.31E+03	2.04E+02	9.33E+03		4.53E+01	4.68E+01	4.73E+01	
N	.24E-04		2.24E+02	7.22E+03	1.90E+02	9.53E+03			4.58E+01		
W	.26E-04		2.22E+02	7.12E+03	2.06E+02	8.71E+03					
W	2.28E-04		2.19E+02	7.04E+03	1.88E+02	8.41E+03					
N	.30E-04		2.18E+02	6.95E+03							

Table 3. Shift and Ratio Data for Halo Devices with L=0.42μm and L=8.4μm

Ratio d shift12	3.71E-02 4.15E-02 3.94E-02	4.02E-02 5.47E-02 7.62E-02 7.90E-02	1.16E-01 2.84E-01 5.89E-01 9.41E-01	2.29E+00 4.07E+00 1.25E+01 1.61E+02 2.73E+02	6.88E+02 9.80E+02 1.29E+03 1.05E+03 1.16E+03 2.21E+02 9.15E+01 6.41E+01 5.29E+01 5.29E+01
Ratio d shift10	1.23E-01 7.28E-02 4.71E-02	3.51E-02 3.05E-02 2.26E-02 1.23E-02	2.47E-02 9.69E-02 1.84E-01 3.66E-01 8.42E-01	1.32E+00 2.51E+00 7.90E+00 9.90E+01 1.56E+02	3.64E+02 5.18E+02 7.08E+02 6.53E+02 1.23E+02 1.23E+01 3.50E+01 3.09E+01 3.07E+01
Ratio d shift08	2.35E-01 3.90E-01 1.57E-01	6.15E-02 3.64E-02 1.98E-02 6.85E-03	7.34E-03 1.51E-02 3.92E-02 1.25E-01 2.63E-01	5.14E-01 1.24E+00 4.56E+00 6.11E+01 9.83E+01	2.24E+02 2.95E+02 3.75E+02 3.14E+02 3.59E+02 6.95E+01 1.95E+01 1.70E+01 1.69E+01
L = 8.4 Sfunc 3.49E+09	4.69E+09 5.24E+09	1.42E+10 2.47E+09 3.80E+08 5.42E+08	2.43E+09 1.10E+09 2.03E+09 2.38E+09	3.10E+09 4.85E+09 2.71E+09 8.68E+09 3.37E+10	4.77E+11 1.38E+11 5.37E+11 6.28E+10 1.41E+10 5.75E+09 3.56E+09 2.24E+09 1.05E+09
L = .42 Sfunc 4.97E+07	2.65E+10 7.61E+10		9.24E+09 1.08E+10 4.05E+10 1.24E+10	3.34E+11 3.08E+11 1.79E+11 3.46E+10	2.79E+10 1.39E+10 7.07E+09 4.12E+09 2.77E+09 1.98E+09 1.51E+09 1.26E+09 1.10E+09 8.56E+08
L = 8.4 Rd -5.03E+08 -5.29E+08 -5.72E+08	-6.22E+08 -6.66E+08	4.02E+08 4.43E+08 4.51E+08 4.51E+08	4.62E+08 -5.00E+08 4.40E+08 4.59E+08	-5.06E+08 -5.50E+08 -6.03E+08 -6.04E+08 -7.76E+08	-1.28E+09 -1.03E+10 1.48E+09 4.33E+08 2.22E+08 1.50E+08 7.93E+07 6.20E+07 5.04E+07
L = .42 Rd 9.96E+08 9.45E+08	1.14E+09 1.53E+09 2.67E+09	4.72E+09 -1.28E+10 -3.08E+09 -2.21E+09	-1.87E+09 -2.39E+09 -1.65E+09 -1.58E+09	-2.28E+09 -5.00E+09 4.41E+09 1.15E+09 8.33E+08	4.62E+08 2.75E+08 1.83E+08 1.34E+08 7.83E+07 6.12E+07 4.81E+07 3.61E+07 2.61E+07
L = 8.4 Id -9.95E-11 -9.46E-11	-8.04E-11 -7.51E-11 -6.88E-11	-1.24E-10 -1.13E-10 -1.11E-10	-1.08E-10 -1.00E-10 -1.14E-10 -1.09E-10	-9.89E-11 -9.10E-11 -8.29E-11 -6.44E-11	4.85E-12 3.39E-11 1.16E-10 2.25E-10 3.32E-10 4.68E-10 6.31E-10 8.07E-10 9.91E-10
L = .42 Id 5.02E-11 5.29E-11	4.37E-11 3.28E-11	1.06E-11 -3.90E-12 -1.63E-11	-2.68E-11 -2.09E-11 -3.03E-11 -3.16E-11	-2.20E-11 -1.00E-11 1.14E-11 4.33E-11 6.01E-11	1.08E-10 1.82E-10 2.73E-10 3.74E-10 4.95E-10 6.39E-10 8.17E-10 1.04E-09 1.38E-09 2.63E-09
					0.05 0.21 0.05 0.21 0.05 0.22 0.05 0.24 0.05 0.26 0.05 0.26 0.05 0.28 0.05 0.28

Ratio	d shift12	6.18E+01	6.95E+01	7.74E+01	8.14E+01	7.76E+01	7.35E+01	7.37E+01	7.14E+01	6.82E+01	6.61E+01	6.48E+01	6.29E+01	6.00E+01	5.74E+01	5.51E+01	5.28E+01	5.04E+01	4.80E+01	4.56E+01	4.33E+01	4.15E+01	3.95E+01	3.75E+01	3.59E+01	3.43E+01	3.28E+01	3.20E+01	3.12E+01	3.02E+01	2.94E+01	2.86E+01	2.74E+01	2.62E+01	2.56E+01	2.51E+01	2.47E+01
Ratio	d shift10	3.40E+01	3.83E+01	4.30E+01	4.55E+01	4.32E+01	4.10E+01	4.14E+01	4.03E+01	3.89E+01	3.80E+01	3.75E+01	3.68E+01	3.54E+01	3.41E+01	3.34E+01	3.26E+01	3.15E+01	3.04E+01	2.94E+01	2.84E+01	2.75E+01	2.66E+01	2.58E+01	2.51E+01	2.44E+01	2.37E+01	2.33E+01	2.29E+01	2.25E+01	2.22E+01	2.18E+01	2.11E+01	2.04E+01	2.01E+01	1.99E+01	1.98E+01
Ratio	d shift08	1.89E+01	2.12E+01	2.37E+01	2.51E+01	2.40E+01	2.29E+01	2.31E+01	2.25E+01	2.18E+01	2.15E+01	2.14E+01	2.11E+01	2.05E+01	1.99E+01	1.97E+01	1.94E+01	1.91E+01	1.88E+01	1.84E+01	1.80E+01	1.77E+01	1.74E+01	1.71E+01	1.69E+01	1.68E+01	1.66E+01	1.65E+01	1.65E+01	1.64E+01	1.63E+01	1.63E+01	1.60E+01	1.56E+01	1.55E+01	1.55E+01	1.55E+01
L = 8.4	Sfunc	8.36E+08	8.09E+08	5.79E+08	3.65E+08	2.96E+08	2.20E+08	1.53E+08	1.09E+08	8.23E+07	6.35E+07	4.60E+07	3.30E+07	2.45E+07	1.86E+07	1.40E+07	1.06E+07	8.04E+06	6.04E+06	4.70E+06	3.67E+06	2.83E+06	2.25E+06	1.80E+06	1.44E+06	1.17E+06	9.65E+05	7.93E+05	6.64E+05	5.90E+05	5.01E+05	4.00E+05	3.43E+05	2.93E+05	2.57E+05	2.24E+05	1.98E+05
L = .42	Sfunc	4.17E+08	3.06E+08	2.35E+08	1.79E+08	1.35E+08	9.96E+07	7.22E+07	5.38E+07	4.05E+07		2.23E+07	1.64E+07	1.23E+07	9.23E+06	6.83E+06	5.11E+06	3.83E+06	2.85E+06	2.14E+06	1.62E+06	1.22E+06	9.44E+05	7.15E+05	5.44E+05	4.21E+05	3.30E+05		2.03E+05	1.62E+05	1.31E+05	1.05E+05	8.54E+04	7.04E+04	5.80E+04	4.87E+04	4.13E+04
L = 8.4	Rd	3.29E+07	2.43E+07	1.67E+07	1.28E+07	9.45E+06	6.84E+06	5.05E+06	3.78E+06		2.14E+06	1.60E+06	1.22E+06	9.37E+05	7.26E+05	5.64E+05	4.46E+05		2.85E+05	2.33E+05	1.91E+05	1.59E+05	1.34E+05	1.14E+05	9.82E+04	8.54E+04	7.48E+04		5.89E+04	5.28E+04	4.71E+04	4.28E+04	3.91E+04	3.59E+04		3.08E+04	2.87E+04
L = .42	R	1.41E+07	1.07E+07	8.01E+06	5.96E+06	4.43E+06	3.27E+06	2.43E+06	1.82E+06	1.36E+06	1.01E+06	7.55E+05	5.65E+05	4.26E+05	3.20E+05	2.42E+05	1.83E+05	1.40E+05	1.07E+05	8.25E+04	6.38E+04	5.00E+04	3.93E+04	3.11E+04	2.50E+04	2.03E+04	1.66E+04	1.37E+04	1.14E+04	9.60E+03	8.15E+03	6.97E+03	6.04E+03	5.27E+03	4.63E+03	4.11E+03	3.66E+03
L = 8.4	<u>D</u>	1.52E-09	2.05E-09	2.99E-09	3.92E-09	5.29E-09	7.31E-09	9.90E-09	1.32E-08	1.74E-08	2.34E-08	3.13E-08	4.11E-08	5.33E-08		8.86E-08	1.12E-07	1.42E-07	1.76E-07	2.15E-07	2.62E-07	3.14E-07	3.72E-07	4.38E-07	5.09E-07	5.86E-07	6.69E-07	7.56E-07	8.49E-07	9.46E-07	1.06E-06	1.17E-06	1.28E-06	1.39E-06	1.51E-06	1.62E-06	1.74E-06
L = .42	므	3.54E-09	4.69E-09	6.24E-09	8.39E-09	1.13E-08	1.53E-08	2.05E-08	2.74E-08	3.68E-08	4.94E-08	6.62E-08	8.84E-08	1.17E-07	1.56E-07	2.07E-07	2.73E-07	3.58E-07	4.69E-07	6.06E-07	7.84E-07	1.00E-06	1.27E-06	1.61E-06	2.00E-06	2.47E-06	3.02E-06	3.66E-06	4.39E-06	5.21E-06	6.14E-06	7.17E-06	8.28E-06	9.49E-06	1.08E-05	1.22E-05	1.37E-05
	7	9	9	9	9	9	92	9	9	9	05	9	9	9	.05	.05	9	9	9	.05	92	9	90	9	.05	9	9	9	05	9	9	9	9	92	0.05 0.64	95	0.

.79E+05 1.55E+01 .58E+05 1.56E+01 .40E+05 1.56E+01 .26E+05 1.56E+01 .15E+05 1.56E+01
. 8 8 8 8 8 8 8 8 8 8 8 8 8 8 8 8 8 8 8
1.58E+05 1.40E+05 1.26E+05 1.15E+05 1.04E+05 9.31E+04
2.54E+04 2.20E+04 1.89E+04 1.65E+04
2.52E+04 2.37E+04 2.24E+04 2.12E+04 2.01E+04
3.28E+03 2.96E+03 2.69E+03 2.45E+03 2.25E+03 2.07E+03 1.92E+03
1.86E-06 1.99E-06 2.11E-06 2.24E-06 2.36E-06 2.49E-06 2.62E-06
1.52E-05 1 1.69E-05 1 1.86E-05 2 2.04E-05 2 2.22E-05 2 2.41E-05 2 2.81E-05 2
0.67 1 0.68 1 0.69 1 0.69 1 0.70 2 0.71 2 0.72 2 0.73 2 0.74 2 0.74 2 0.74 2

5	\$	L = .42	L = 8.4 Id	L = .42 Rd	L = 8.4 Rd	L = .42 Sfunc	L = 8.4 Sfunc	Ratio d shift08	Ratio d shift10	Ratio d shift12
0.05	1.03	Τ.	6.49E-06	5.44E+02	7.70E+03	1.27E+03	1.47E+04		1.89E+01	2.04E+01
0.05	2.	4	6.62E-06	5.31E+02	7.55E+03	1.20E+03	1.49E+04	1.73E+01	1.87E+01	2.01E+01
0.05	1.05	9.62E-05	6.75E-06	5.20E+02	7.41E+03	1.14E+03	1.39E+04	1.74E+01	1.88E+01	2.04E+01
0.05	1.06	w	6.88E-06	5.09E+02	7.27E+03	1.09E+03	1.27E+04	1.74E+01	1.87E+01	2.06E+01
0.05	1.07	ب	6.99E-06	4.98E+02	7.15E+03	1.20E+03	1.24E+04	1.71E+01	1.86E+01	2.03E+01
0.05	1.08	1.03E-04	7.12E-06	4.84E+02	7.03E+03	1.17E+03	1.23E+04	1.69E+01	1.85E+01	2.01E+01
0.05	1.09	1.05E-04	7.24E-06	4.75E+02	6.91E+03	9.47E+02	1.13E+04	1.71E+01	1.87E+01	2.05E+01
0.05	1.10	1.07E-04	7.35E-06	4.66E+02	6.80E+03	8.90E+02	1.09E+04	1.73E+01	1.88E+01	2.04E+01
0.05	1.11	1.09E-04	7.48E-06	4.57E+02	6.69E+03	8.56E+02	1.09E+04	1.72E+01	1.89E+01	1.99E+01
0.05	1.12	1.12E-04	7.60E-06	4.48E+02	6.58E+03	8.16E+02	1.02E+04	1.74E+01	1.89E+01	2.01E+01
0.05	1.13	1.13E-04	7.71E-06	4.41E+02	6.48E+03	7.86E+02	9.89E+03	1.77E+01	1.86E+01	2.01E+01
0.05	1.14	1.16E-04	7.83E-06	4.33E+02	6.38E+03	7.60E+02	9.65E+03	1.75E+01	1.86E+01	1.98E+01
0.05	1.15	1.18E-04	7.95E-06	4.26E+02	6.29E+03	7.24E+02	9.18E+03	1.73E+01	1.87E+01	1.98E+01
0.05	1.16	1.20E-04	8.06E-06	4.18E+02	6.20E+03	7.09E+02	8.77E+03	1.74E+01	1.86E+01	2.01E+01
0.05	1.17	1.22E-04	ထ	4.11E+02	6.11E+03		8.75E+03	1.74E+01	1.85E+01	2.01E+01
0.05	1.18	1.24E-04	8.30E-06	4.05E+02	6.02E+03	6.63E+02	8.50E+03	1.74E+01	1.88E+01	2.02E+01
0.05	1.19	1.26E-04	8.41E-06	3.98E+02	5.94E+03	5.96E+02	7.97E+03	1.76E+01	1.91E+01	2.05E+01
0.05	1.20	1.27E-04	8.52E-06	3.93E+02	5.87E+03	5.70E+02	7.93E+03	1.78E+01	1.90E+01	2.06E+01
0.05	1.21	1.29E-04	8.64E-06	3.87E+02	5.79E+03	5.84E+02	7.92E+03	1.75E+01	1.88E+01	2.04E+01
0.05	1.22	1.31E-04	8.76E-06	3.81E+02	5.71E+03	5.45E+02	7.28E+03	1.74E+01	1.88E+01	2.02E+01
0.05	1.23	1.33E-04	8.86E-06	3.76E+02	5.64E+03	5.23E+02	6.48E+03	1.76E+01	1.91E+01	2.01E+01
0.05	1.24	1.35E-04	8.96E-06	3.71E+02	5.58E+03	5.08E+02	6.61E+03	1.76E+01	1.88E+01	1.99E+01
0.05	1.25	1.37E-04	9.08E-06	3.66E+02	5.51E+03	5.14E+02	6.95E+03	1.78E+01	1.87E+01	1.95E+01
0.05	1.26	1.39E-04	O	3.60E+02	5.44E+03	4.82E+02	6.55E+03	1.81E+01	1.91E+01	1.97E+01
0.05	1.27	1.40E-04	9.30E-06	3.56E+02	5.38E+03	4.50E+02	6.21E+03	1.81E+01	1.89E+01	2.01E+01
0.05	1.28	1.42E-04	0,	3.51E+02	5.31E+03	4.57E+02	6.25E+03	1.78E+01	1.84E+01	1.98E+01
0.05	1.29	1.44E-04	9.52E-06	3.47E+02	5.25E+03	4.28E+02	5.77E+03	1.74E+01	1.85E+01	1.97E+01
0.05	1.30	1.46E-04	9.62E-06	3.43E+02	5.20E+03	4.11E+02	5.52E+03	1.72E+01	1.86E+01	1.99E+01
0.05	1.31	1.48E-04	9.72E-06	3.39E+02	5.14E+03	4.07E+02	5.47E+03	1.74E+01	1.86E+01	1.99E+01
0.05	1.32	1.49E-04	9.82E-06	3.35E+02	5.09E+03	3.76E+02	5.40E+03	1.75E+01	1.87E+01	2.00E+01
0.05	1.33	1.51E-04	9.93E-06	3.31E+02	5.03E+03	3.78E+02	5.35E+03	1.76E+01	1.88E+01	2.00E+01
0.05	1.3 4	1.53E-04	1.00E-05	3.27E+02	4.98E+03		5.03E+03	1.77E+01	1.89E+01	2.01E+01
0.05	1.35	1.54E-04	1.01E-05	3.24E+02	4.93E+03		4.75E+03	1.78E+01	1.90E+01	2.01E+01
0.05	1.36	1.56E-04	1.02E-05	3.21E+02	4.89E+03		4.77E+03	1.77E+01	1.88E+01	.97
0.05	1.37	1.58E-04	1.03E-05	~	4.84E+03	3.32E+02	4.80E+03	1.78E+01	1.89E+01	1.96E+01
0.05	1.38	1.59E-04	1.04E-05	3.14E+02	4.79E+03	3.29E+02	4.37E+03	1.82E+01	1.91E+01	

Ratio	d shift12														
Ratio	d shift 10	1.87E+01													
Ratio	d shift08	1.80E+01	1.77E+01	1.78E+01											
L = 8.4	Sfunc	4.51E+03	4.54E+03	3.91E+03	3.95E+03	4.09E+03	3.82E+03	3.75E+03	3.79E+03	3.63E+03	3.48E+03	3.23E+03	3.37E+03	3.23E+03	
L = .42	Sfunc	3.28E+02	3.02E+02	2.87E+02	2.82E+02	2.81E+02	2.76E+02	2.58E+02	2.41E+02	2.45E+02	2.41E+02	2.41E+02	2.33E+02	2.22E+02	
L = 8.4	Rd	4.75E+03	4.70E+03	4.66E+03	4.62E+03	4.58E+03	4.54E+03	4.50E+03	4.47E+03	4.43E+03	4.39E+03	4.36E+03	4.33E+03	4.29E+03	4.26E+03
L = .42	Rd	3.10E+02	3.07E+02	3.04E+02	3.02E+02	2.99E+02	2.96E+02	2.93E+02	2.91E+02	2.88E+02	2.86E+02	2.83E+02	2.81E+02	2.79E+02	2.77E+02
L = 8.4	D													1.17E-05	
L = .42	ㅁ	1.61E-04	1.63E-04	1.64E-04	1.66E-04	1.67E-04	1.69E-04	1.71E-04	1.72E-04	1.73E-04	1.75E-04	1.76E-04	1.78E-04	1.79E-04	1.81E-04
	٧g	1.39	1.40	1.41	1.42	1.43	1 .44	1.45	1.46	1.47	1.48	1.49	1.50	1.51	1.52
	P/	0.05	0.05	0.05	0.05	0.05	0.05	0.05	0.05	0.05	0.05	0.05	0.05	0.05	0.05

Table 4. Shift and Ratio Data for Halo Devices with L=0.21μm and L=8.4μm

Ratio d shift18	3.26E-01 6.80E-01 1.08E+00 1.45E+00 7.04E-01 9.20E-01 1.61E+00 3.57E+00 8.84E+00 1.66E+01 7.00E+02 1.17E+03 7.00E+03 4.00E+03 4.36E+03 4.36E+03 4.36E+03 5.29E+03 5.29E+03 5.29E+03 7.25E+02 7.25E+02 7.25E+02 7.25E+03 7.25E+03 7.25E+03	2.11E+02 2.19E+02
	5.14E-02 1.07E-01 5.26E-01 6.09E-01 3.25E-01 1.46E+00 2.08E+00 3.05E+00 3.05E+00 3.05E+00 1.59E+03 2.22E+03 2.93E+02 1.44E+02 1.26E+03 2.08E+02 1.26E+03	1.18E+02 1.23E+02
	1.58E-02 4.34E-02 8.24E-02 1.55E-01 1.18E-01 1.97E-01 3.99E-01 6.95E-01 1.11E+00 2.92E+00 2.92E+00 2.92E+00 1.73E+01 2.25E+02 3.79E+02 3.79E+02 1.26E+03 1.35E+03 1.49E+03 2.84E+02 8.08E+01	6.60E+01 6.88E+01
	9.70E-03 1.04E-02 1.33E-02 1.48E-02 2.45E-02 1.45E-01 3.13E-01 3.13E-01 1.56E+00 1.01E+01 1.33E+02 5.09E+02 5.09E+02 7.18E+02 6.46E+01 4.51E+01	3.71E+01 3.85E+01
	1.34E-02 9.78E-03 8.20E-03 7.52E-03 7.94E-03 7.94E-01 7.99E-02 7.99E-01 7.22E-01 7.25E+02 8.36E+02 7.36E+	2.07E+01 2.16E+01
	5.24E+09 1.32E+10 2.47E+09 3.80E+08 5.42E+09 2.43E+09 1.10E+09 2.33E+09 2.33E+09 2.33E+09 3.37E+10 4.77E+11 1.38E+10 5.75E+09 3.37E+10 5.75E+09 3.56E+09 3.56E+09	1.05E+09 8.75E+08
L = .21 Sfunc 4.82E+09 3.39E+09	3.27E+08 5.08E+09 1.23E+10 1.91E+10 4.26E+10 1.21E+11 1.92E+11 1.92E+11 1.27E+12 6.13E+11 7.56E+11 7.56E+11 7.56E+11 7.37E+10 7.37E+10 7.37E+10 7.37E+09 3.57E+09 3.57E+09	9.65E+08 7.92E+08
L = 8.4 Rd -5.03E+08 -5.29E+08 -5.72E+08	6.66E+08 4.02E+08 4.51E+08 4.51E+08 4.51E+08 4.51E+08 4.50E+08 4.59E+08 4.59E+08 5.00E+08 6.03E+08 6.03E+08 7.76E+08 1.28E+09 1.28E+09 1.28E+09 1.28E+09 7.76E+08 7.93E+07 6.20E+08	5.04E+07 4.11E+07
L = .21 Rd 1.10E+09 1.04E+09 1.00E+09	9.49E+08 1.05E+09 1.21E+09 1.21E+09 2.06E+09 3.86E+09 2.06E+09 2.36E+09 6.49E+09 6.49E+09 1.96E+09 1.96E+09 8.66E+08 4.91E+08 1.96E+09 1.96E+09 7.98E+07 7.98E+07 5.97E+07	3.54E+07 2.62E+07
L = 8.4 Id -9.95E-11 -9.46E-11 -8.74E-11		9.91E-10 1.22E-09
L = .21 Id 4.56E-11 4.81E-11 5.00E-11	5.27E-11 5.18E-11 7.28E-11 7.30E-11 7.30E-11 7.30E-11 7.30E-11 7.70E-12 7.7	1.41E-09 1.91E-09
		0.29
Vd 0.05 0.05 0.05	0 0 0 0 0 0 0 0 0 0 0 0 0 0 0 0 0 0 0	0.05

	2.96E+01 2.96E+01 3.12E+01 2.96E+01 2.82E+01 2.74E+01 2.59E+01 2.59E+01	8.09E+08 2.6EE+01 3.65E+08 2.96E+01 2.26E+08 2.96E+01 2.20E+08 2.96E+01 1.53E+08 2.80E+01 1.09E+08 2.82E+01 4.60E+07 2.65E+01 8.23E+07 2.65E+01 6.35E+07 2.59E+01 3.30E+07 2.56E+01	3.16E+08 8.09E+08 2.66E+01 3.16E+08 3.65E+08 2.96E+01 2.46E+08 3.65E+08 3.12E+01 1.86E+08 2.96E+01 1.40E+08 2.96E+01 1.04E+08 1.53E+08 2.80E+01 1.04E+08 1.53E+08 2.80E+01 2.65E+07 3.30E+07 2.53E+01 2.40E+07 3.30E+07 2.53E+01 2.80E+07 2.65E+01 2.40E+07 3.30E+07 2.53E+01 2.80E+07 2.65E+01 2.80E+07 2.53E+01 2.80E+07 2.55E+01 2.80E+07 2.53E+01 2.80E+07 2.60E+07 2.6	.43E+07 4.16E+08 8.09E+08 2.66E+01 6.79E+07 3.16E+08 8.09E+08 2.66E+01 28E+07 2.46E+08 3.65E+08 3.12E+01 2.46E+06 1.86E+08 2.96E+08 2.96E+01 2.86E+06 1.86E+08 2.20E+08 2.96E+01 2.58E+06 1.40E+08 2.20E+08 2.80E+01 2.78E+06 1.04E+08 1.53E+08 2.74E+01 2.8E+06 5.69E+07 8.23E+07 2.55E+01 2.22E+06 3.23E+07 3.30E+07 2.53E+01 2.22E+06 2.40E+07 3.30E+07 2.53E+01 2.22E+06 2.40E+07 3.30E+07 2.53E+01 2.22E+06 2.40E+07 3.30E+07 2.53E+01 2.22E+06 2.40E+07 2.22E+06 2.40E+07 2.53E+07 2.22E+06 2.40E+07 2.22E+06 2.40E+07 2.22E+06 2.40E+07 2.22E+06 2.40E+07 2.40E+0	2.43E-07 4.16E+08 8.09E+08 2.66E+01 1.67E+07 3.16E+08 8.09E+08 2.66E+01 1.28E+07 2.46E+08 3.65E+08 3.12E+01 9.45E+06 1.86E+08 2.96E+08 2.96E+01 6.84E+06 1.40E+08 2.20E+08 2.80E+01 5.05E+06 1.04E+08 1.53E+08 2.82E+01 3.78E+06 7.61E+07 1.09E+08 2.74E+01 2.87E+06 5.69E+07 6.35E+07 2.59E+01 1.60E+06 3.23E+07 2.56E+01 1.60E+06 3.23E+07 2.50E+01 1.60E+06 3.23E+01 1.60E+06 3.23E+07 2.50E+01 1.60E+06 3.23E+07 2.50E+01 1.60E+06 3.23E+01 1.60E+06 3.23E+07 2.50E+01 1.60E+06 3.23E+07 2.50E+01 1.60E+06 3.24E+00 3.2
	2.96E+01 3.12E+01 2.96E+01 2.80E+01 2.74E+01 2.65E+01 2.59E+01	5.79E+08 2.96E+01 3.65E+08 3.12E+01 2.96E+08 2.96E+01 1.53E+08 2.80E+01 1.09E+08 2.82E+01 1.09E+08 2.74E+01 8.23E+07 2.65E+01 6.35E+07 2.59E+01 4.60E+07 2.59E+01 3.30E+07 2.53E+01	3.16E+08 5.79E+08 2.96E+01 2.46E+08 3.65E+08 3.12E+01 1.86E+08 2.96E+08 2.96E+01 1.40E+08 2.20E+08 2.80E+01 1.04E+08 1.53E+08 2.82E+01 7.61E+07 1.09E+08 2.74E+01 5.69E+07 8.23E+07 2.65E+01 3.23E+07 6.35E+07 2.59E+01 2.40E+07 3.30E+07 2.53E+01	.67E+07 3.16E+08 5.79E+08 2.96E+01 2.8E+07 2.46E+08 3.65E+08 3.12E+01 2.45E+06 1.86E+08 2.96E+08 2.96E+01 2.84E+06 1.40E+08 2.20E+08 2.80E+01 2.95E+01 2.95E+06 1.04E+08 1.53E+08 2.82E+01 2.8E+06 7.61E+07 1.09E+08 2.74E+01 2.87E+06 5.69E+07 6.35E+07 2.59E+01 2.60E+06 3.23E+07 2.53E+07 2.53E+01 2.22E+06 2.40E+07 2.53E+01 2.22E+06 2.40E+07 2.53E+07 2.53E+07 2.53E+07 2.53E+07 2.53E+01 2.22E+06 2.40E+07 2.53E+01 2.20E+07 2.53E+01 2.20E+07 2.53E+01 2.20E+07 2.53E+01 2.20E+07 2.53E+01 2.20E+07 2.53E+01 2.20E+08 2.40E+07 2.53E+01 2.20E+08 2.40E+07 2.53E+01 2.20E+08 2.40E+08 2.40E+	1.67E+07 3.16E+08 5.79E+08 2.96E+01 1.28E+07 2.46E+08 3.65E+08 3.12E+01 9.45E+06 1.86E+08 2.96E+08 2.96E+01 6.84E+06 1.40E+08 2.20E+08 2.80E+01 5.05E+06 1.04E+08 1.53E+08 2.82E+01 3.78E+06 7.61E+07 1.09E+08 2.74E+01 2.87E+06 5.69E+07 8.23E+07 2.65E+01 1.60E+06 3.23E+07 4.60E+07 2.56E+01 1.60E+06 3.23E+07 4.60E+07 2.56E+01
	3.12E+01 2.96E+01 2.80E+01 2.74E+01 2.59E+01 2.59E+01	3.65E+08 3.12E+01 2.96E+08 2.96E+01 2.20E+08 2.80E+01 1.53E+08 2.82E+01 1.09E+08 2.74E+01 8.23E+07 2.65E+01 6.35E+07 2.59E+01 4.60E+07 2.56E+01 3.30E+07 2.56E+01	2.46E+08 3.65E+08 3.12E+01 1.86E+08 2.96E+08 2.96E+01 1.40E+08 2.20E+08 2.80E+01 1.04E+08 1.53E+08 2.82E+01 7.61E+07 1.09E+08 2.74E+01 5.69E+07 8.23E+07 2.65E+01 3.23E+07 6.35E+07 2.59E+01 2.40E+07 3.30E+07 2.53E+01	28E+07 2.46E+08 3.65E+08 3.12E+01 4.5E+06 1.86E+08 2.96E+08 2.96E+01 0.5E+06 1.40E+08 2.20E+08 2.96E+01 0.5E+06 1.04E+08 1.53E+08 2.82E+01 0.5E+06 7.61E+07 1.09E+08 2.74E+01 0.5E+06 5.69E+07 8.23E+07 2.65E+01 0.5E+06 3.23E+07 4.60E+07 2.56E+01 0.5E+06 2.40E+07 3.30E+07 2.53E+01 0.5E+06 0.5E+07	1.28E+07 2.46E+08 3.65E+08 3.12E+01 9.45E+06 1.86E+08 2.96E+08 2.96E+01 6.84E+06 1.40E+08 2.20E+08 2.96E+01 5.05E+06 1.04E+08 1.53E+08 2.82E+01 3.78E+06 7.61E+07 1.09E+08 2.74E+01 2.87E+06 5.69E+07 8.23E+07 2.65E+01 2.14E+06 4.27E+07 6.35E+07 2.59E+01 1.60E+06 3.23E+07 4.60E+07 2.56E+01
	2.80E+01 2.82E+01 2.74E+01 2.65E+01 2.59E+01	2.20E+08 2.80E+01 1.53E+08 2.82E+01 1.09E+08 2.74E+01 8.23E+07 2.65E+01 6.35E+07 2.59E+01 4.60E+07 2.59E+01 3.30E+07 2.53E+01	1.80E+08 2.30E+08 2.30E+01 1.40E+08 2.20E+08 2.80E+01 1.04E+08 1.53E+08 2.82E+01 2.6E+07 1.09E+08 2.74E+01 2.3E+07 8.23E+07 2.59E+01 3.23E+07 3.30E+07 2.53E+01 2.40E+07 2.46E+01 2.40E+01 2.40E+07 2.40E+07 2.40E+01 2.40E+07 2.40E+01 2.40E		9.45E+06 1.80E+08 2.30E+08 2.30E+01 6.84E+06 1.40E+08 2.20E+08 2.80E+01 5.05E+06 1.04E+08 1.53E+08 2.82E+01 3.78E+06 7.61E+07 1.09E+08 2.74E+01 2.87E+06 5.69E+07 8.23E+07 2.65E+01 1.60E+06 3.23E+07 4.60E+07 2.56E+01 1.60E+08 4.60E+07 4.6
	2.82E+01 2.74E+01 2.65E+01 2.59E+01 2.56E+01	1.53E+08 2.82E+01 1.09E+08 2.74E+01 8.23E+07 2.65E+01 6.35E+07 2.59E+01 4.60E+07 2.56E+01 3.30E+07 2.53E+01 2.45E+07 2.46E+01	1.04E+08 1.53E+08 2.82E+01 7.61E+07 1.09E+08 2.74E+01 5.69E+07 8.23E+07 2.65E+01 4.27E+07 6.35E+07 2.59E+01 3.23E+07 4.60E+07 2.56E+01 2.40E+07 3.30E+07 2.53E+01	.05E+06	5.05E+06 1.04E+08 1.53E+08 2.82E+01 3.78E+06 7.61E+07 1.09E+08 2.74E+01 2.87E+06 5.69E+07 8.23E+07 2.65E+01 2.14E+06 4.27E+07 6.35E+07 2.59E+01 1.60E+06 3.23E+07 4.60E+07 2.56E+01
	2.74E+01 4. 2.65E+01 4. 2.59E+01 4. 2.56E+01 4.	1.09E+08 2.74E+01 8.23E+07 2.65E+01 6.35E+07 2.59E+01 4.60E+07 2.59E+01 3.30E+07 2.53E+01 2.45E+07 2.46E+01	7.61E+07 1.09E+08 2.74E+01 5.69E+07 8.23E+07 2.65E+01 4.27E+07 6.35E+07 2.59E+01 3.23E+07 4.60E+07 2.56E+01 2.40E+07 3.30E+07 2.53E+01	.78E+06 7.61E+07 1.09E+08 2.74E+01 .87E+06 5.69E+07 8.23E+07 2.65E+01 .14E+06 4.27E+07 6.35E+07 2.59E+01 .60E+06 3.23E+07 4.60E+07 2.56E+01 .22E+06 2.40E+07 3.30E+07 2.53E+01	3.78E+06 7.61E+07 1.09E+08 2.74E+01 4. 2.87E+06 5.69E+07 8.23E+07 2.65E+01 4. 2.14E+06 4.27E+07 6.35E+07 2.59E+01 4. 1.60E+06 3.23E+07 4.60E+07 2.56E+01 4.
	2.59E+01 4. 2.59E+01 4. 2.56E+01 4.	8.23E+07 2.65E+01 6.35E+07 2.59E+01 4.60E+07 2.56E+01 3.30E+07 2.56E+01 2.45E+07 2.46E+01	5.69E+07 8.23E+07 2.65E+01 4.27E+07 6.35E+07 2.59E+01 3.23E+07 4.60E+07 2.56E+01 2.40E+07 3.30E+07 2.53E+01 4.78E+07 2.46E+07 2.65E+01	.87E+06 5.69E+07 8.23E+07 2.65E+01 .14E+06 4.27E+07 6.35E+07 2.59E+01 .60E+06 3.23E+07 4.60E+07 2.56E+01 .22E+06 2.40E+07 3.30E+07 2.53E+01	2.87E+06 5.69E+07 8.23E+07 2.65E+01 4. 2.14E+06 4.27E+07 6.35E+07 2.59E+01 4. 1.60E+06 3.23E+07 4.60E+07 2.56E+01 4.
	2.59E+01 4. 2.56E+01 4.	6.35E+07 2.59E+01 4.60E+07 2.56E+01 3.30E+07 2.53E+01 2.45E+07 2.46E+01	4.27E+07 6.35E+07 2.59E+01 3.23E+07 4.60E+07 2.56E+01 2.40E+07 3.30E+07 2.53E+01 4.78E+07 2.46E+07	.14E+06 4.27E+07 6.35E+07 2.59E+01 .60E+06 3.23E+07 4.60E+07 2.56E+01 .22E+06 2.40E+07 3.30E+07 2.53E+01	2.14E+06 4.27E+07 6.35E+07 2.59E+01 4. 1.60E+06 3.23E+07 4.60E+07 2.56E+01 4.
	2.56E+01 4.	4.60E+07 2.56E+01 3.30E+07 2.53E+01 2.45E+07 2.46E+01	3.23E+07 4.60E+07 2.56E+01 2.40E+07 3.30E+07 2.53E+01 4.78E+07 2.46E+07	.60E+06 3.23E+07 4.60E+07 2.56E+01	1.60E+06 3.23E+07 4.60E+07 2.56E+01 4
		3.30E+07 2.53E+01 2.45E+07 2.46E+01	2.40E+07 3.30E+07 2.53E+01 4 78E+07 2 46E+07 2 46E+04	.22E+06	
	2.53E+01	10:10:2		. */L+U+ 1 /XL+U/	1.22E+06 2.40E+0/ 3.30E+0/ 2.53E+01 0 37E+07 2 45E+01
	.86E+07 2.40E+01	1.86E+07 2.40E+01	1.34E+07 1.86E+07 2.40E+01	.26E+05 1.34E+07 1.86E+07 2.40E+01	7.26E+05 1.34E+07 1.86E+07 2.40E+01
2.37E+01 4.06E+01	2.37E+01	1.40E+07 2.37E+01	1.00E+07 1.40E+07 2.37E+01	1.00E+07 1.40E+07 2.37E+01	5.64E+05 1.00E+07 1.40E+07 2.37E+01
2.35E+01 3.99E+01	2.35E+01	1.06E+07 2.35E+01	7.55E+06 1.06E+07 2.35E+01	1.06E+07 2.35E+01	4.46E+05 7.55E+06 1.06E+07 2.35E+01
-	2.32E+01	8.04E+06 2.32E+01	5.61E+06 8.04E+06 2.32E+01	5.61E+06 8.04E+06 2.32E+01	3.53E+05 5.61E+06 8.04E+06 2.32E+01
- ,	2.30E+01	6.04E+06 2.30E+01	4.18E+06 6.04E+06 2.30E+01	4.18E+06 6.04E+06 2.30E+01	2.85E+05 4.18E+06 6.04E+06 2.30E+01
2.2/E+01 3./UE+01 2.24E+01 3.61E+01	2.2/E+01 2.24E+01	3.67E+06 2.27E+01	3.17E+U6 4.70E+U6 2.27E+U1 2.39E+06 3.67E+06 2.24E+01	3.17E+U6 4.70E+U6 2.27E+U1 2.39E+06 3.67E+06 2.24E+01	. 2.33E+U5 3.1/E+U6 4./UE+U6 2.2/E+U1 . 191E+U5 2.39E+06 3.67E+06 2.24E+01
1 3.55E+01	2.23E+01 3.55E+01	2.83E+06 2.23E+01 3.55E+01	1.78E+06 2.83E+06 2.23E+01 3.55E+01	1.78E+06 2.83E+06 2.23E+01 3.55E+01	1.59E+05 1.78E+06 2.83E+06 2.23E+01 3.55E+01
3.49E+01	2.22E+01 3.49E+01	2.25E+06 2.22E+01 3.49E+01	1.36E+06 2.25E+06 2.22E+01 3.49E+01	1.36E+06 2.25E+06 2.22E+01 3.49E+01	. 1.34E+05 1.36E+06 2.25E+06 2.22E+01 3.49E+01
3 42F+01		4 OOF 106 0 04E 104 0 40E 104	1.03E+06 1.80E+06 2.21E+01 3.42E+01	4 02E+06 4 00E+06 0 04E+04 0 40E+04	1 14E+05 1 03E+06 1 80E+06 2 21E+01 3 42E+01
3 42F+01		4 OUE TUE 10 10 11 11 11 11 11 11 11 11 11 11 11	1.03E+06 1.80E+06 2.21E+01 3.42E+01	A MODERNE A BONETON OFFICE OF THE PORT OF	1 14E+05 1 03E+06 1 R0E+06 221E+01 3 42E+01
	2.21E+01 3.42E+01	1.60E+06 2.21E+01 3.42E+01		1.03E+06 1.80E+06 2.21E+01 3.42E+01	
	2.21E+01 3.42E+01	1.60E+06 2.21E+01 3.42E+01		1.03E+06 1.80E+06 2.21E+01 3.42E+01	1.14E+03 1.03E+00 1.00E+00 2.21E+01 0.42E+01
10:11:0	2.21E+01 3.42E+01	1.60E+06 2.21E+01 3.42E+01		1.03E+U6 1.8UE+U6 2.21E+U1 3.4ZE+U1	
1 3.37E+01	2.21E+01 3.42E+01 2.22E+01 3.37E+01	1.44E+06 2.22E+01 3.37E+01	7.76E+05 1.44E+06 2.22E+01 3.37E+01	1.03E+06 1.80E+06 2.21E+01 3.42E+01 7.76E+05 1.44E+06 2.22E+01 3.37E+01	9.82E+04 7.76E+05 1.44E+06 2.22E+01 3.37E+01
. —	2.21E+01 3. 2.22E+01 3.	1.44E+06 2.22E+01 3	7.76E+05 1.44E+06 2.22E+01	7.76E+05 1.80E+06 2.21E+01 3.	. 9.82E+04 7.76E+05 1.44E+06 2.22E+01 3.
		4 OF THE 2 2 24 E + 0.4	1.03E+06 1.80E+06 2.21E+01	4 02E+06 4 00E+06 2 24E+04	1 14E+05 1 03E+06 1 80E+06 2 21E+01
2.27E+01 2.24E+01 2.23E+01 2.22E+01	0 0 0 0	4.70E+06 3.67E+06 2.83E+06 2.25E+06 2.25E+06	3.17E+06 4.70E+06 2.39E+06 3.67E+06 2.178E+06 2.83E+06 2.25E+06 2.136E+06 1.80E+06 2.25E+06 2.180E+06 2.25E+06 2.2	3.17E+06 4.70E+06 2.239E+06 3.67E+06 2.1.78E+06 2.83E+06 2.25E+06 2.05E+06	2.33E+05 3.17E+06 4.70E+06 2.191E+05 2.39E+06 3.67E+06 2.159E+05 1.78E+06 2.25E+06 2.134E+05 1.36E+06
	86E+07 40E+07 .06E+07 .04E+06 .04E+06 .70E+06 .67E+06		1.34E+07 1.00E+07 7.55E+06 5.61E+06 4.18E+06 3.17E+06 2.39E+06 1.78E+06 1.36E+06	.26E+05 1.34E+07 .64E+05 1.00E+07 .46E+05 7.55E+06 .53E+05 5.61E+06 .85E+05 4.18E+06 .33E+05 3.17E+06 .91E+05 2.39E+06 .34E+05 1.78E+06 .34E+05 1.36E+06	E+05 7.26E+05 1.34E+07 E+05 5.64E+05 1.00E+07 E+05 4.46E+05 7.55E+06 E+05 3.53E+05 5.61E+06 E+05 2.35E+05 4.18E+06 E+04 1.91E+05 2.39E+06 E+04 1.34E+05 1.36E+06 E+04 1.34E+05 1.36E+06
08 6.17E+05 9.37E+05 1.78E+07 1.08 4.64E+05 7.26E+05 1.34E+07 07 2.63E+05 5.64E+05 7.55E+06 07 1.99E+05 3.53E+05 5.61E+06 07 1.51E+05 2.33E+05 3.17E+06 07 8.74E+04 1.91E+05 2.39E+06 07 6.72E+04 1.59E+05 1.36E+06 07 6.72E+04 1.34E+05 1.36E+06 07 6.72E+04 1.44E+05 1.36E+06 07 6.72E+06 07 6	08 8.20E+05 1.22E+06 08 6.17E+05 9.37E+05 08 4.64E+05 7.26E+05 08 3.50E+05 5.64E+05 07 2.63E+05 4.46E+05 07 1.99E+05 3.53E+05 07 1.51E+05 2.85E+05 07 8.74E+04 1.91E+05 07 6.72E+04 1.59E+05	08 4.64E+05 7 08 3.50E+05 5 07 2.63E+05 3 07 1.99E+05 3 07 1.51E+05 2 07 8.74E+04 1 07 6.72E+04 1	008 4.64 008 3.50 007 2.63 007 1.51 007 8.74 007 6.72	004 004 004 004 004 004 004	
5.33E-08 6.17E+05 9.37E+05 1.78E+07 6.89E-08 4.64E+05 7.26E+05 1.34E+07 8.86E-08 3.50E+05 5.64E+05 1.00E+07 1.12E-07 2.63E+05 4.46E+05 7.55E+06 1.42E-07 1.99E+05 3.53E+05 5.61E+06 1.76E-07 1.51E+05 2.35E+05 3.17E+06 2.62E-07 8.74E+04 1.91E+05 2.39E+06 3.72E-07 5.18E+04 1.34E+05 1.36E+06 4.25E-07 5.18E+04 1.34E+05 1.36E+06 4.25E-07 5.18E+04 1.34E+05 1.36E+06 4.25E+06 4.2	4.11E-08 8.20E+05 1.22E+06 5.33E-08 6.17E+05 9.37E+05 6.89E-08 4.64E+05 7.26E+05 8.86E-08 3.50E+05 5.64E+05 1.12E-07 2.63E+05 3.53E+05 1.42E-07 1.99E+05 2.35E+05 2.15E-07 1.15E+05 2.33E+05 2.62E-07 8.74E+04 1.91E+05 3.72E-07 5.18E+04 1.34E+05 3.72E-07 5.18E+04 1.34E+05	6.89E-08 4.64E+05 7.886E-08 3.50E+05 5.1.12E-07 2.63E+05 3.1.42E-07 1.99E+05 3.1.76E-07 1.51E+05 2.62E-07 8.74E+04 1.3.72E-07 5.18E+04 1.3.72E-07 5.18E-07 5.00E-0.4 5.4.72E-07 5.18E-0.4 1.3.72E-07 5.18E-0.4 1.3.72E-07 5.00E-0.4 5.4.72E-0.4 5.	6.89E-08 4.64 6.89E-08 3.50 1.12E-07 2.63 1.42E-07 1.99 1.76E-07 1.15 2.15E-07 1.15 3.14E-07 6.72 3.72E-07 5.18	5.33E-08 6.89E-08 8.86E-08 1.12E-07 1.76E-07 2.15E-07 3.14E-07	• • • • • • • • • • • • • • • • • • • •

Ratio	shift18	5.83E+01	5.70E+01	5.50E+01	5.27E+01	5.15E+01	5.06E+01	4.99E+01	5.04E+01	5.13E+01	5.08E+01	5.01E+01	4.95E+01	4.89E+01	4.84E+01	4.79E+01	4.78E+01	4.74E+01	4.68E+01	4.63E+01	4.61E+01	4.58E+01	4.55E+01	4.56E+01	4.59E+01	.59E+01	.55E+01	53E+01	4.55E+01	4.52E+01	4.50E+01	4.49E+01	4.45E+01	4.45E+01	4.45E+01	4.38E+01	4.39E+01
_	ס			_ ص	- 5	_ 2	_ ى	4	_	- 5	_	_	4	_	_	_	_	_	4	4	4	_	_	_		4.	4	_		-		_	_	4	4	_	_
Ratio	d shift16	4.79E+01	4.71E+01	4.65E+01	4.58E+01	4.43E+01	4.29E+01	4.25E+01	4.20E+01	4.15E+01	4.25E+01	4.36E+01	4.32E+01	4.28E+01	4.23E+01	4.20E+01	4.19E+01	4.17E+01	4.14E+01	4.10E+01	4.09E+01	4.08E+01	4.08E+01	4.12E+01	4.14E+01	4.12E+01	4.11E+01	4.13E+01	4.12E+01	4.08E+01	4.12E+01	4.12E+01	4.06E+01	4.04E+01	4.02E+01	4.03E+01	4.09E+01
Ratio	d shift 14	3.87E+01	3.84E+01	3.82E+01	3.79E+01	3.75E+01	3.73E+01	3.65E+01	3.55E+01	3.53E+01	3.53E+01	3.53E+01	3.61E+01	3.72E+01	3.70E+01	3.67E+01	3.66E+01	3.65E+01	3.62E+01	3.61E+01	3.62E+01	3.61E+01	3.62E+01	3.67E+01	3.71E+01	3.72E+01	3.71E+01	3.70E+01	3.72E+01	3.73E+01	3.73E+01	3.72E+01	3.73E+01	3.71E+01	3.67E+01	3.66E+01	3.70E+01
Ratio	d shift12	3.06E+01	3.07E+01	3.09E+01	3.09E+01	3.08E+01	3.08E+01	3.09E+01	3.09E+01	3.04E+01	2.99E+01	3.00E+01	3.01E+01	3.01E+01	3.09E+01	3.19E+01	3.20E+01	3.19E+01	3.17E+01	3.16E+01	3.17E+01	3.18E+01	3.20E+01	3.25E+01	3.29E+01	3.31E+01	3.33E+01	3.35E+01	3.36E+01	3.34E+01	3.37E+01	3.40E+01	3.37E+01	3.35E+01	3.37E+01	3.36E+01	3.38E+01
Ratio	d shift10	2.38E+01	2.41E+01	2.44E+01	2.47E+01	2.49E+01	2.51E+01	2.54E+01	2.55E+01	2.57E+01	2.60E+01	2.58E+01	2.55E+01	2.56E+01	2.57E+01	2.58E+01	2.68E+01	2.77E+01	2.77E+01	2.76E+01	2.77E+01	2.78E+01	2.80E+01	2.86E+01	2.91E+01	2.93E+01	2.95E+01	2.98E+01	3.01E+01	3.02E+01	3.04E+01	3.05E+01	3.04E+01	3.06E+01	3.05E+01	3.04E+01	3.10E+01
L = 8.4	Sfunc	1.79E+05	1.58E+05	1.40E+05	1.26E+05	1.15E+05	1.04E+05	9.31E+04	8.49E+04	7.91E+04	7.21E+04	6.70E+04	6.19E+04	5.67E+04	5.29E+04	4.89E+04	4.54E+04	4.25E+04	4.03E+04	3.72E+04	3.37E+04	3.19E+04	3.09E+04	2.96E+04	2.80E+04	2.66E+04	2.51E+04	2.34E+04	2.25E+04	2.18E+04	2.09E+04	1.92E+04	1.87E+04	1.77E+04	1.66E+04	1.63E+04	1.48E+04
L = .21	Sfunc	3.53E+04	2.94E+04	2.47E+04	2.08E+04	1.75E+04	1.48E+04	1.28E+04	1.11E+04	9.61E+03	8.41E+03	7.42E+03	6.50E+03	5.75E+03	5.11E+03	4.58E+03	4.09E+03	3.69E+03	3.36E+03	3.06E+03	2.78E+03	2.52E+03	2.31E+03	2.37E+03	2.22E+03	1.79E+03	1.64E+03	1.53E+03	1.42E+03	1.34E+03	1.26E+03	1.17E+03	1.09E+03	1.02E+03	9.66E+02	9.04E+02	8.41E+02
L = 8.4	Rd	2.68E+04	2.52E+04	2.37E+04	2.24E+04	2.12E+04	2.01E+04	1.91E+04	1.82E+04	1.74E+04	1.66E+04	1.59E+04	1.53E+04	1.47E+04	1.41E+04	1.36E+04	1.32E+04	1.27E+04	1.23E+04	1.19E+04	1.16E+04	1.13E+04	1.09E+04	1.06E+04	1.03E+04	1.01E+04	9.81E+03		9.34E+03	9.12E+03	8.91E+03	8.71E+03		8.33E+03	•	8.00E+03	•
L = .21	Rd	2.68E+03	2.36E+03	2.09E+03	1.87E+03	1.68E+03	1.52E+03	1.38E+03	1.26E+03	1.16E+03	1.07E+03	9.89E+02	9.20E+02	8.59E+02	8.05E+02	7.56E+02	7.13E+02	6.75E+02	6.39E+02	6.07E+02	5.78E+02	5.52E+02	5.28E+02	5.06E+02	4.80E+02	4.61E+02	4.44E+02	4.28E+02	4.14E+02	4.00E+02	3.87E+02	3.75E+02	3.64E+02	3.53E+02	4	3.34E+02	.25
L = 8.4	므	1.86E-06	1.99E-06	2.11E-06	2.24E-06	2.36E-06	2.49E-06	2.62E-06	2.75E-06	2.88E-06	3.01E-06	3.14E-06	3.27E-06	3.40E-06	3.53E-06	3.67E-06	3.80E-06	3.93E-06	4.06E-06	4.19E-06	4.32E-06	4.44E-06	4.57E-06	4.70E-06	4.83E-06	4.96E-06	5.10E-06	5.22E-06	5.35E-06	5.48E-06	5.61E-06	5.74E-06	5.87E-06	6.00E-06	6.12E-06	.25	6.37E-06
L = .21	<u> </u>	1.87E-05	2.12E-05	2.39E-05	2.68E-05	2.98E-05	3.30E-05	3.62E-05	3.97E-05	4.32E-05	4.68E-05	5.06E-05	5.44E-05	5.82E-05	6.21E-05	6.61E-05	7.01E-05	7.41E-05	7.82E-05	8.23E-05	8.65E-05	9.06E-05	9.48E-05	9.89E-05	1.04E-04	1.08E-04	1.13E-04	1.17E-04	1.21E-04	1.25E-04	1.29E-04	1.33E-04	1.38E-04	1.42E-04	1.46E-04	Ш	1.54E-04
	δ	0.67	0.68	0.69	0.70	0.71	0.72	0.73	0.74	0.75	9.76	0.77	0.78	0.79	0.80	0.81	0.82	0.83	0.8 4	0.85	0.86	0.87	0.88	0.89	0.90	0.91	0.92	0.93	0.9 4	0.95	96.0	0.97		0.99	1.00	1.01	1.02
	P	0.05	0.05	0.05	0.05	0.05	0.05	0.05	0.05	0.05	0.05	0.05	0.05	0.05	0.05	0.05	0.05	0.05	0.05	0.05	0.05	0.05	0.05	0.05	0.05	0.05	0.05	0.05	0.05	0.05	0.05	0.05	0.05	0.05		0.05	

Ratio Ratio shift16 a shift16 a. 3.75E+01 4.04E+01 3.75E+01 4.11E+01 3.75E+01 4.10E+01 3.95E+01
Ratio 3.75E+0 3.75E+0 3.75E+0 3.75E+0 3.75E+0 3.69E+0 3.66E+0 3.67E+0
5 55555555555555555555555555555555555
2 555555555555555555555555555555555555
Sfunc d shift - Sfunc d shift - 3.13E+1.49E+04 3.13E+1.24E+04 3.15E+1.24E+04 3.15E+1.13E+04 3.16E+1.09E+04 3.19E+1.09E+04 3.19E+1.02E+04 3.19
12. 12. 12. 12. 12. 12. 12. 12. 12. 12.
Rd Sfu Rd Sfu 7.70E+03 7.94 7.55E+03 7.51 7.41E+03 7.16 7.27E+03 6.75 7.05E+03 6.29 7.03E+03 6.29 6.91E+03 5.92 6.80E+03 5.97 6.69E+03 5.07 6.58E+03 4.97
Rd 1.31 L.3 Rd 3.17E+02 7.7 3.09E+02 7.5 3.02E+02 7.5 2.95E+02 7.1 2.88E+02 7.1 2.82E+02 7.0 2.70E+02 6.8 2.65E+02 6.5 5.5 6.5 6.5 6.5 6.5 6.5 6.5 6.5 6.5
14 8.4 1 1 1 1 1 1 1 1 1 1 1 1 1 1 1 1 1 1 1
L=.21 Id 1.58E-04 6.1.62E-04 6.1.70E-04 6.1.73E-04 7.77E-04 7.77E-04 7.81E-04 7.89E-04 7.99E-04 7.99E-04
Vd Vg 0.05 1.03 0.05 1.04 0.05 1.05 0.05 1.07 0.05 1.09 0.05 1.10 0.05 1.10

_	18														
Ratio	d shift -														
Ratio	dshift 16 dshift 18														
Ratio	dshift 10 dshift 12 dshift 14														
Ratio	d shift12														
Ratio	d shift10	3.29E+01													
L = 8.4	Sfunc	4.51E+03	4.54E+03	3.91E+03	3.95E+03	4.09E+03	3.82E+03	3.75E+03	3.79E+03	3.63E+03	3.48E+03	3.23E+03	3.37E+03	3.23E+03	
L = .21	Sfunc	1.77E+02	1.72E+02	1.77E+02	1.60E+02	1.56E+02	1.49E+02	1.51E+02	1.45E+02	1.37E+02	1.37E+02	1.32E+02	1.38E+02	1.27E+02	
L = 8.4	Rd	4.75E+03	4.70E+03	4.66E+03	4.62E+03	4.58E+03	4.54E+03	4.50E+03	4.47E+03	4.43E+03	4.39E+03	4.36E+03	4.33E+03	4.29E+03	4.26E+03
L = .21	Rd	1.79E+02	1.77E+02	1.75E+02	1.74E+02	1.72E+02	1.71E+02	1.69E+02	1.68E+02	1.66E+02	1.65E+02	1.64E+02	1.62E+02	1.61E+02	1.60E+02
L = 8.4	<u> </u>	1.05E-05	1.06E-05	1.07E-05	1.08E-05	1.09E-05	1.10E-05	1.11E-05	1.12E-05	1.13E-05	1.14E-05	1.15E-05	1.16E-05	1.17E-05	1.17E-05
L = .21	<u> </u>	2.80E-04	2.82E-04	2.85E-04	2.88E-04	2.90E-04	2.93E-04	2.96E-04	2.98E-04	3.01E-04	3.03E-04	3.06E-04	3.08E-04	3.11E-04	3.13E-04
	δ	1.39	1.40	1.41	1.42	1.43	1 .	1.45	1.46	1.47	1.48	1.49	1.50	1.51	1.52
	₽	0.05	0.05	0.05	0.05	0.05	0.05	0.05	0.05	0.05	0.05	0.05	0.05	0.05	0.05

APPENDIX D

DATA MANIPULATION IN EXCEL

This appendix describes how the different values needed for applying the shift and ratio method were determined. They are described in terms of the columns and rows as well as the equations used in the Excel file.

The resistance (R_d) values for the short channel gate length device (column 5) are calculated in the Excel files by dividing the first column (V_d) by the drain current (column 3) for all gate voltages. Thus the Nth entry for the resistance value would use the following equation.

$$R_d(N) = \frac{V_d(N)}{I_d(N)} \tag{26}$$

The resistance of the long channel device is calculated similarly by using the drain current values in column 4.

The S-function (Sfunc) for the short channel device (column 7) is calculated in the Excel file by taking the difference between the resistance values for the short channel device (column 5) divided by the difference in gate voltages (column 2) for the respective resistance values. The absolute value of this division gives the S-function value. The Nth entry for the S-function uses the equation below.

$$S^{i}(N) = abs \left(\frac{R_{d}(N-1) - R_{d}(N+1)}{V_{g}(N-1) - V_{g}(N+1)} \right)$$
 (27)

The S-function for the long channel device (column 8) is calculated similarly using the resistance values from column 6.

The different ratio values are calculated by dividing the running average of the S-function of the long channel device (column 8) by the running average of the S-function of the short channel device (column 7). The Nth entry for the ratio for a defined 'd' shift value is calculated using the equation below.

$$r(N,\delta) = \frac{average\left(S^{0}(N-2), S^{0}(N-1), S^{0}(N), S^{0}(N+1), S^{0}(N+2)\right)}{average\left(S^{i}(N-2-\delta), S^{i}(N-1-\delta), S^{i}(N-\delta), S^{i}(N+1-\delta), S^{i}(N+2-\delta)\right)}$$
(28)

BIBLIOGRAPHY

- [1] H. van Meer, K. Henson, J-H Lyu, M. Rosmeulen, S. Kubicek, N. Collaert, and K. de Meyer, "Limitations of shift and ratio based L_{eff} extraction techniques for MOS transistors with halo or pocket implants," IEEE Electron Device Letters, vol. 21, pp. 133-136, March (2000)
- [2] K. K. Ng and J. R. Brews, "Measuring the Effective Channel Length of MOSFETs," IEEE Circuits and Devices, November, pp. 33-38 November (1990)
- [3] Y. Taur, "MOSFET channel length: extraction and interpretation," IEEE Transactions on Electron Devices, vol. 47 pp. 160-170, January (2000)
- [4] Y. Taur, D. S. Zicherman, D. R. Lombardi, P. J. Restle, C. H. Hsu, H. I. Hanafi, M. R. Wordeman, B. Davari, and G. G. Shahidi, "A new shift and ratio method for MOSFET channel length extraction," IEEE Electron Device Letters, vol. 13, pp. 267-269, May (1992)
- [5] J. W. Mayer, L. Eriksson, and J. A. Davies, "Ion Implantation in Semiconductors," Academic Press Inc., NY, 1970
- [6] K. Miyashita, H. Yoshimura, M. Takayanagi, M. Fujiwara, K. Adachi, T. Nakayama, and Y. Toyoshima, "Optimized Halo Structure for 80nm Physical Gate CMOS Technology with Indium and Antimony Highly Angled Ion Implantation," IEDM, pp. 645-648, (1999)
- [7] Hewlett-Packard, "Operation and Service Manual Model 4145B Semiconductor Parameter Analyzer," Yokogawa-Hewlett-Packard, September (1986)
- [8] K.-S. Yeo, S. S. Rofail, and W.-L. Goh, "CMOS/BiCMOS ULSI Low Voltage, Low Power," Prentice Hall, NJ, 2002
- [9] H. C. Casey, "Devices for Integrated Circuits' Silicon and III-V Compound Semiconductors," John Wiley, NY, pp. 349, (1999)
- [10] S. Thompson, P. Packan, and M. Bohr, "MOS Scaling: Transistor Challenges for the 21st Century, "Intel Technology Journal, Q3 (1998)
- [11] Hewlett-Packard Co, "HP-IB Command Library for MS-DOS," Hewlett-Packard, Edition 2, June (1986)
- [12] K. Ahmed, I. De, C. Osburn, J. Wortman, and J. Hauser, "Limitations of the Modified Shift-and-Ratio Technique for Extraction of the Bias Dependence of Leff and Rsd of LDD MOSFET's," IEEE Transactions on Electron Devices, vol. 47, pp. 891-893, April (2000)

- [13] B. Cretu, T. Boutchacha, G. Ghibaudo, and F. Balestra, "New ratio method for effective channel length and threshold voltage extraction in MOS transistors," Electronics Letters, vol. 37, pp. 717-719, May (2001)
- [14] J. Y.-C. Sun, M. R. Wordeman, and S. E. Laux, "On the Accuracy of Channel Length Characterization of LDD MOSFET's," IEEE Transactions on Electron Devices, vol. ED-33, pp. 1556-1562, October (1986)
- [15] B. Yu, H. Wang, O. Milic, Q. Xiang, W. Wang, J. X. An, and M.R. Lin, "50nm Gate-length CMOS transistor with Super-Halo: design, process, and reliability," IEDM, pp.653-656, (1999)
- [16] Y. Taur, C. H. Wann, and D. J. Frank, "25nm CMOS design considerations," IEDM, pp. 789-792, (1998)
- [17] T. B. Hook, S. Biesemans, and J. Slinkman, "The dependence of channel length on channel width in narrow-channel CMOS devices for 0.35-0.13 mm technologies," IEEE Electron Device Letters, vol. 21, pp. 85-87, February (2000)
- [18] J.-C. Guo, S. S.-S. Chung, and C. C.-H. Hsu, "A new approach to determine the effective channel length and the drain-and-source series resistance of miniaturized MOSFET's," IEEE Transactions on Electron Devices, vol. 41, pp. 1811-1818, October (1994)
- [19] B. J. Sheu and P. K. Ko, "A capacitance method to determine channel lengths for conventional and LDD MOSFET's," IEEE Electron Device Letters, vol. EDL-5, pp. 491-493, November (1984)
- [20] Y. Taur, S. Wind, Y. J. Mii, Y. Lii, D. Moy, K. A. Jenkins, C. L. Chen, P. J. Coane, D. Klaus, J. Bucchignano, M. Rosenfield, M. G. R. Thomson, and M. Polcari, "High performance 0.1mm CMOS devices with 1.5 V Power Supply," IEDM, pp. 127-130, (1993)
- [21] Y. Taur, Y.-J. Mii, R. Logan, H.-S. Wong, "On 'effective channel length' in 0.1-mm MOSFET's," IEEE Electron Device Letters, vol. 16, pp. 136-138, April (1995)
- [22] M. S. Lundstrom, "On the mobility versus drain current relation for a nanoscale MOSFET," IEEE Electron Device Letters, vol. 22, pp. 293-295, June (2001)
- [23] G. Niu, J. D. Cressler, S. J. Mathew, and S. Subbanna, "A channel resistance derivative method for effective channel length extraction in LDD MOSFET's," IEEE Transactions on Electron Devices, vol. 47, pp. 648-650, March (2000)

- [24] S. M. Sze, "High-Speed Semiconductor Devices," John Wiley and Sons, Inc., NY, 1990
- [25] G. Carter and W. A. Grant, "Ion Implantation of Semiconductors," Halsted Press, NY, 1976
- [26] G. Niu, J. D. Cressler, S. J. Mathew, and S. Subbanna, "A total resistance slope-based effective channel mobility extraction method for deep submicrometer CMOS technology," IEEE Transactions on Electron Devices, vol. 46, pp. 1912-1914, September (1999)
- [27] S. Biesemans, M. Hendriks, S. Kubicek, and K. de Meyer, "Practical accuracy analysis of some existing effective channel length and series resistance extraction methods for MOSFET's," IEEE Transactions on Electron Devices, vol. 45, pp. 1301-1316, June (1998)
- [28] P. C. Liu and H. Lin, "Measuring and characterizing sub-micron short channel LDD MOSFETs"
- [29] X. Zhou and K. Y. Lim, "Experimental determination of electrical, metallurgical, and physical gate lengths of submicron MOSFET's"
- [30] K. Y. Lim and X. Zhou, "A physically-based semi-empirical series resistance model for deep-submicron MOSFET I-V modeling," IEEE Transactions on Electron Devices, vol. 47, pp. 1300-1302, June (2000)
- [31] P. Antognetti and G. Massobrio, "Semiconductor Device Modeling with SPICE," McGraw-Hill, New York, 1988

